Dynamic management of spectral resources in LTE networks

Amine Mohamed Adouane

THÈSE

Présentée à

Université de Versailles Saint-Quentin-en-Yvelines

pour obtenir le grade de

DOCTEUR de l'Université de Versailles

Mention "**Informatique**"

par

Amine Mohamed Adouane

Dynamic management of spectral resources in LTE networks

Soutenue le 16 Février 2015 devant la Commission d'Examen :

Directeur de Thèse :	
Samir Tohme, Professeur des universités	Université de Versailles Saint-Quentin-en-Yvelines
Co-encadrante :	
Kinda Khawam, Maitre de conférences	Université de Versailles Saint-Quentin-en-Yvelines
Rapporteurs :	
Stefano Secci, Maitre de conférences HDR	Université Pierre et Marie Curie
Bernard Cousin, Professeur des universités	IRISA Université de Rennes 1
Examinateurs :	
Steven Martin, Professeur des universités	LRI, Université Paris-Sud
Djamal Zeglache, Professeur	Telecom Sudparis
Invité :	
Samer Lahoud, Maitre de conférences,	IRISA, Université de Rennes 1.

To my parents

Remerciements

Ce manuscrit conclut trois ans de travail, je tiens en ces quelques lignes à exprimer ma reconnaissance envers tous ceux qui de prés ou de loin y ont contribué.

Je tiens à remercier en premier lieu Mr Samir Tohme, mon directeur de thèse pour m'avoir donné la chance de faire cette thèse, ainsi que pour son encouragement, son expérience, ses conseils et sa sympathie qui m'ont permis de mener à bien cette thèse.

Je tiens à exprimer mes plus vifs remerciements à Kinda Khawam qui fut pour moi une encadrante de thèse attentive et disponible malgré ses nombreuses charges. Sa compétence, sa rigueur scientifique et sa clairvoyance m'ont beaucoup appris. Ils ont été et resteront des moteurs de mon travail de chercheur.

J'exprime tous mes remerciements à l'ensemble des examinateurs : Djamal ZEGHLACHE, Paul MüHLETHALER et Steven MARTIN. Je remercie également Bernard COUSIN et Stefano SECCI qui ont accepté d'être les rapporteurs de cette thèse, et pour l'effort qu'ils ont fait pour lire mon manuscrit et l'intérêt qu'ils ont porté à mon travail. Je remercie aussi Samer LAHOUD d'avoir accepté d'être présent pour ma soutenance.

Ce travail a été réalisé au sein du laboratoire PRISM de l'Université de Versailles dans le cadre du projet SOAPS. Je tiens donc à remercier toutes les personnes que j'ai rencontrées et qui m'ont aidé et encouragé tout au long de cette thèse.

Mes remerciements iront également à tous les membres de ma famille. Je pense surtout à mes parents sans qui l'enfant que j'étais ne serait pas devenu l'homme que je suis. C'est avec émotion qu'à mon tour je leur dévoile le fruit de mes efforts. J'espère être à la hauteur de leur fierté. Une pensée profonde va directement vers mon père qui sans lui rien de cela n'aurait existé et à maman pour toute son aide au fil de ses années. Je remercie également mon oncle Seddiki Zakari pour ses conseils et orientations.

Sans oublier de remercier tous ceux qui ont participé de près ou de loin à l'accomplissement de cette thèse.

Table des matières

Summary

The exponential growth in the number of communications devices has set out new ambitious targets to meet the ever-increasing demand for user capacity in emerging wireless systems. However, the inherent impairments of communication channels in cellular systems pose constant challenges to meet the envisioned targets. High spectral reuse efficiency was adopted as a solution to higher data rates. Despite its benefits, high spectral reuse leads to increased interference over the network, which degrades performances of mobile users with bad channel quality. To face this added interference, OFDM (Orthogonal Frequency Division Multiplexing) is used for the new 4th generation wireless network. Thanks to its orthogonality OFDM eliminates the intra-cellular interference, but when the same resources are used in two adjacent cells, the inter-cell interference becomes severe. To get rid of the latter, several methods for Inter-Cell Interference Coordination (ICIC) have been proposed. ICIC allows coordinated radio resources management between multiple cells. The eNodeBs can share resource usage information and interference levels over the X2 interface through LTE-normalized messages. Non-cooperative game theory was largely applied where eNodeBs selfishly selects resource blocks (RBs) in order to minimize interference. In this thesis, we stress on ICIC for the downlink of a cellular OFDMA system in the context of the SOAPS (Spectrum Opportunistic Access in Public Safety) project. This project focuses on the improvement of frequency resource scheduling for Broadband Services provision by PMR (Private Mobile Radio) systems using LTE technologies. Hence, our first addresses the problem of downlink ICIC where the resource selection process is apprehended as a potential game for which we propose a fully decentralized algorithm based on replicator dynamics to attain the pure Nash equilibriums of the game. Extensive simulations assessed the good performances of the algorithm for low to medium load. Results are in adequacy with the project need and with the system latency constraints. Our second work is devoted to a more general solution for the ICIC problem not limited to narrow band systems (with limited number of RBs). It portrays the problem of downlink ICIC as a load balancing game. We adapt a stochastic version of a best-response dynamics algorithm to attain the pure Nash equilibriums of the modeled game. Each eNodeB strives to select a pool of favorable resources with low interference based on local knowledge only. Proof of convergence is provided, and the efficiency of the tailored algorithm is proven

through extensive simulations. However, in this first solution the userś position in the cell is not taken into account for ease of computation. The shortcoming of this first adaptation is treated in a second version where a greedy algorithm is used to achieve faster convergence times. The new simulation results show a significant improvement for both time convergence and system performance even for larger system bandwidth. Finally, the ICIC issue was treated through adequate power allocation on RBs. The power level selection process of RBs is apprehended as a sub-modular game and a semi distributed algorithm based on best response dynamics is proposed to attain the NEs of the modeled game, striking a good balance between system performance and power economy.

Résumé

La croissance exponentielle du nombre de dispositifs communicants et des services sans fil émergents fixe des objectifs toujours plus haut pour répondre à la demande de capacité sans cesse croissante des utilisateurs. Cependant, les déficiences inhérentes des canaux de communication dans les systèmes cellulaires posent des défis constants pour atteindre les objectifs envisagés. Pour pallier à ce problème le spectre fréquentiel est utilisé avec une forte efficacité (High efficiency spectral reuse) comme solution pour atteindre des débits plus élevés. Malgré ses avantages, la réutilisation spectrale élevée conduit à des interférences accrues sur le réseau, ce qui dégrade dáutant plus les performances des utilisateurs mobiles qui ont une mauvaise qualité de canal. Pour faire face à ces interférences, l'OFDM (Orthogonal Frequency Division Multiplexing) est utilisé dans les réseaux de 4 ème génération. Grace à son orthogonalité, l'OFDM élimine l'interférence intra-cellulaire, mais quand les mêmes ressources sont utilisées dans deux cellules adjacentes, l'interférence inter-cellule devient importante. Pour se débarrasser de ces interférences, plusieurs méthodes connues sous le nom d'Inter-Cell interferences coordination (ICIC) ont été proposées. L'ICIC permet la gestion des ressources radio coordonnée entre plusieurs cellules appelées eNodeB. Ces eNodeB peuvent partager des informations sur l'utilisation des ressources et les niveaux d'interférence grâce à l'interface X2 qui les relient, ces informations sont transmises par des messages LTE normalisée. Lorsque les eNodeBs sélectionnent égoïstement les ressources blocs (RBS) afin de minimiser les interférences, la théorie des jeux non-coopératifs est largement appliquée pour trouver un juste équilibre. Dans cette thése, nous mettons l'accent sur l'ICIC pour la liaison descendante d'un système OFDMA cellulaire dans le contexte du projet SOAPS (Spectrum Opportunistic Access in Public Safety). Ce projet a pour but l'amélioration de la planification des ressources de fréquences pour fournir des services à large bande dans les systèmes PMR (Private Mobile Radio) en utilisant les technologies LTE. Nous adressons en premier le problème d'ICIC sur le lien descendent où le processus de sélection des ressources est appréhendé comme un jeu potentiel, pour cela nous proposons un algorithme entièrement décentralisé basé sur la dynamique de réplication pour atteindre les équilibres de Nash purs du jeu. Des simulations approfondies ont permis d'évalué les bonnes performances de l'algorithme à faible et à moyenne charge. Les résultats ainsi obtenus sont en adéquation avec les besoins du projet et avec

les contraintes de latence du systéme. Notre deuxième travail est consacré a une solution plus générale au problème d'ICIC, ne se limitant pas aux systèmes à bande étroite (avec un nombre limité de RBs). Le problème d'ICIC est décrit comme un jeu d'équilibrage de charge (Load Balancing). Nous adaptons une version stochastique d'un algorithme dynamique de best-response pour atteindre l'équilibre de Nash pur du jeu modélisé. Chaque eNodeB s'efforce de sélectionner un pool de ressources favorables à faible interférence sur la base des connaissances locales du système seulement. La preuve de convergence de cet algorithme est apportée, et son efficacité est prouvée par de nombreuses simulations. Cependant, la position de l'utilisateur dans la cellule dans cette première solution n'est pas prise en compte pour la facilité du calcul. La faiblesse de cette première adaptation est traitée dans une seconde version où un algorithme glouton est utilisé pour obtenir des temps de convergence plus rapide. Les nouveaux résultats de simulation montrent une amélioration significative à la fois en temps de convergence, et en termes de performances du système, même pour des systèmes à plus grande bande passante. Enfin, le problème d'ICIC a été traité comme un problème d'allocation adéquate en puissance sur les RBs. Le processus de sélection du niveau de puissance pour les RBS est appréhendé comme un jeu sous-modulaire, ainsi, un algorithme semi distribué basé sur la dynamique de best-response est proposé pour atteindre l'équilibre de Nash du jeu modélisé, un bon équilibre entre les performances du système et l'économie d'énergie devant etre trouvé.

List of Publications

IEEE ISCC 2014, Replicator Dynamics for Distributed Inter-Cell Interference Coordination, Amine Adouane, Kinda Khawam, Johanne Cohen, Dana Marinca, Samir Tohmes, University of Versailles PRISM Laboratory, University of Paris Sud LRI lab.

IEEE European Wireless 2014, Distributed Load Balancing Game for Inter-Cell Interference Coordination, Amine Adouane, Lise Rodier, Kinda Khawam, Johanne Cohen, Samir Tohme, University of Versailles PRISM Laboratory, University of Paris Sud LRI lab.

IEEE WCNC 2014, Game Theoretic Framework for InterCell Interference Coordination, Amine Adouane, Lise Rodier, Kinda Khawam, Johanne Cohen, Samir Tohme, University of Versailles PRISM Laboratory, University of Paris Sud LRI lab.

IEEE IFIP Networking 2014, Game Theoretic Framework for Power control in InterCell Interference Coordination, Kinda Khawam, Amine Adouane, Samer Lahoud, Johanne Cohen, Samir Tohme, University of Versailles PRISM Laboratory, University of Paris Sud LRI lab.

Table des figures

List of Abbreviations

3GPP	Third Generation Partnership Project
ABSF	Almost Blank Sub-Frame
BBU	Base Band Unit
CN	Core Network
CoMP	Cooperative Multi-Point
CP	Cyclic Prefix
CQI	Channel State Indicator
CSB	Cell Selection Bias
CSI	Channel State Information
DCCH	Dedicated Control Channel
EPC	Evolved Packet network
FDD	Frequency Division Multiplexing
FFR	Fractional Frequency Reuse
FRF	Frequency Reuse Factor
ICI	Inter-Cell Interference
ICIC	Inter-Cell Interference Coordination
i.i.d.	independent and identically distributed
IMT	International Mobile Telecommunications
IP	Internet Protocol
ISI	Inter Symbol Interference
ITU-R	International Telecommunication Union-Radiocommunication
LTE	Long Term Evolution

MIMO	Multiple Input, Multiple Output
MILP	Mixed Integer linear Problem
MME	Mobile Management Entity
ODE	Ordinary Differential Equations
OFDMA	Orthogonal Frequency Division Multiple Access
OI	Overload Indicator
PAPR	Peak to Average Power Ratio
PDSCH	Physical Downlink Shared Channel
PER	Paquet Error Rate
PFR	Partial Frequency Reuse
PMI	Precoding Matrix indicator
PMR	Private Mobile Radio
PNE	Pure Nash Equilibrium
PUCCH	Physical Uplink Control Channel
PUSCH	Physical Uplink Shared Channel
QAM	Quadrature Amplitude Modulation
QPSK	Quadrature Phase-Shift Keying
RAN	Radio Access Network
RB	Resource Block
RE	Resource Elements
RI	Rank Indicator
RNC	Radio Network Coordinator
RNTP	Relative Narrowband Transmit Power
RRH	Radio Remote Head
RRM	Radio Resource Management
RS	Reference Signal
RSRP	Reference Signal Received Power
RSRQ	Reference Signal Received Quality
RSSI	Received Strength Signal Indicator
SC-FDMA	Single Carrier FDMA
SFFR	Soft FFR
SFR	Soft Frequency Reuse
S-GW	Serving Gateway
SINR	Signal to Interference-plus-Noise Ratio

SOAPS	Spectrum Opportunistic Access in Public Safety
TDD	Time Division Multiplexing
TTI	Transmit Time Interval
UE	User Equipement
WIMAX	Worldwide Interoperability for Microwave Access
ZFBF-SUS	Zero Forcing BeamForming with Semi-orthogonal User Selection

Chapitre 1

Introduction

The 21^{st} century is the century of communication that has set out new ambitious targets to meet the ever-increasing demand for UE (User Equipment) capacity in emerging wireless systems. However, the physical channel of cellular networks has many constraints, and meeting the requested target is very hard. In order to overcome the bounded capacity of such networks, there is a crucial need for higher spectral efficiency. Unfortunately, this comes at the cost of increased interference level, which renders the expected solutions even more challenging. Thanks to its various merits, Orthogonal Frequency Division Multiplexing (OFDM) has been adopted as the key physical layer technique in 4G wireless system. Hence, to face the challenges ahead, the OFDM technology represents a key asset for intra-cell interference mitigation owing to its orthogonality feature. Yet, for Inter-Cell Interference (ICI), and in particular for dense frequency reuse, high interference on the cell border can be encountered. Remedy to this ICI is paramount and can be treated with efficient inter-cell interference coordination (ICIC) techniques which are the object of this thesis. This chapter recaptures some key components of ICIC and highlights some of the most relevant previous work. The plan of the thesis is given at the end of the chapter.

1.1 Introduction

The frequency reuse-1 is advocated by the Third Generation Partnership Project (3GPP) [Pro06] for the LTE/LTE-Advanced networks. This allows to use the same resources all over the network cells, taking benefits from the OFDM special features. OFDM has been chosen as the 4G physical access due to its resistance to the Inter-Symbol Interference (ISI), frequency selective fading, and to its high spectral efficiency. These benefits stem from the orthogonality of sub-carriers composing the system frequency band, which allows to virtually eliminate the intra-cell interference. Unfortunately, the UEs suffering from poor channel quality will be exposed to ICI, and experience low throughput. Therefore, a

lot of effort is being deployed to hinder ICI, the corresponding devised schemes are known as Inter-Cell Interference Coordination (ICIC) techniques [DSZ12]. The main goal of ICIC is to decrease the interference in order to provide better throughput for UEs suffering from bad channel quality. We begin by reminding the reader of the main characteristics of LTE then detail the various ICIC techniques used in the literature.

1.2 The LTE network

The long term evolution LTE was proposed as a solution to reduce data transfer time in the cellular network, it was standardized in December 2008 and the first LTE service was launched by TeliaSonera in Oslo and Stockholm on December 14, 2009 as a data connection with a USB modem. The LTE main features are :

- Peak download rates up to 299.6 Mbit/s and upload rates up to 75.4 Mbit/s depending on the UE category (with 4x4 antennas using 20 MHz of spectrum). Five different terminal classes have been defined from a voice centric class up to a high end terminal class that supports the highest peak data rates. All terminals will be able to process 20 MHz bandwidth.
- Low data transfer latency (sub-5 ms latency for small IP packets in optimal conditions), lower latency for handover and connection setup time than with previous radio access technologies.
- Improved support for mobility, exemplified by support for terminals moving at up to 350 km/h or 500 km/h depending on the frequency band.
- OFDMA (Orthogonal Frequency Division Multiple Access) for the downlink and SC-FDMA (Single-Carrier FDMA) for the uplink to preserve power.
- Support for both Frequency and Time Division Duplexing FDD and TDD communication systems as well as half-duplex FDD with the same radio access technology.
- Support for all frequency bands currently used by IMT (International Mobile Telecommunications) systems by ITU-R (International Telecommunication Union-Radiocommunication).
- Increased spectrum flexibility : 1.4 MHz, 3 MHz, 5 MHz, 10 MHz, 15 MHz and 20 MHz wide cells are standardized.
- Support for cell sizes from tens of meters radius (femto and picocells) up to 100 km radius (macro-cells).
- Supports of at least 200 active data clients in every 5 MHz cell.
- Simplified architecture : The network side of E-UTRAN is composed only of intelligent eNodeBs
- Support for inter-operation and co-existence with legacy standards (e.g., GSM/EDGE, UMTS and CDMA2000).
- Packet switched radio interface.

1.2.1 The LTE architecture

The goal of LTE is to increase the capacity and speed of wireless data networks, it was then designed for full packet services ; it provides IP connection between the UE and the network. Like the other cellular networks, the LTE network is formed by a wired Core Network (CN) called Evolved Packet Core (EPC), and a wireless part called Evolved-UTRAN (E-UTRAN), as we can see in Figure 1.1 [Cha13].

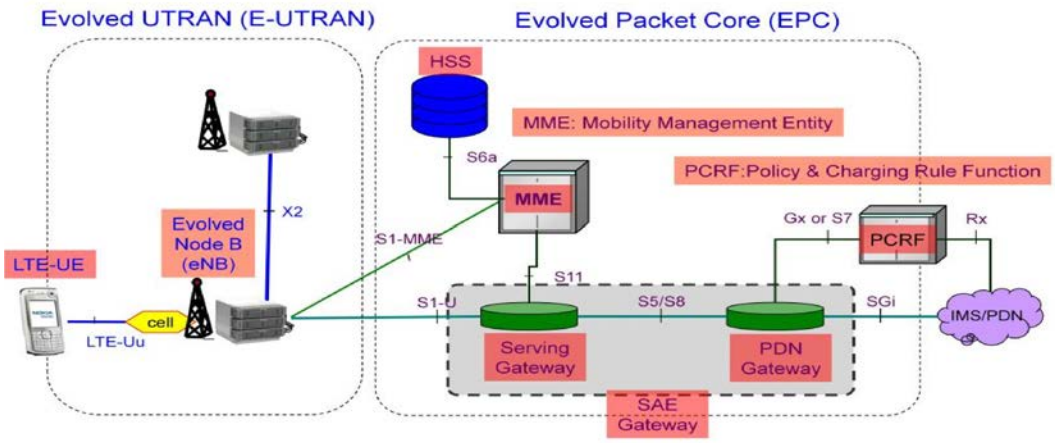

FIGURE 1.1: LTE Global Architecture

We are only concerned in this thesis with the access network detailed below in subsection 1.2.2.

1.2.2 The access network E-UTRAN

The access network of LTE is called E-UTRAN, it consists of a batch of eNodeBs with no centralized controller ; the E-UTRAN architecture is said to be flat as shown in Figure 1.2.

The eNodeBs are interconnected with each others over the X2 interfaces, each eNodeB is connected with the MME (Mobility Management Entity) via the S1-MME interface and with the S-GW (Serving Gateway) via the S1-U interface. In the E-UTRAN, the eNodeB are the intelligent entity responsible of all the radio functions. Integrating the radio controller functions into the eNodeB is one of the major upgrades of the LTE architecture by virtue of which the system latency is reduced and efficiency increased.

The eNodeB functions can be summarized as follows :

– Radio Resource Management : it includes scheduling and dynamic allocation of resources to UEs in both uplink and downlink, radio bearer control, radio mobility control and radio admission control.

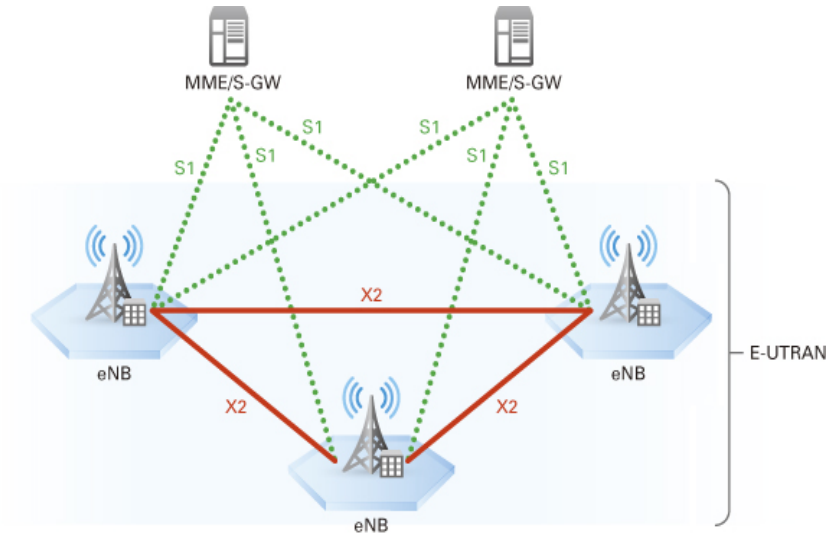

FIGURE 1.2: LTE E-UTRAN architecture

– Header Compression : it consists of compressing the IP packet headers in order to get a better resource usage.
– Security : encryption of the data sent over the air.
– Positioning : help the E-SMLC (Evolved Serving Mobile Location Center) to position the UE by sending relevant measurement.
– Connectivity to the EPC : providing the signaling towards the MME and the bearer path towards the S-GW.

1.2.3 LTE frame structures

As it was done for the previous releases of cellular networks, the 3gpp has standardized the frame structure of the wireless access network. The LTE frame is differently conceived depending on the chosen division duplex : it is called Type 1 frame for the LTE FDD (frequency division duplex mode) systems and Type 2 frame for the LTE TDD (time division duplex) systems.

1.2.3.1 Type 1 LTE frame structure

The Type 1 LTE frame has a length of 10 ms, it is divided into 20 individual slots as shown in Figure 1.3. Each frame slot has a duration of 0.5 ms, in this case a slot represents exactly a Resource Block (RB), which is the smallest radio resource we can allocate to a UE [Com09].

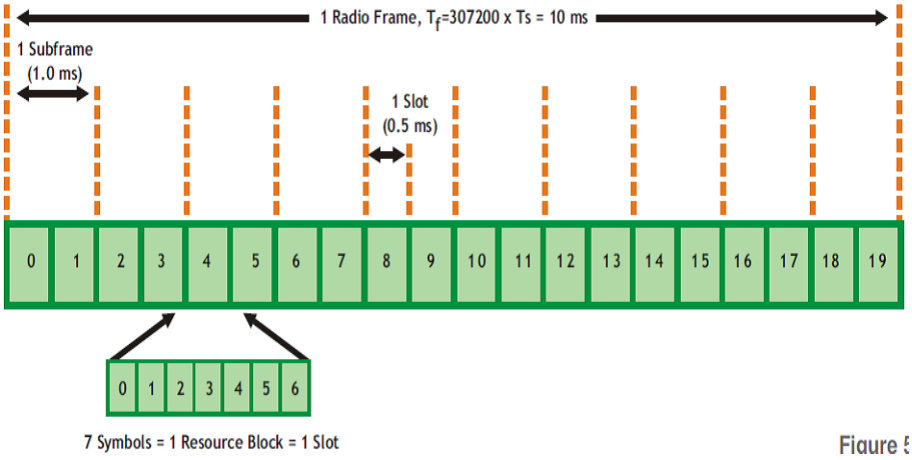

FIGURE 1.3: LTE Type-1 frame structure

1.2.3.2 Type 2 LTE frame structure

The Type 2 frame is composed of 2 half frames of 5 ms as shown in Figure 1.4 ; each half frame is divided into five sub-frames of 1ms each. According to the switch time, at least one of the half frames contains three fields :

– DwPTS - Downlink Pilot Time Slot
– GP - Guard Period
– UpPTS - Uplink Pilot Time Slot.

When the switch time is 10 ms, only the first half frame will carry this field ; whereas if the switch time is 5ms, both half frames are used [Com09].

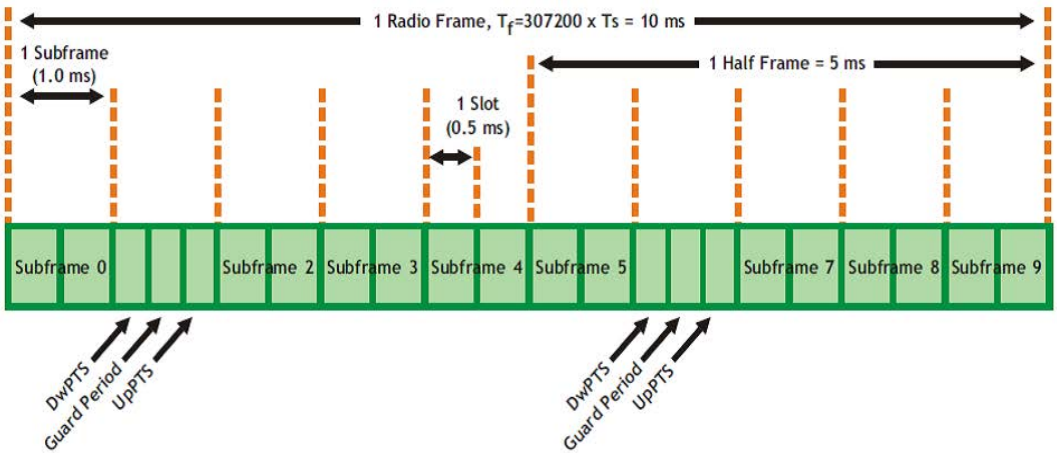

FIGURE 1.4: LTE Type-2 frame structure

1.2.3.3 Resource Block RB

A Physical Resource Block (PRB) is composed of six or seven symbols by twelve subcarriers as displayed in Figure 1.5 [Com09], it is represented by a table of 6 or 7 rows and 12 lines, each cell of the table is called a resource element and consist in a subcarrier of 15 kHz for one symbol. This gives the RB a frequency band of 180 KHz. The number of symbols is determined by the Cyclic Prefix (CP), if a normal CP is used the RB will have seven symbols, if an extended CP is used it is composed of six symbols.

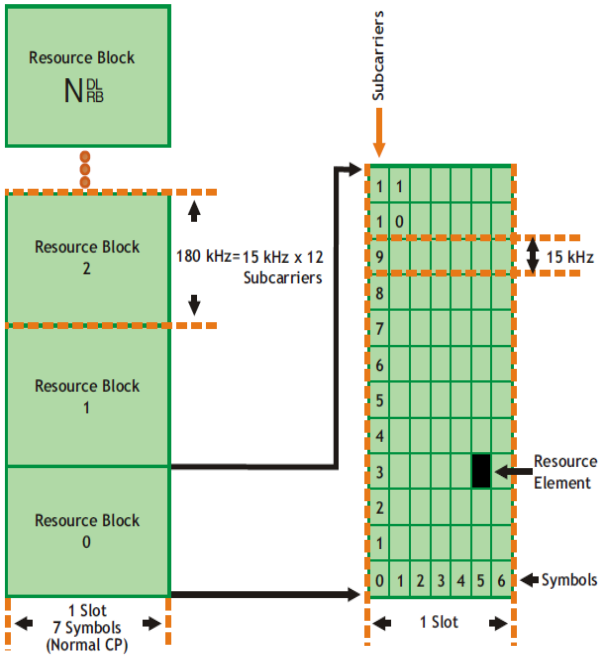

FIGURE 1.5: LTE RB composition

1.2.4 The X2 Interface

The X2 interface is used to interconnect the eNodeBs in order to exchange signaling information when needed for load or interference management and for handover information. We will focus on the load and interference messages since they are intimately related to our work.

1.2.4.1 Load and interference management Over X2

Since there is no central entity for Radio Resource Management (RRM) in the E-UTRAN, the exchange of load and interference messages is essential among eNodeBs through the so-called X2 interface. The physical characteristics of the X2 interface brings some latency

to the system, this latency imposes a message periodicity of approximately 200 ms. In the following, we explain some of the important messages exchanged over the X2 link.

1.2.4.2 Relative Narrowband Transmit Power message RNTP

The eNodeB sends this message on the downlink in order to inform the neighboring eNodeBs about its power use on each RB. This message contains information relative to a power threshold, when exceeded, the other eNodeBs should avoid using the corresponding RB. The RNTP message is defined as follows [3gp12] :

$$RNTP = \begin{cases} 1 & \text{if used power is greater than a given threshold,} \\ 0 & \text{otherwise.} \end{cases} \tag{1.2.1}$$

1.2.4.3 High Interference Indicator HII

It indicates the PRB interference sensibility on the uplink, this allows the eNodeB to warn other eNodeBs about the RB allocated with high power transmission ; in that case, the neighboring eNodeBs will avoid allocating these resources to the mobile UEs with bad channel quality [3gp11a].

1.2.4.4 the Overload Indicator OI

The eNodeB sends information about the received interference to the adjacent eNodeBs through the overload indicator message. Receiving an OI allows the eNodeB to manage the resource scheduling to lower the interference received by mobile UEs with bad channel quality [3gp11a].

1.2.5 The LTE Uu interface

This interface links the UE to the access network (the eNodeBs). In addition to carrying the UEs data, the LTE-Uu interface allows the exchange of signaling messages between the UE and the eNodeBs, some of these messages can be used to manage the interference in the network. The UE sends to the eNodeB a CSI (Channel State Information) which consists of channel quality indicator (CQI), precoding matrix indicator (PMI) and rank indication (RI). Since in this thesis we consider only single antenna transmissions, the PMI and RI messages are not considered. Hence, the most relevant message sent through this interface for our work is the CQI (Chanel Quality Indicator) which has significant impact on the system performance. It is sent by the UE to indicate to its serving antenna the channel quality it perceives. In fact, downlink channel dependent scheduling in LTE requires specific information to be sent by the terminals to the network. Such information

is transmitted through channel state reports that contain CQI feedback. CQI represents the highest modulation and coding scheme that guarantee a block error rate less than 10% for physical downlink shared channel transmissions. There are two types of channel state reports in LTE : periodic and aperiodic. The periodic CQI report is sent over the PUCCH (Physical Uplink Control Channel) if no data is sent over the uplink, or in the PUSCH (Physical Uplink Shared Channel) piggybacked with UE data in the same subframe, in this case, the periodic PUCCH resource will be idle. The minimum periodicity could be 2 ms. If the eNodeB needs more detailed CQI report, it can trigger an aperiodic CQI sent over the PUSCH together with UL data or alone [3gp12]. Three levels of CQI report granularity can be enumerated : wideband, UE selected subband, and higher layer configured subband. The wideband report is responsible of the CQI information for the whole system bandwidth. The UE selected CQI report provide wideband CQI information along with differential CQI value, this CQI value indicates the report for multiple subband (the best M subbands perceived by the UE). The highest layer configured subband is the most detailed report, it provides wideband CQI value and multiple differential CQI for all the subbands. The higher the CQI value (from 0 to 15) reported by UE, the higher the modulation scheme (from QPSK to 64QAM) and higher the coding rate will be used by eNodeB to achieve higher efficiency. Having information on UE channel quality, the eNodeBs can give low interfered RBs to UEs with bad channel quality for acceptable performances. On the contrary, the eNodeB can reserve low interfered RBs to UEs with good channel quality to enhance system performances.

1.3 Inter-Cell Interference Coordination ICIC

In 4G networks, OFDM is used for the radio access as it allows increased spectral efficiency while mitigating the intra-cell interference owing to its orthogonality feature. However, for the inter-cell interference, when the frequency reuse one is deployed, close neighboring UEs with same frequency will suffer from bad channel quality as highlighted by Figure 1.6. Inter-Cell Interference Coordination (ICIC) has proved to be one of the best solutions to overcome this problem and has been adopted as a resource management mechanism to enhance system performance. One of the first proposed solutions was the Fractional Frequency Reuse (FFR) which manages statically the frequency resource distribution within each cell in order to decrease the inter-cell interference [Ass08]. Instead of using all the available RBs in adjacent cells, FFR gives them disjoint spectrum for their edge zones (UEs at the cell periphery, usually suffering from bad channel quality). Hence, frequency reuse 3 model is used for edge zones, and frequency reuse 1 for the cell center zone (UEs close to the serving antenna, usually enjoying good channel quality). The ICI can also be mitigated through power control on the allocated RBs. A good example is the well-known Soft Frequency Reuse (SFR) [MMT08] which allocates lower power for cell-center

RBs while cell-edge RBs get higher transmission power. Hence, interference mitigation is achieved by either transmit power control [JL03] or by radio resource allocation schemes [SAR09]. ICIC can also by a joint (complex) resource allocation and power adaptation problem. Hence, FFR technique imposes restrictions on RB usage within each cell, while SFR modifies both RB allocation and downlink power allocation. However, both schemes are static schemes that fail to cope with a variable traffic.

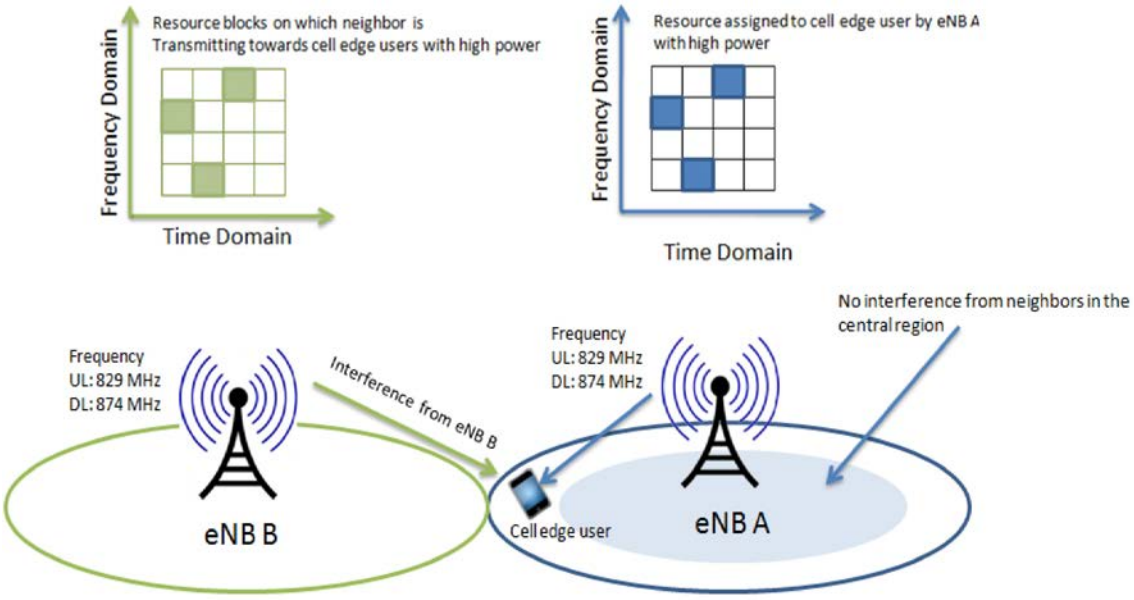

FIGURE 1.6: Inter-cell interference

In order to manage the inter-cell interference, different methods are used as shown in Figure 1.7. They are divided into 2 main categories : *Frequency Reuse-based schemes* and *Cell Coordination-based schemes.*

– The Frequency Reuse-based schemes are static methods characterized by the frequency reuse factor (FRF) which is the rate at which the same frequency can be used in the network. We can divide the frequency reused based schemes into :
  1. The conventional frequency reuse which encompasses the frequency reuse 1 and 3,
  2. The fractional frequency reuse (FFR) where we find the known Partial Frequency Reuse (PFR), Soft Frequency Reuse (SFR), and Soft Fractional Frequency Reuse (SFFR) among others.
– The Cell Coordination-based schemes are dynamic methods that include :
  1. Centralized methods where a central entity takes decisions on behalf of a group of eNodeBs using CoMP (Coordinated Multi-Point) [3GP11b], along with enhanced-ICIC (e-ICIC) transmissions in LTE-A (LTE Advanced). This approach is optimal but suffers from high complexity and long delays. Therefore, it is not suited for quick network management.

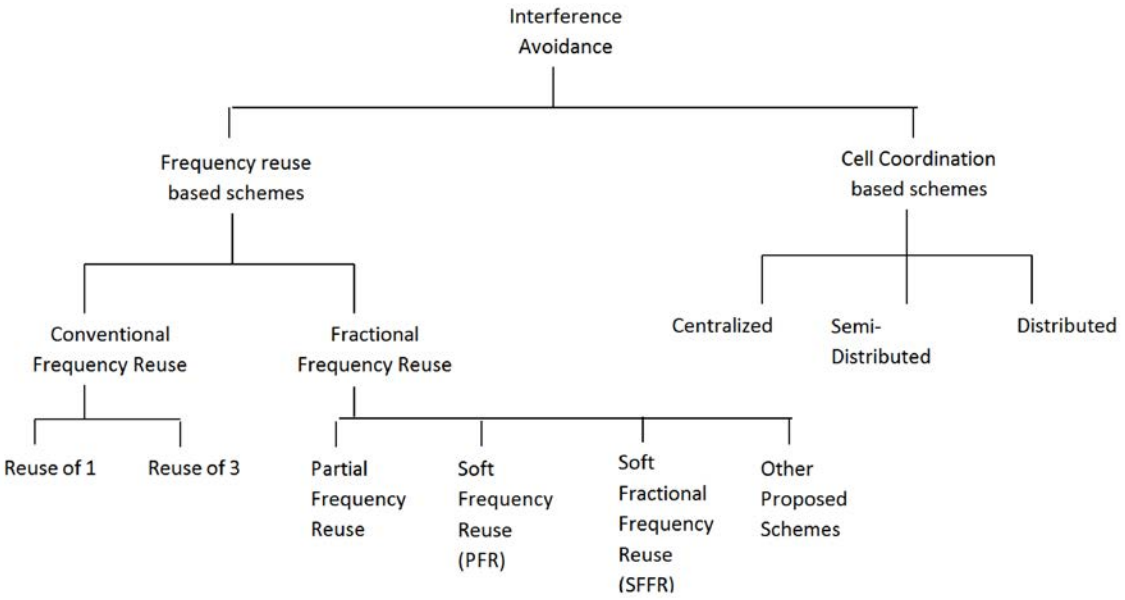

FIGURE 1.7: Interference Mitigation Classification

2. Semi-distributed networks where the different eNodeBs are the decision makers; however, their decisions are made by a central entity or aided by exchanged signaling information among them. Hence, radio resource allocation, power allocation, or both, are made using information sent over the X2 interface.
3. Distributed scheme are characterized by complete absence of cooperation among eNodeBs. Hence, each eNodeB takes its decisions without relying on any assistance or on any external signaling messages.

In the following section we will explain in more details all the methods just enumerated.

1.3.1 Frequency reuse based schemes

The main goal of the interference avoidance schemes is to control the allocation of radio resources (frequency, time and power) in order to obtain higher SINRs (Signal to Interference and Noise Ratio) and reduce interference between adjacent eNodeBs.

1.3.1.1 Conventional frequency reuse

The LTE network is configured by default to be deployed with a Frequency Reuse Factor (FRF) of 1. In this configuration, the whole frequency band is available in the entire cell coverage area as shown in Figure 1.8. As already said, owing to the orthogonality feature of OFDM, the intra-cell interference is mostly mitigated and can be ignored. However, inter-cell interference is still problematic and UEs with bad channel quality can endure high interference from adjacent cells.

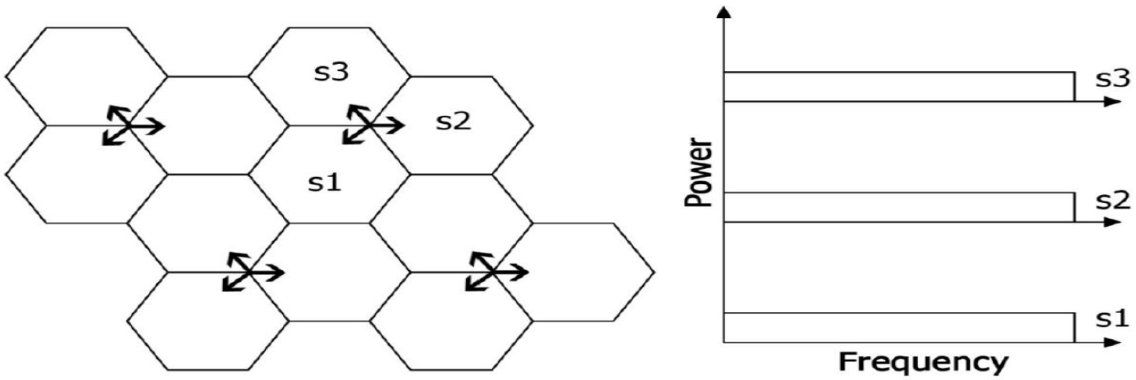

FIGURE 1.8: Frequency reuse 1 scheme

In order to face this problem, an easy solution is to adopt the FRF of 3. It consists in dividing the entire frequency band into 3 parts, attributing each part to a cell in a way to avoid using the same frequencies in any two adjacent cells as we see in Figure 1.9. This method leads to a better SINR in the system and improves inter-cell interference, but since the frequency band is divided by 3, the channel capacity decreases. This problem becomes even more relevant when the system is loaded.

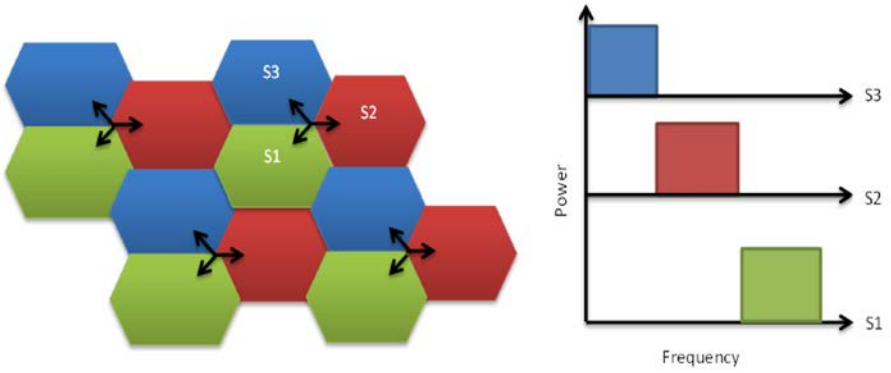

FIGURE 1.9: Frequency reuse 3 scheme

1.3.1.2 Fractional Frequency Reuse (FFR)

With the aim of improving the shortcomings of the FRF 3 scheme, the Fractional Frequency Reuse FFR was developed. The main idea is to divide the cell into two geographical areas, the area close to the eNodeB (with cell center UEs) and the area far away from the eNodeB (with cell edge UEs). Each area will get a part of the frequency band : the cell-edge UEs will get a fraction of the resources that are different from those of neighboring cell edge UEs, while the rest of the frequency band will be allocated to the cell center UEs (protected from adjacent interference by the edge area).

Many derivative schemes from the FFR have been proposed, here are some of them :

1.3.1.2.1 Partial Frequency Reuse (PFR) FFR with full isolation (FFR-FI)

In the PFR scheme, the part of the spectrum allocated to the cell-edge UEs is divided into three fractions as depicted in Figure 1.10. This results in an under-utilization of the radio resource as some frequencies are not used in some sectors at all [KM11].

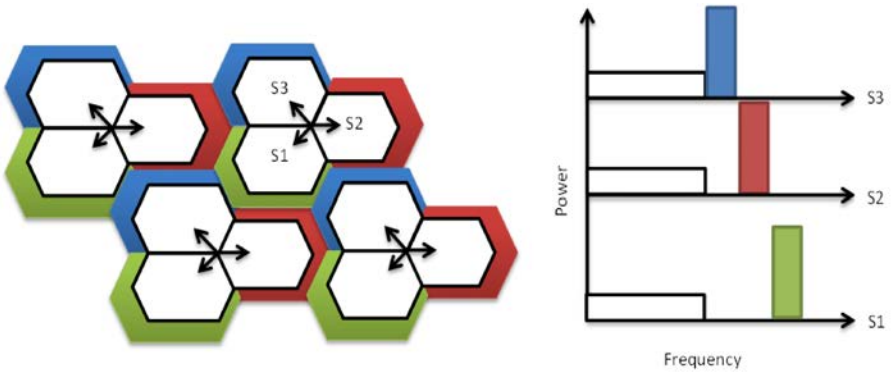

FIGURE 1.10: Partial Frequency Reuse Scheme

1.3.1.2.2 Soft Frequency Reuse (SFR)

In order to overcome the deficiency of the PFR scheme, the SFR scheme was proposed in [EE13] to provide some flexibility to the latter. In the SFR scheme, the available bandwidth is divided into orthogonal segments, and each neighboring cell is assigned a cell-edge band with a higher power allocation, as shown in Figure 1.11 ; while the cell-center UEs can still have access to the cell-edge bands selected by neighboring cells, but at a reduced power level. In this way, each cell can utilize the entire bandwidth while reducing interference caused to the neighboring cells. As a consequence, a lower ICI is achieved at cell-edges at the expense of reduced spectrum utilization.

1.3.2 Cell coordination based schemes

Unlike the frequency reuse schemes, the cell coordination schemes are dynamic and hence able to adapt the resource allocation to the actual network state and traffic load at the cost of increased complexity. The cell coordination schemes can be classified into three main categories according to their operation mode.

1.3.2.1 Centralized schemes

The LTE architecture is characterized by the absence of a central entity that coordinates base stations (such as the BSC Base Station Controller) and the RNC (Radio Network

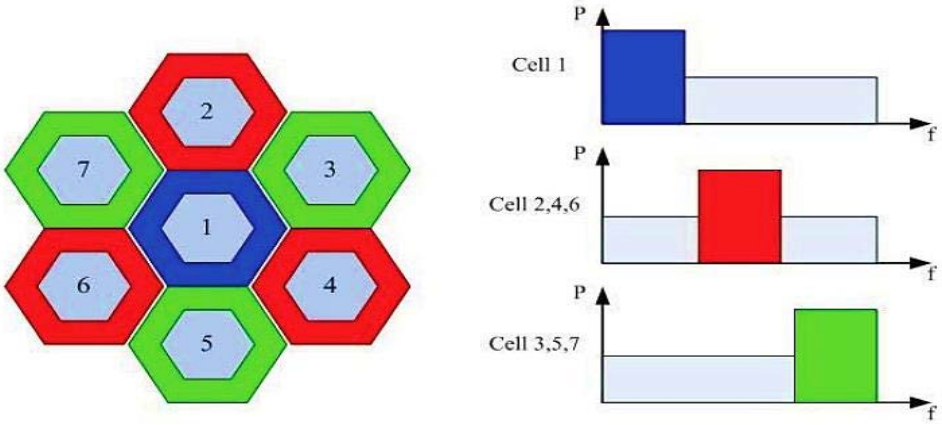

FIGURE 1.11: Soft Frequency Reuse scheme

Controller) as in 2G and 3G networks. A novel architecture based on the cloud is introduced in [HDDM13] under the name Cloud-Radio Access Network (C-RAN), it allows the coordination and management of the eNodeB over the cloud. This new solution allows the connection of several aloof Radio Remote Heads (RRH) and Base Band Unit (BBU) to a central point over the cloud. In the LTE-A [3GP08], a Coordinated Multi-Point (CoMP) transmission and reception [3GP11b] is introduced, along with enhanced-ICIC (e-ICIC) which brings a solution to the RB selection for the layered network (macro, small, pico and femto cells). It also introduces the Almost Blank Subframe (ABSF) allowing time sharing of resources between different cells [DMMS14].

Cooperative ICIC techniques benefit from the communication between network entities to coordinate RBs distribution in a way to reduce ICI and improve system performance. However, the cooperation between different base stations increases computational complexity and generates an additional signaling load. More importantly, the resource management issue may be related to a complex optimization problem where many constraints are handled (interference level, SINR, ...). This problem can be seen as a multi-dimensional allocation problem with resource restriction to mitigate the interference and it is proven to be NP-HARD [RLLS98]. The issue of the NP-HARD complexity can be faced using binary/integer linear programming [LCK08, RY07]. Nonetheless, the linearized problems remain highly complex [LPJZ09].

In particular, in [NSV+14], the authors put forward a centralized ICIC management method applied to a LTE-A network, where a layered solution divides the network into groups of few cells. This step is called "Small-scale" coordination where the goal is to optimize the total throughput, and then coordinate the optimized group to reach a better system performance by lowering the interference. The authors showed that this problem is NP-HARD complex and used a mixed-integer-linear problem (MILP) to bypass it. In [ENJA08], the

interference problem in OFDMA based network (WIMAX) is addressed where a mathematical model was proposed to mitigate the interference level. This is done by finding the best routing and assigning slots to the end connection, the effect of the hidden terminal and neighboring interference was considered. In [AADM07], the benefit of a centralized schemes over distributed ones is highlighted, and an optimal resource allocation is proposed with hard complexity. The proposed centralized scheme considers the constraints of transmission quality and throughput while minimizing transmission power. In [BZGA10], a solution for CoMP transmissions is proposed using the Medium Access Control (MAC) scheduling in the LTE-A network. Each UE is served jointly by several cells that form clusters, and each cluster is managed by its own central entity. These central entities are aware of all the Channel State Information (CSI), Channel Quality Indicator (CQI), Precoding Matrix Index (PMI) and Ranking Indicator (RI) of UEs served by their cluster. The resource allocation for each cluster is done according to these messages. In [WWS$^+$], the problem of multi-layer network with macro and femto cells is treated. A dynamic centralized approach was proposed whose goal is to increase the forward link performance for best effort and real time transmission in the femto cell network. The system is divided into clusters, then a comprehensive research for optimal allocation between femto cells of the same cluster is done. Finally, a conventional static scheme is applied (SFR, PFR, ...) at the femto cell layer in order to reduce the radio Packet Error Rate PER. In [SSC11], the downlink resource allocation problem is studied where the proposed solution comes into two levels. The solution for the first level (the main level) is done using projected-subgradient method. At the second level, minimum-cost network flow optimization was used to solve each sub-problem. The authors showed through simulations that the obtained results are comparable to those with frequency reuse 3 scheme for cell edge UEs.

1.3.2.2 Semi-distributed schemes

As already mentioned, in semi-distributed schemes there is not a classic central entity that controls LTE base stations ; however, neighboring eNodeBs are connected via the X2 interface through which they can exchange information relative to their load and interference level. In such an approach, the intelligence of the network is dispatched on many components as part of the decision is taken by the eNodeBs themselves. A central entity can be responsible of giving the eNodeB the global framework of the allocation. This approach allows working on different time scales, for example the central entity can give a pool of resources to each eNodeB, and then the distributed algorithm on each eNodeB will manage the allocation of these resources to their UEs.

In [SMB$^+$14], a semi-distributed method has been used to overcome the ICI problem by minimizing the total time needed by an eNodeB to send data over the network. An algorithm was proposed based on the LTE-A new message (Almost Blank Sub-Frame) ABSF,

which allows a sub-frame to be empty (Blank) for some eNodeBs, in order to avoid using these sub-frames when the interference override a threshold. In [SEH14], the authors addressed the problem of interference with a new Location Aware multicellular Cooperation (LAC) scheme where they combined two existing methods. The first method is a joint zero-forcing beamforming with semi-orthogonal UE selection (ZFBF-SUS) transmission, and the second method is a semi-distributed power allocation optimization. They used CoMP transmission to serve the UEs with bad SINR, while the other UEs are served using multiuser MIMO. A two steps algorithm is used : a distributed resource allocation is done on each eNodeB for the non-CoMP UEs, and then a central entity serves the CoMP UEs. In [MMT08], the uplink resource allocation is tackled through a semi-decentralized dynamic soft frequency reuse scheme. The proposal tends to overcome the problem of throughput harvesting for the cell edge UEs with the respect of RBs reuse minimization via the use of a per frequency sub-band indicator sent over the X2 link to neighboring cells. Hence, when a cell faces a need of supplementary RBs for cell edge UEs, it will send a message over the X2 link to loan the requested RBs from adjacent cells. The coexistence of macro and small cells is becoming a relevant problem with the growing demand for capacity, which induces an important traffic load on the system and co-channel interference. For instance, in [LLK+11], the authors introduced the time domain ICIC using the ABS for heterogeneous networks. A cooperative system was used to overcome the interference caused by the small cells .

1.3.2.3 Distributed schemes

In the case of decentralized ICIC, the eNodeBs optimize their local parameters without the help of central controllers or signaling exchange among peers. Decentralized ICIC can react to relatively fast change of situation but it is difficult to avoid converging to local optimums. The non-cooperative game theory is quite suitable to model the way eNodeBs compete in a distributed manner for limited resources. The goal is to maximize a utility function to match the best resource allocation for each cell. Planning a game theoretical RBs selection scheme depends on the existence of Nash equilibriums for the modeled game, where no player will take advantage from moving unilaterally from the attained equilibrium.

In [MPS07], each UE tries to maximize the utility function which can be the transmit power, carrier allocation strategy, transmission rate or modulation. A Nash equilibrium is proved to be reached for this power control game. In [EHB08], a decentralized scheduling algorithm is proposed aiming at lowering the interference with a local knowledge of the system. Each eNodeB chooses a pool of low interfered resources, and then a fast allocation algorithm will schedule them for active UEs. A Nash equilibrium is proven to be attained. In [EASH09], the authors show that a decentralized game theoretical approach, where a

Nash equilibrium is reached, gives better system performances, especially for non-uniform traffic load compared to the frequency reuse 1 and 3 deployments.

In [MDV13], a distributed cognitive interference alignment method is proposed to address the interference problem. Using only autonomous operations and local Channel State Information (CSI), they optimized the spectral efficiency by means of a distributed one-shot strategy. In [DMMS14], the author addressed the problem of interference with a decentralized eICIC algorithm. They used Almost Blank Sub-frame (ABSF) and Cell Selection Bias (CSB) to manage the interference between macro and pico cells. The algorithm was implemented in a real network in New York city and showed promising results on the deployed LTE network. In [PWSF13], the use of eICIC in a decentralized manner is also discussed ; the problem of mixed deployment of macro and small cells is addressed using eICIC and ABSF. Further, benefits of time domain resource sharing over network layers are outlined.

To avoid converging to local optimum, many works rely on non-cooperative game theory, it appears to be suitable to model the competition between eNodeBs for the scarce radio resources. In [AKG11], the interference problem in cognitive radio is portrayed as a non-cooperative game to allocate resource in a distributed fashion while overcoming the problem of co-channel interference. The goal is to provide autonomous behavior with dynamic resource allocation inside the femto cell component of the network. In [KZM12], the uplink resource allocation in a cognitive network is tackled where a price based mechanism is used to manage the interference among femto cells. A Stackelberg game is used to address the sharing of resources between the macro and femto cells, with the macro cell acting as the master and the femto cells as the followers. In [LYW+11], the ICI problem in a LTE-A network is tackled using an evolutionary potential game, a jointly optimization of resource allocation and power control is treated as a cross-layer ICIC framework. The author used a Lagrangian multiplier method to optimize the constraints of the system, then a potential game is introduced to allocate the RBs and tune their power to increase the throughput. Simulation results highlighted the benefits of such a solution. Another game to overcome co-channel interference in a heterogeneous macro/femto cells network is presented in [ZCM+12]. A weighted technique is used, where the impact of the interference of each allocation is given a price. Simulation results show that the proposed scheme strikes a good balance between fairness and efficiency of resource allocation among both macro and femto cells.

1.4 Downlink Power Control in LTE

In LTE networks, power allocation is a sensitive parameter as it has a significant impact on system interference, and hence on the achieved data throughput. The physical layer uses a

special signal named Reference Signal (RS) that allows the UE to figure out the downlink cell power. Two types of RS exist, the cell specific RS which is sent all over the bandwidth and for all the sub-frames, and the UE specific RS which is sent over the dedicated UE RB. The RS is sent on the downlink transmission every 6 subframe for the Frequency domain, and every 4 OFDMA symbols for the time domain as shown in Figure 1.12 [AR11]. The RS is sent as a clear reference for the power estimation, more precisely with the Reference Signal Received Power (RSRP) and the Reference Signal Received Quality (RSRQ).

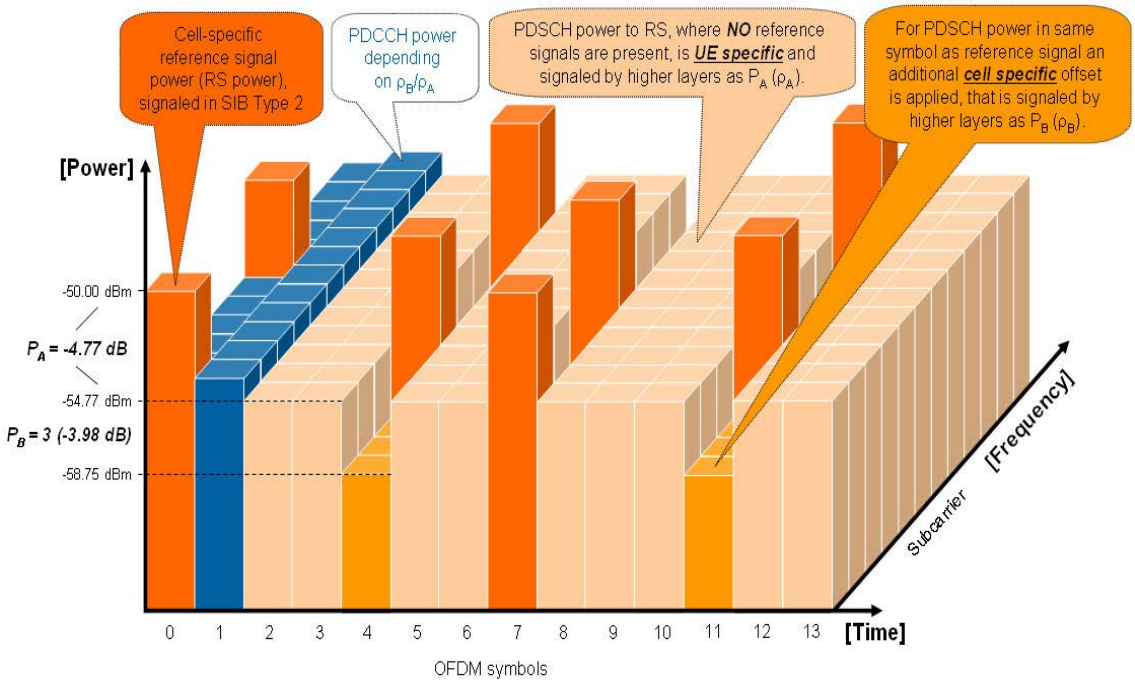

FIGURE 1.12: Downlink LTE FDD frame

The RSRP signal is used to estimate the downlink power, it represents the average power of Resource Elements (RE) that carry cell specific Reference Signals over the entire bandwidth. It is used for handover and cell selection/re-selection. The measurement of the RSRP ranges from -44 to-140 dBm and the RSRP levels for usable signal typically range from -75 dBm (for UEs close to the cell antenna) to -120 dBm (at the edge coverage). Reference Signal Received Quality (RSRQ) is defined as the following ratio :

$$RSRQ = \frac{N * RSRP}{E - UTRAcarrierRSSI} \tag{1.4.1}$$

Where N is the number of Physical Resource Blocks (PRBs) over which the Received Strength Signal Indicator (RSSI) is measured, typically equal to system bandwidth. RSSI is a parameter which provides information about total received wide-band power (measured for all symbols) including total interference and thermal noise. Owing to the relevance of the RS signal, it will be assigned the highest power during transmission, this power is

cell-specific and must be constant over the whole bandwidth since all the other signals (PDSCH, DCCH, synchronization, etc.) are calculated relatively to it. The RS power goes from -60 to 50 dBm. Since the transmit power of an eNodeB is shared on all subcarriers, the larger the bandwidth is, the lower the power on each subcarrier. Therefore, LTE uses P_A and P_B parameters to adjust the power in order to have a constant power for all the OFDMA symbols at the receiver :

- P_A indicates the ratio of the data subcarrier power of OFDM symbols excluding pilot symbols to the pilot subcarrier power.
- P_B indicates the ratio of the data subcarrier power of OFDM symbols including pilot symbols to the pilot subcarrier power.

Power allocation in OFDMA based networks has been widely studied and addressed in different works. In [CLL13], the authors addressed the ICIC interference with a sequential frequency reuse. Better SINR to cell edge UE is obtained by allocating more power for them, while each cell is given sequentially a sub-channel of the frequency bandwidth to avoid interfering with neighboring cells. In [YKS13], the problem of interference is studied for both multicellular networks and layered networks with macro, pico and femto cells. A power spectrum adaptation algorithm with a heuristic joint proportionally fair scheduling and spatial multiplexing scheme was proposed. Authors showed that a relevant improvement of system performances is realized in comparison with a fixed power allocation. In [HMLN13], the authors presented an energy efficient power allocation for a point-to-point multi-carrier link. A two level algorithm is adopted : first, a power optimization is performed without constraints ; second, the obtained power allocation is made in respect to the system power constraints through a joint time and frequency optimization. In [SQ09], a closed loop adaptive power control is proposed that aims at providing fair SINR from the UEs point of view. Simulation results confirmed that power saving was possible while lowering system interference and increasing fairness for UEs. In [CAM+09], the interference problem between macro and femto cells is addressed where a distributed power allocation algorithm is applied by femtocells in a way that the SINR is optimized without harming the macro cell. In [BCRG14], the power control on the uplink is studied where authors proposed a fully distributed algorithm where a limit on power is imposed to the UEs to avoid interference with neighboring cells. In [PTLa14], a cognitive radio network was studied where a decentralized beamforming algorithm where only local CSI information to manage power allocation. In [LAV14], another beamforming decentralized approach is proposed using the SRS message and the reciprocity of the radio channel. The results show a significant improvement of the UEs throughput. In [BPVG06], the authors tried to minimize the allocated power to UEs while guaranteeing a constant throughput. A non-collaborative algorithm is proposed where each eNodeB performs its resource allocation independently, taking into account the interference level among adjacent nodes.

Another important aspect of the OFDMA systems is the Peak-to-Average power Ratio

(PAPR). The authors of [AkI08] used a hybrid algorithm with an inverse relation between power control and adaptive modulation (when the modulation order increases, the power decreases). This leads to the lowest possible power while using high modulation order. The authors in [SQ09] pointed out that the use of high power for center UEs leads to performance degradation at the edge of the cell. Hence, they propose a solution with an adaptive ower control scheme that aims at providing a fair SINR to the UEs.

Distributed power control schemes are sought for in 4G networks and are preferred to RRM schemes with no power tuning due to lack of cooperation among serving nodes [KW11]. In [SV09, WKSV10], dynamic Soft Frequency Reuse (SFR) schemes are put forward with proved efficiency. Furthermore, several solutions have been proposed to overcome interference in OFDM systems using joint dynamic power and subcarrier allocation as in [KLL03]. Further, the joint power and RB allocation in [WCLM99, CKKL04] takes advantage of the channel quality fluctuation [WCLM99, CKKL04]. This dynamicity permits to decrease the power without degrading the BER (Bit Error Rate).

1.5 Plan of the Thesis

The main ICIC techniques are surveyed in Chapter 1. We discuss and classify a wide range of methods that are either static or dynamic. A brief description of the LTE architecture is provided for a full comprehension of the ICIC framework. The rest of the thesis is organized as follows. The work in Chapter 3 has been done for the purpose of the SOAPS project where downlink performances of OFDMA narrow band systems is enhanced. A fully decentralized algorithm based on replicator dynamics was put forward to attain the PNEs of the ICIC potential game. Chapters 4 and 5 address the problem of downlink ICIC where the resource selection process is apprehended as a congestion game. A fully decentralized algorithm was adapted to the paper context to attain the PNE of the modeled game. Each eNodeB strives to select a pool of favorable resources with low interference based on local knowledge only. Furthermore, performance improvement is realized in a time coherent with the signaling period of the X2 interface. In chapter 6, the ICIC issue is treated through adequate power allocation on selected resource blocks. The power level selection process is apprehended as a sub-modular game and a semi distributed algorithm based on best response dynamics is proposed to attain the NEs of the modeled game. Based on local knowledge conveyed by the X2 interface, each eNodeB will first select a pool of favorable resource blocks with low interference. Second, each eNodeB will strive to fix the power level adequately on those selected RBs realizing performances comparable with the Max Power policy that uses full power on selected RBs while achieving substantial power economy. We summarize our contributions in the last chapter and give insights to future research directions.

Chapitre 2

System Framework

This thesis have been done in the context of the SOAPS (Spectrum Opportunistic Access in Public Safety) project. The SOAPS project addresses low layer protocols issues for Broadband Services provision by PMR (Private Mobile Radio) systems using LTE technologies with particular focus on the improvement of frequency resource scheduling. The work of this thesis goes beyond the project (dedicated for systems with only 6 RBs) and propose more general solution for the ICI problem in wide band OFDMA systems (with a large number of resource blocks). We introduce in this chapter the general framework we have used along this thesis.

2.1 The Network Model

In order to validate our theoretic approach, our simulations are done in a cellular OFDM based network model suitable for LTE, and hence for the SOAPS project. We present hereafter the radio network framework :

- We model the system as a cellular network comprising $N = \{1, ..., n\}$ hexagonal cells.
- The work focuses on the downlink scenario.
- The SOAPS project relays on LTE, hence OFDMA is used as the multiple access scheme.
- The time and frequency radio resources are grouped into time-frequency Resource Blocks (RB).
- Each RB consists of N_s OFDM symbols in the time dimension and N_f sub-carriers in the frequency dimension (in LTE, $N_s = 7$ and $N_f = 12$).
- The set of RBs are represented by $M = \{1, .., m\}$ where m is the total number of RBs.
- We do not consider the MIMO configuration, therefore both eNodeBs and UE have single antenna each.
- We consider without loss of generality, that each UE gets only one RB at each scheduling iteration.

2.1.1 The Data Rate on the Downlink

One of the relevant parameters indicating a channel quality for the end UE is the data rate perceived on the UE equipment. In order to calculate this data rate, we have to estimate the SINR (Signal to Interference plus Noise Ratio) per RB.

The SINR observed on RB k allocated to UE u by eNodeB i can be expressed as :

$$SINR_{i,k,u} = \frac{P_0 \cdot G_i \cdot (\frac{1}{d^i_{u,i}})^\beta}{P_0 \cdot \sum_{\substack{j \in M, \\ j \neq i}} G_j \cdot x_{j,k} \cdot (\frac{1}{d^i_{u,j}})^\beta + P_N} \tag{2.1.1}$$

where the used parameters are such as :

- P_0 represents the maximal transmitted power per RB. No power control, other than on/off with equal power levels, is assumed. As said, chapter 6 tackles power control for ICI.
- P_N represents the thermal noise power per RB.
- G_i is the antenna gain of eNodeB i.
- $d^i_{u,j}$ is the distance between eNodeB j and UE u served by eNodeB i.
- β is the path-loss factor varying between 2 and 6.

Finally, the binary variable $x_{j,k}$ are such that :

$$x_{j,k} = \begin{cases} 1 & \text{if RB } k \text{ is used by eNodeB } j, \\ 0 & \text{otherwise.} \end{cases} \tag{2.1.2}$$

We denote by $\mathbb{B}$ the set $\{0, 1\}$. Note that $x_{j,k} \in \mathbb{B}$.

We denote by $D_{i,k,u}$ the data rate achieved by UE u on RB k in eNodeB i given by what follows :

$$D_{i,k,u} = \frac{W}{E_b/N_0} \cdot SINR_{i,k,u},$$

where W is the bandwidth per RB. Given a target error probability, it is necessary that $E_b/N_0 \geq \gamma$, for some threshold γ which is UE specific.

Each cell will be logically divided into n_z concentric discs of radii R_z and the area between two adjacent circles of radii R_{z-1} and R_z is called zone $z \in \mathcal{N}_z$ where $\mathcal{N}_z = \{1, .., n_z\}$ represents the set of zones. We consider that the UE belonging to the same zone z have the same radio conditions leading to the same γ (denoted by γ_z) and the same mean rate

per zone $D_{i,k,z}$ according to what follows :

$$\begin{aligned} D_{i,k,z} &= \frac{\frac{W}{\gamma_z}\int_{R_{z-1}}^{R_z}\rho_{zmobile}\frac{2\pi r dr}{r^\beta}\cdot G_i\cdot P_0}{P_0\cdot\sum_{\substack{j\in M,\\ j\neq i}} G_j\cdot x_{j,k}\cdot\frac{1}{(d^i_{i,j})^\beta}+P_N} \\ &= \frac{\frac{W}{\gamma_z}(R_z^{2-\beta}-R_{z-1}^{2-\beta})\cdot\rho_{zmobile}\cdot G_i\cdot x_{i,k}}{\sum_{\substack{j\in M,\\ j\neq i}} x_{j,k}\cdot\frac{G_j}{(\delta^z_{i,j}\cdot R_{cell})^\beta}+\eta} \end{aligned} \tag{2.1.3}$$

where R_{cell} is the cell radius. As for interference, we consider mainly for simplification the impact of eNodeB j on eNodeB i by replacing $d^i_{u,j}$ with $d^i_{z,j}=\delta^z_{i,j}\cdot R_{cell}$ the distance between eNodeB i and eNodeB j (the value of $\delta^z_{i,j}$ depends on how far is eNodeB j from zone z of eNodeB i). Finally, $\eta=\frac{P_N}{P_0}$. As $\eta << 1$, it will be neglected in what follows.

2.1.2 The Bit Transfer Time

We denote by $T_{i,k,z}$ the amount of time necessary to send a data unit through RB k in eNodeB i for UEs in zone z. In fact, the delay needed to transmit a bit for a given UE is the inverse of the data rate $D_{i,k,z}$ perceived by this UE :

$$\begin{aligned} T_{i,k,z} &= \frac{1}{D_{i,k,z}} \\ &= \frac{\sum_{\substack{j\in M,\\ j\neq i}} y_{j,k}\cdot H^z_{i,j}}{H_{i,z}} \end{aligned} \tag{2.1.4}$$

where $H^z_{i,j}=\frac{G_j}{(\delta^z_{i,j}\cdot R_{cell})^\beta}$ captures distance-dependent attenuation between eNodeB j and eNodeB i and for eNodeB i and $H_{i,z}=\frac{W}{\gamma_z}(R_z^{2-\beta}-R_{z-1}^{2-\beta})\cdot\rho_{zmobile}\cdot G_i$ captures distance-dependent attenuation inside zone z.

2.2 Non-Cooperative game for RBs selection

Non-Cooperative game theory models the interactions between players competing for a common resource. Hence, it is well adapted to distributed ICIC modeling. Here, eNodeBs are the decision makers or players of the game. We define a multi-player game $\mathcal{G}$ between the n eNodeBs. The eNodeBs are assumed to make their decisions without knowing the decisions of each other. We present hereafter the general framework of the game used in Chapters 3, 4 and 5. The final game is devoted to power control and will be presented in details in the sequel of Chapter 6.

– The set of players is $N=\{1,..,n\}$.
– The set of available RBs is $M=\{1,..,m\}$.

– Each eNodeB is a player that has to pick several RBs among the m available RBs.
– The strategy of eNodeB i is denoted by the m-dimensional binary vector $x_i \in S_i$ whose components are the $x_{i,k}$ variables defined in Equation (2.1.2) and where S_i is the set of eNodeB i's strategies ($S_i = \mathbb{B}^m$).
– $X = (X_i)_{i \in N} \in \mathcal{S} = \{1, 2, \cdots, m\}^N$ is a pure strategy profile, where $\mathcal{S}$ is the set of strategy profiles.
– In every chapter, we define $c_i(x_i, X_{-i})$ the cost function of eNodeB i that selects action x_i, where X_{-i} denotes the vector of strategies played by all other eNodeBs except eNodeB i.

The cost function varies from chapter to chapter and will be detailed in each chapter for clarity.

2.2.1 The Nash Equilibrium

In a non-cooperative game, an efficient solution is obtained when all players adhere to a Nash Equilibrium (NE). A NE is a profile of strategies in which no player will profit from deviating its strategy unilaterally. Hence, it is a strategy profile $X^* \in \mathcal{S}$ where each player's strategy is an optimal response to the other players' strategies :

$$c_i(X^*) = c_i(x_i^*, X_{-i}^*) \leq c_i({x_i}', X_{-i}^*), \forall i \in N, \forall {x_i}' \in S_i \tag{2.2.1}$$

In general, finite games possess mixed NE but are not guaranteed to have pure NEs. For mixed NE, each eNodeB has to continually change its RBs selection according to a distribution probability over the strategy set. Implementing such solutions is cumbersome, hence, for our portrayed games, we only want to allow deterministically chosen actions, the so-called pure strategies.

Our games are distributed and need a local feedback from the system to compute the cost of each allocation, we relies on the CQI sent back from the UE to calculate that cost.

2.3 Conclusion

The defined framework presented in this chapter will be used for all the upcoming chapters, however some added aspects will be detailed for each contribution.

Chapitre 3

Replicator Dynamics for Distributed Inter-Cell Interference Coordination

This chapter addresses the problem of ICIC in the downlink of cellular OFDMA systems where the resource selection process is apprehended as a load balancing game. Proving the existence of Pure Nash equilibriums (PNE) shows that stable resource allocations can be reached by selfish eNodeBs. We resort to a fully decentralized algorithm based on a replicator dynamic to reach the PNE of the ICIC game. Each eNodeB will strive to select a pool of favorable resources with low interference based on local knowledge only[AKC+14].

3.1 Introduction

In this chapter, we focus on the problem of inter-cell interference in the context of the SOAPS. In this context, we propose an ICIC scheme modeled as an exact potential game. Furthermore, we prove that a replicator dynamics algorithm converges to the pure NEs of our game. The result of the devised coordination process in each cell will be a pool of RBs that is not too highly interfered.

The rest of the chapter is organized as follows. The network model and cost characterization are given in the reference model in Section 2.1 presented in Chapter 2. The RBs selection scheme is presented as a non-cooperative potential game in Section 3.3. The distributed learning algorithm based on replicator dynamics to reach pure NE is presented in Section 3.4. Simulation results are portrayed in Section 3.5. Conclusion is given in Section 3.6.

3.2 Non-Cooperative game for RBs selection

Non-Cooperative game theory is used to model the ICIC, where selfish eNodeBs share common resources in a way to enhance their own local performance. We adopt the multi-player game $\mathcal{G}$ between the n eNodeBs defined in Section 2.2. We will define the cost function of a eNodeB i that selected strategy x_i as follows :

$$\begin{aligned} c_i(x_i, X_{-i}) &= \sum_{k \in M} \sum_{z \in \mathcal{N}_z} x_{i,k} \cdot T_{i,k,z} \\ &= \sum_{k \in M} \sum_{z \in \mathcal{N}_z} x_{i,k} \frac{\sum_{\substack{j \in N, \\ j \neq i}} x_{j,k} \cdot H^z_{i,j}}{H_{i,z}} \end{aligned} \tag{3.2.1}$$

Where X_{-i} denotes the vector of strategies played by all other eNodeBs except eNodeB i. Note that the eNodeB will single out the strategy that minimizes the total bit transfer time in its cell.

3.3 Potential games

Potential games [Ros73] form a special class of normal form games where the unilateral change of one UEs strategy x_i to x'_i results in a change of its utility function that is equal to the change of a so-called potential function $\phi : \mathcal{S} \to \mathbb{R}$ as follows :

$$c_i(x_i, X_{-i}) - c_i(x'_i, X_{-i}) = \phi(x_i, X_{-i}) - \phi(x'_i, X_{-i})$$

A potential game [Ros73] admits at least one pure NE which is a desired property in this context for practical reasons.

Proposition 1. The game $\mathcal{G}$ is an exact potential game.

Démonstration. We will define our potential function which maps a profile $X = (x_1, x_2, \ldots, x_n)$ to a real :

$$\phi(X) = 1/2 \sum_{i \in N} \sum_{k \in M} \sum_{z \in \mathcal{N}_z} x_{i,k} \frac{\sum_{\substack{j \in N, \\ j \neq i}} x_{j,k} \cdot H^z_{i,j}}{H_{i,z}} \tag{3.3.1}$$

Now, we will prove that if X and X' are two pure profiles which only differ on the strategy of one eNodeB ℓ, then $c_\ell(x_\ell, X_{-\ell}) - c_\ell(x'_\ell, X_{-\ell}) = \phi(x_\ell, X_{-\ell}) - \phi(x'_\ell, X_{-\ell})$.

As for the potential function, we have the following :

$$
\begin{aligned}
&2\phi(Y) - 2\phi(Y') = \\
&\sum_{\substack{i\in N,\\ i\neq\ell}} \sum_{k\in M} \sum_{z\in\mathcal{N}_z} \frac{x_{i,k}}{H_{i,z}} \Big(\sum_{\substack{j\in N,\\ j\neq i,\\ j\neq\ell}} x_{j,k} H^z_{i,j} + x_{\ell,k} H^z_{i,\ell}\Big) \\
&- \sum_{\substack{i\in N,\\ i\neq\ell}} \sum_{k\in M} \sum_{z\in\mathcal{N}_z} \frac{x_{i,k}}{H_{i,z}} \Big(\sum_{\substack{j\in N,\\ j\neq i,\\ j\neq\ell}} x_{j,k} H^z_{i,j} + x'_{\ell,k} H^z_{i,\ell}\Big) \\
&+ \sum_{k\in M} \sum_{z\in\mathcal{N}_z} \left(\frac{x_{\ell,k}}{H_{\ell,z}} \Big(\sum_{\substack{j\in N,\\ j\neq\ell}} x_{j,k} H^z_{\ell,j}\Big) - \frac{x'_{\ell,k}}{H_{\ell,z}} \Big(\sum_{\substack{j\in N,\\ j\neq\ell}} x_{j,k} H^z_{\ell,j}\Big) \right) \\
&= \sum_{\substack{i\in N,\\ i\neq\ell}} \sum_{k\in M} \sum_{z\in\mathcal{N}_z} \frac{x_{i,k}}{H_{i,z}} H^z_{i,\ell} \cdot (x_{\ell,k} - x'_{\ell,k}) \\
&+ c_\ell(x_\ell, X_{-\ell}) - c_\ell(x'_\ell, X_{-\ell}) \\
=&\sum_{k\in M} \sum_{z\in\mathcal{N}_z} x_{\ell,k} \sum_{\substack{i\in N,\\ i\neq\ell}} \frac{x_{i,k}}{H_{i,z}} H^z_{i,\ell} - \sum_{k\in M} \sum_{z\in\mathcal{N}_z} x'_{\ell,k} \sum_{\substack{i\in N,\\ i\neq\ell}} \frac{x_{i,k}}{H_{i,z}} H^z_{i,\ell} \\
&+ c_\ell(x_\ell, X_{-\ell}) - c_\ell(x'_\ell, X_{-\ell}) \\
=&2 \cdot (c_\ell(x_\ell, X_{-\ell}) - c_\ell(x'_\ell, X_{-\ell}))
\end{aligned}
$$

□

3.4 Distributed Learning of PNE

Implementing a practical distributed RBs selection policy to reach pure NE is not straightforward and must be carried out carefully. In this chapter, we resort to replicator dynamic ([BC13]) to learn Nash equilibriums.

A *mixed strategy* $q_i = (q_{i,1}, q_{i,2}, \ldots, q_{i,m})$ corresponds to a probability distribution over pure strategies. In other words, pure strategy s is chosen with probability $q_{i,s} \in [0,1]$, with $\sum_{s=1}^{m} q_{i,s} = 1$. Let K_i be the simplex of mixed strategies for eNodeB i. Any pure strategy s can be considered as a mixed strategy e_s, where vector e_s denotes the unit probability vector with s^{th} component being a unity component, hence a corner of K_i.

Let $\mathbb{K} = \prod_{i=1}^{n} K_i$ be the space of all mixed strategies. A *strategy profile* $Q = (q_1, ..., q_n) \in \mathbb{K}$ specifies the (mixed or pure) strategies of all players. Following classical convention, we write $Q = (q_i, Q_{-i})$, where Q_{-i} denotes the vector of strategies played by all other eNodeBs besides eNodeB i.

Definition 3.1. The game mechanics work as follows : at $t = 0$, we begin with $q(0) = (q_1(0), ..., q_n(0))$ any random vector of probabilities. At each iteration $t > 0$:

1. Each eNodeB i chooses an action $x_i(t)$ according to probability distribution $q_i(t)$.
2. Each eNodeB i learns the cost $c_i(t)$ resulting from the RBs allocation $x_i(t)$ it used and the set of all actions of other players.
3. Each eNodeB i updates the probability vectors $q_i(t+1)$ in the following way :

$$q_{i,s}(t+1) = \begin{cases} q_{i,s}(t) + b(1 - \frac{c_i(t)}{c_{max}})(1 - q_{i,s}(t)) \\ \text{if} \quad s = x_i(t), \\ q_{i,s}(t) - b(1 - \frac{c_i(t)}{c_{max}})q_{i,s}(t) \\ \text{otherwise,} \end{cases} \tag{3.4.1}$$

where $0 < b < 1$ is a parameter and c_{max} is the maximum cost.

Theorem 3.1. *Let G be an instance of game $\mathcal{G}$. Let $\mathbb{K}^*$ be a set of mixed profiles where at most one player plays a pure strategy. The learning algorithm, for any initial condition in $\mathbb{K} - \mathbb{K}^*$, always weakly converges to a Nash Equilibrium.*

Proof of convergence of Theorem 3.1 is given in the appendix A at the end of this thesis.

Algorithms of this form are fully distributed as decisions made by eNodeBs are completely decentralized : at any iteration t, eNodeB i only needs to know its own cost $c_i(t)$ and mixed strategy $q_i(t)$. To compute the cost $c_i(t)$, any eNodeB i makes use of signaling information already present in the downlink of an LTE system. In fact, a UE assigned to a specific RB measures its channel quality based on pilots, i.e. Cell Specific Reference Signals (CRS) that are spread across the whole band independently of the individual UE allocation. Hence, the cost function can be easily inferred through the CQI (Channel Quality Indicator) sent every TTI (Transmit Time Interval) by serviced UEs. We consider that a time iteration in our algorithm is equal to a TTI ($1ms$).

3.5 Simulation Results

For the needs of the SOAPS project, we consider a bandwidth of 1.4 MHz with 6 RBs used for PMR systems. The choice of the replicator dynamics is well adapted for the present context to reach NE. In fact, the replicator dynamics algorithm is efficient but is known to converge slowly to NE especially for games with a large set of actions. With m RBs, the number of possible actions is $\begin{pmatrix} m \\ k \end{pmatrix} = \frac{m!}{k! \cdot (m-k)!}$ for a eNodeB with k active UEs. With either 1 or 5 active UEs, we only have 6 possible actions. But with 50% of load (3 UEs), we reach 20 possible actions. With larger bandwidth systems, the set of strategies

becomes very large. For instance, for a system with 15 RBs and 50% of load, we get 6435 possible actions rendering convergence times prohibitively long. For comparison, we considered for all simulation results a system with 10 RBs and hence with a maximum of 252 actions at 50% of load.

Moreover, for LTE networks, a convergence time smaller than 200 TTI is sought for. In fact, the RNTP (Relative Narrow-band Transmit Power) indicator, received from neighboring eNodeBs every 200 TTI through the X2 interface, advertises on which RBs a neighboring eNodeB will use high power. Hence, each eNodeB can aggregate information about transmit power levels from adjacent cells and decides accordingly to preclude some RBs that will be highly interfered (or alternatively allocate them to mobile UEs with good channel quality) as already explained in the introductory chapter. Although this mechanism is not taken into account as this thesis is dedicated to distributed ICIC, the convergence time to NE should be nonetheless coherent with the RNTP signaling time to cope with semi-distributed schemes.

We consider the following additional parameters listed in the 3GPP technical specifications TS 36.942 :

– The mean antenna gain in urban zones is 12 dBi (900 MHz).
– Transmission power is 43 dBm (according to TS 36.814) which corresponds to 20 Watts (on the downlink).
– eNodeBs have a frequency reuse of 1, with $W = 180$ KHz.

As for noise, we consider that the UE noise figure is 7.0 dB and the thermal noise is -104.5 dBm which gives a receiver noise floor of $p_N = -97.5$ dBm.

We consider 10 hexagonal cells where the distance between two neighboring eNodeB is 2 Km. Two zones are taken into account : zone 1 which stands for cell-center UEs located at a distance smaller than $R_0 = 0.5Km$ and zone 2 stands for cell-edge UEs located at a distance ranging between $R_0 = 0.5Km$ and $R_1 = R_{cell} = 1Km$. We assume that for cell-center UEs 64-QAM modulation is used while for cell-edge UEs 16-QAM modulation is used. The path-loss factor is set to 3. For each scenario, 400 simulations were run, where in each cell a random number of UEs is chosen at the beginning of the simulation, they are uniformly distributed among zones and correspond to a snapshot of the network.

3.5.1 Speed of Convergence

In Figure 3.1, we depict the strategy dynamics q_i of two randomly selected eNodeB (eNodeB 0 and eNodeB 3) as a function of the number of iterations.
All eNodeBs have only one center UE which gives them 6 possible actions $(1, 0, 0, 0, 0, 0)$; $(0, 1, 0, 0, 0, 0)$; $(0, 0, 1, 0, 0, 0)$; $(0, 0, 0, 1, 0, 0)$; $(0, 0, 0, 0, 1, 0)$; $(0, 0, 0, 0, 0, 1)$. We can see that the eNodeBs strategies converge to either 0 or 1, opting for one single action which can be practical. We recorded this behavior through all the extensive simulations we performed

(convergence to pure NE is proven in the appendix).

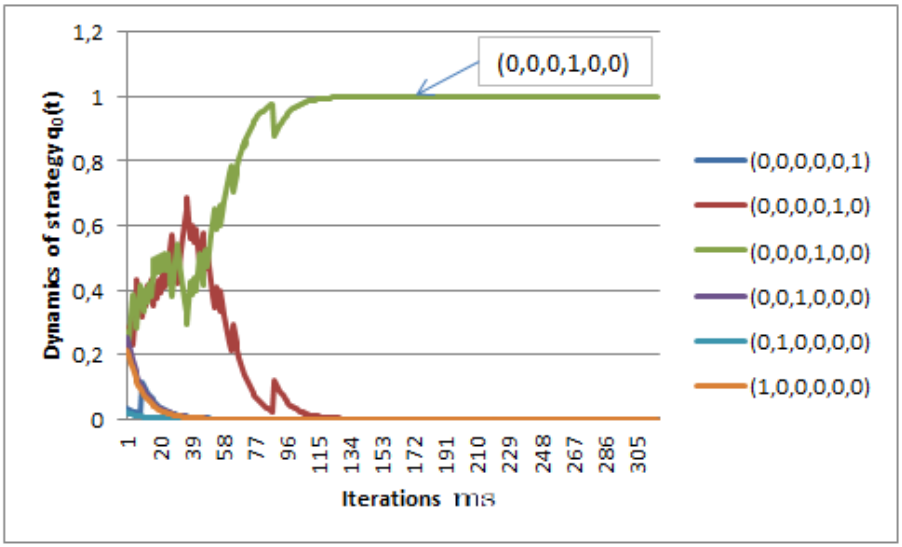

(a) eNodeB 0

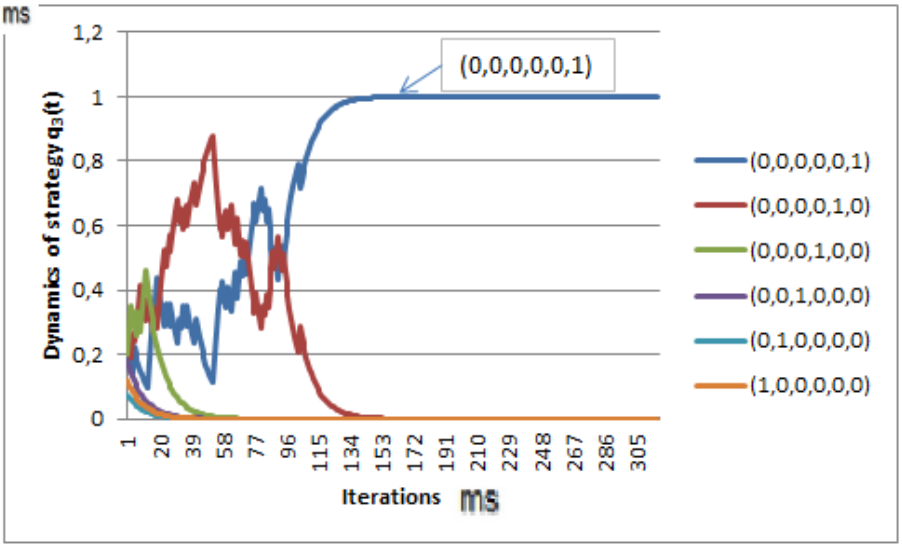

(b) eNodeB 3

FIGURE 3.1: Replication Dynamics : strategy updates for 2 random eNodeBs

We also notice the slow convergence of the algorithm (around 300 iterations are required for the present case) which hinders the benefits of a distributed approach. As mentioned, we wish to reach convergence faster than 200 iterations. However, we see through the extensive simulations we ran that the convergence is relatively fast at the beginning of the algorithm but slows down drastically half way through. At that point, the set of RBs that will be ultimately selected by each eNodeB is clearly designated (we can see this behavior in Figure 3.1 around 100 iterations) and it is useless to pursue the RB selection process. Hence, we propose an accelerated mode of the algorithm such that whenever for a

given eNodeB the probability of selecting any action surpasses 0.8, convergence is assumed to be reached and the eNodeB chooses this particular action. In Figure 3.2, we run 100 simulations to compare the number of iterations of the accelerated mode (denoted REP ACC) vs. the normal mode (denoted REP) for respectively 6 and 10 RBs as a function of the mean number of active UEs per eNodeB.

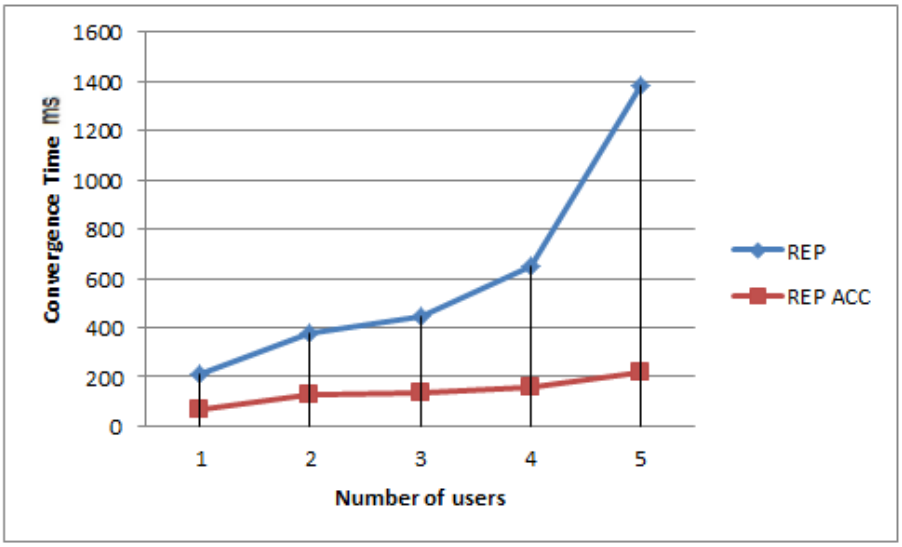

(a) 6 RBs

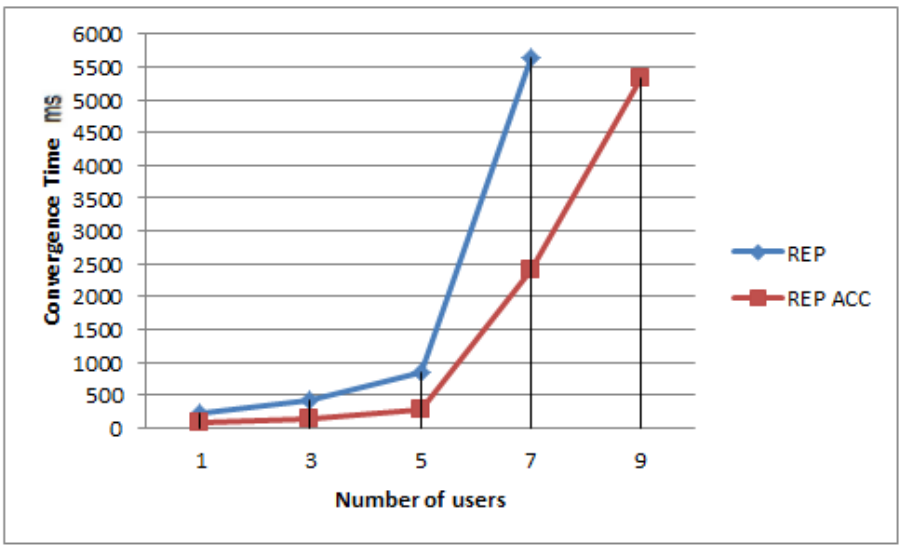

(b) 10 RBs

FIGURE 3.2: Normal Mode vs. Accelerated Mode

We can see in Figure 3.2 the tremendous improvement in speed for the accelerated mode as compared to the normal implementation of the replicator dynamics algorithm. However, although for the 6 RBs system (which is the system of interest in this chapter), convergence time is now coherent with the RNTP signaling time (limited to 220 iterations at 90% load),

it largely surpasses this threshold for the 10 RBs system (around 5000 iterations at 90% load). Note that the convergence time for the normal mode at 90% load is not reported in the figure for clarity as it reaches a mean of 1.970.213.913 iterations.

3.5.2 Performance Evaluation

In order to show the benefit of our solution, the performances are compared against a Random algorithm where actions are chosen at random. For every snapshot, 400 runs of the random algorithm were made. In Figure 3.3, we depicted the total cost $c_{total} = \sum_{i \in N} c_i$ (where c_i is given in equation (4.3.1)) as a function of the mean number of UEs per eNodeB for 6 RBs and 10 RBs. We reported the total cost for the random algorithm and the replicator dynamics in normal mode and accelerated mode. Further, we captured results for the replicator dynamics in normal mode at three different instants : at 100 iterations (denoted REP 100IT), at 200 iterations (denoted REP 200IT) and at convergence (denoted REP CONV). In Figure 3.4, the mean relative change of cost is displayed as a function of the mean number of UEs per eNodeB where the relative change in eNodeB i is given by $\frac{c_i^{REP} - c_i^{Random}}{c_i^{REP}} * 100$ with c_i^{Random} and c_i^{REP} being the cost function according to Equation (4.3.1) for the random algorithm and the replicator dynamics respectively.

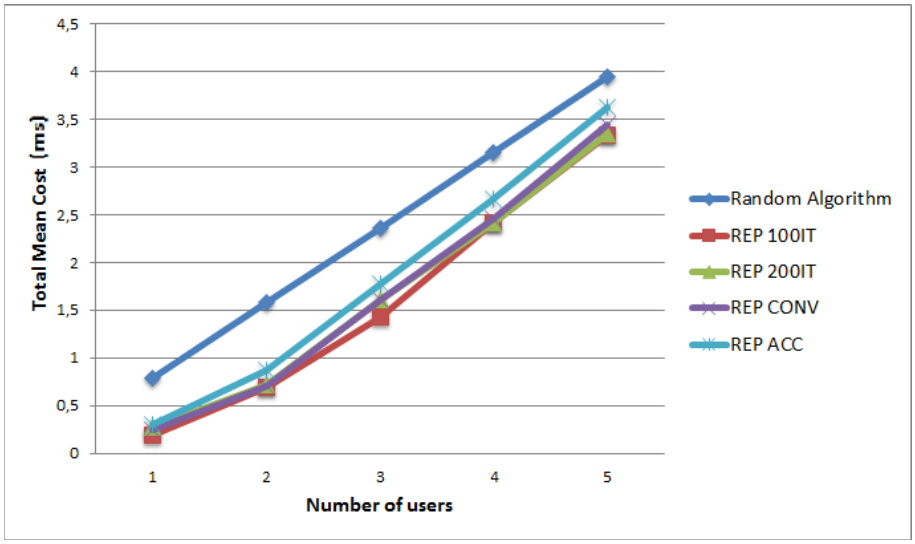

(a) 6 RB

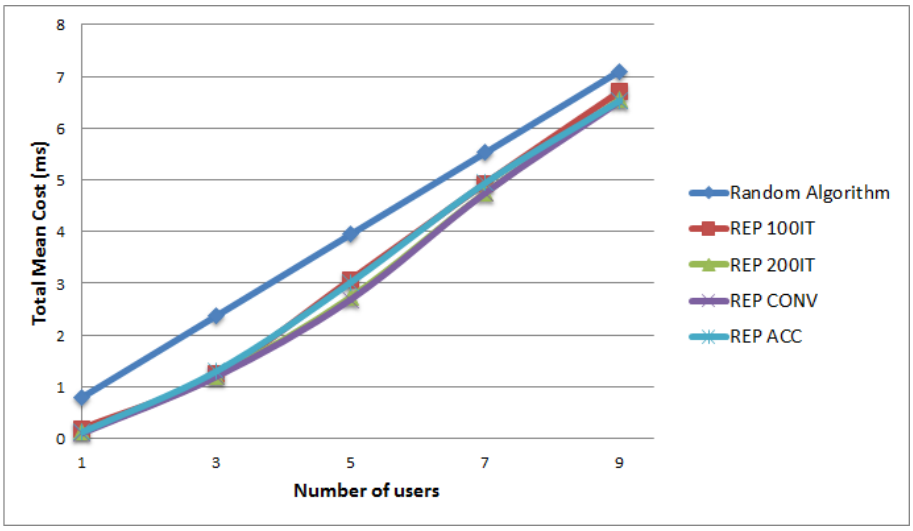

(b) 10 RB

FIGURE 3.3: Total Mean Cost : Random Algorithm vs. Replicator Dynamics Algorithm

We can see that the main performance improvement is achieved during the first 100 iterations in comparison with the random algorithm especially for the PMR system (6 RBs). All proposed versions are roughly equivalent in terms of performance although the accelerated version impedes slightly the performance improvement due to its aggressive approach. Considering an iteration to be equivalent to a TTI, this result is quite attractive since we obtain good results before eNodeBs exchange the RNTP messages among them through the X2 interface. The latter signaling information should normally incite eNodeBs to exclude certain actions from their strategy space (due to potentially high interference on some of their RBs) before restarting the algorithm with new initial conditions set according to the RNTP message content. Furthermore, as expected, the reduction in total cost

decreases as load increases in comparison with the random algorithm (around 10% for the maximum load for the 6 RBs system and falling below that for the 10 RBs system) as can be seen in Figure 3.4. This behavior was expected, with the increase of system load, there is fewer room for the algorithm to change the allocated strategy, most resources are being already used rendering interference inevitable.

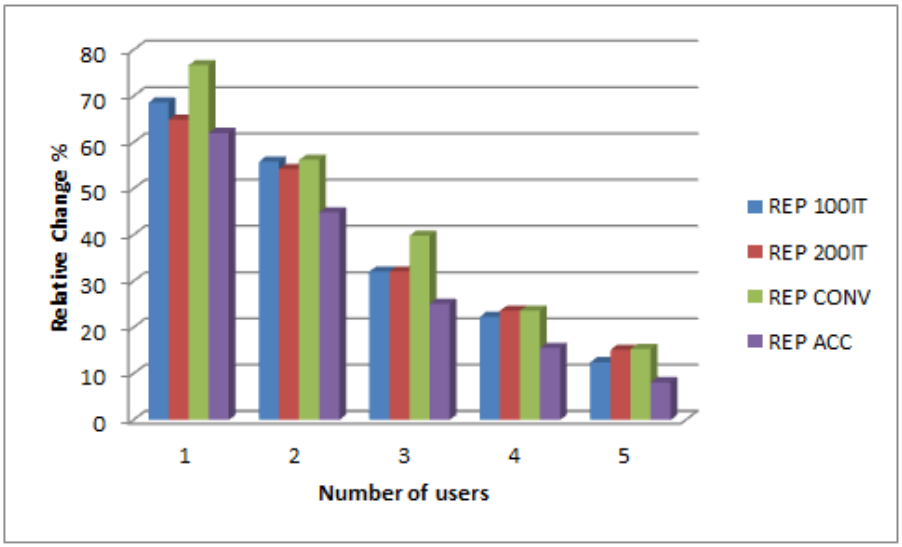

(a) 6 RB

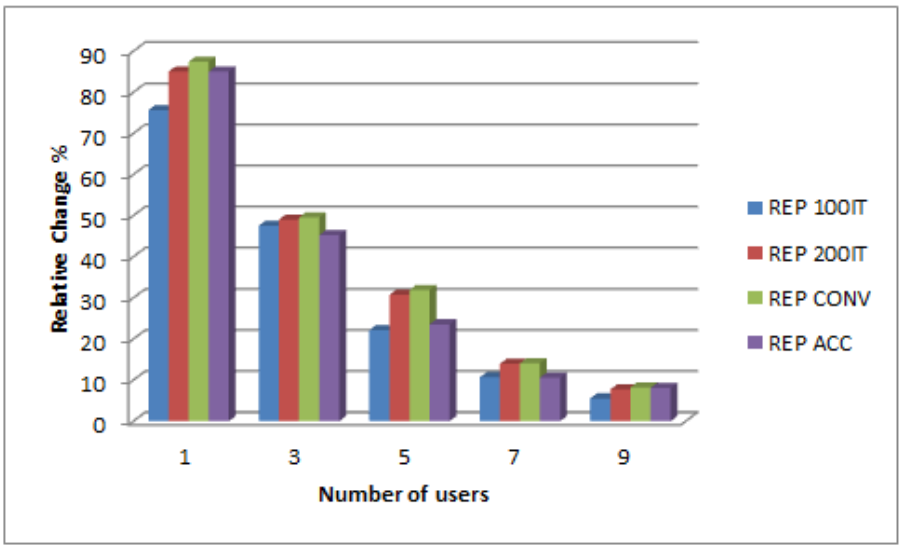

(b) 10 RB

FIGURE 3.4: Relative Change : Random Algorithm vs. Replicator Dynamics Algorithm

3.6 Conclusion

In this chapter, the Inter Cell Interference problem was addressed for the special case of the PMR network where RBs are astutely allocated in a distributed fashion. We put forward a potential game to model the interference coordination among eNodeBs and propose a fully distributed algorithm based on replicator dynamics to reach pure NEs. Numerical simulations assessed the good performances of the proposed approach in comparison with a random resource allocation. More importantly, improvement is realized in a time coherent with the RNTP signaling time.

In future work, the RNTP messages will be taken into account to evaluate their impact on the replicator dynamics algorithm performances. In fact, after receiving new RNTP messages, the replicator dynamics algorithm will be restarted with an initial mixed strategy that is no longer random but biased against actions comprising highly interfered RBs.

In this work, we put forward an efficient distributed algorithm suitable for narrow band systems like PMR. However, it is of limited interest for more widespread OFDM-based networks with larger number of spectral resources. Therefore, we put into light through the next chapters more adapted game theoretic distributed algorithms with fast convergence times.

Chapitre 4

Distributed Load Balancing Game for Inter-Cell Interference Coordination

This chapter reconsiders the problem tackled in Chapter 3 where the ICIC resource selection process is apprehended as a potential game in the downlink of a cellular OFDMA system. However, contrary to the work displayed in the previous chapter, there is no restriction on the system bandwidth size. We consider here a game theoretic approach where the ICIC problem is modeled as a congestion game[ARK+14a]. We adapt the distributed algorithm proposed by Berenbrinck et al. [AB12] to attain the PNE of the considered game. Proof of convergence is obtained in a limited time.

4.1 Introduction

Turning to non-cooperative game theory is quite fit to model the way eNodeBs compete in a distributed way for scarce and shared resources. We adapt a stochastic version of the best-response dynamics proposed by Berenbrink et al. [AB12, BFHH12] where players only have a local view of the system. Hence, all eNodeBs are able to simultaneously change their strategy in a fully distributed way. The result of the devised coordination process in each cell will be a pool of RBs that is not too highly interfered and which can then be used for fast intra-cell scheduling by the eNodeB. More importantly, we provide proof of convergence to PNE in a bounded time. Unfortunately, proof of convergence is obtained at the cost of reduced model accuracy : in this chapter we overlooked the impact of UEs position in a given cell. The rest of the chapter is organized as follows. The network model and cost characterization are given in Chapter 2. The RB selection scheme is presented as a non-cooperative congestion game in Section 4.3. Proof of convergence to PNE in a

bounded time is presented in Section 4.4. Simulation results are portrayed in Section 4.5. Conclusion is given in Section 4.6.

4.2 The network model

We use the reference model of Section 2.1 presented in Chapter 2. To model the amount of interference endured by eNodeBs, we use the model proposed in [EHB08]. A resource allocation by any eNodeB consists in selecting a subset of RBs to be used in its cell. The choice of eNodeB i is denoted by the m-dimensional vector X_i whose components $x_{i,k}$ are defined in 2.1.2.

The different geographic positions of individual UEs are not taken into consideration : the use of any RB k by eNodeB i is impacted by the concurrent use of that same RB by other eNodeBs, the goal will be to lower the use of each RB over the adjacent cells, leading to a load balancing situation. Furthermore, we consider that any eNodeB is interfered only by its 6 neighboring eNodeBs. The impact of further away cells is neglected. Building on that, we define $I_{i,k}$ as the interference endured by eNodeB i on RB k as follows :

$$I_{i,k} = \sum_{\substack{j \in N, \\ j \neq i}} x_{j,k} \tag{4.2.1}$$

4.3 Non-cooperative congestion game for RBs selection

Non-Cooperative game theory models adequately the interactions between selfish eNodeBs competing for a common pool of RBs. The higher is the number of eNodeBs that select concurrently the same RB k, the higher is the interference produced on the latter (congestion impact). Hence, the highest will be the cost of eNodeBs that chose that RB k in particular. Consequently, the ICIC problem at hand is adequately modeled by a congestion game where eNodeBs (the decision makers or players of the game) will try on their own to avoid RBs that are increasingly solicited by adjacent cells.

We adopt the multi-player game $\mathcal{G}$ between the n eNodeBs defined in Section 2.2. We will define the cost function of a eNodeB i that selected strategy x_i as follows :

$$\begin{aligned} c_i(X_i, X_{-i}) &= \sum_{k \in M} x_{i,k} \cdot I_{i,k} \\ &= \sum_{k \in M} \sum_{\substack{j \in N, \\ j \neq i}} x_{i,k} \cdot x_{j,k} \end{aligned} \tag{4.3.1}$$

Where X_{-i} denotes the vector of strategies played by all other eNodeBs except eNodeB i. Every eNodeB i needs a certain amount of N_i RBs depending on the number of active

UEs in its cell. The action set X_i is hence cell-specific as only actions with $\sum_{k=1}^{m} x_{i,k} = N_i$ are allowed in eNodeB i.

4.3.1 The load balancing game

A load balancing game is a congestion game where every player chooses only one resource. In our case, every eNodeB (player) chooses concurrently many RBs (resources). Hence, we need to tailor our game so that it boils down to a load balancing game as follows : the system starts with an initial state where D_i RBs are randomly alloted in eNodeB i. In each round, every eNodeB migrates randomly and uniformly the allocation of only one UE from an occupied RB to an available RB. The goal is to adapt the algorithm proposed by Berenbrinck et al in [AB12, BFHH12] where authors studied distributed load balancing in networks with selfish players. They consider n resources and $m > n$ selfish players that unilaterally decide to move from one resource to another if this improves their experienced load. Concurrent migration is possible based only on local information which is pretty suitable for distributed ICIC. The adapted algorithm is sketched hereafter :

Algorithm 1 Distributed Load Balancing Algorithm

1: At each iteration
2: **for** i = 1 to n **do**
3: eNodeB i selects a RB l uniformly at random among the b used RBs
4: eNodeB i selects a free RB j uniformly at random in $m - b$ (strategy x'_i)
5: **if** $(c_i(x_i, X_{-i}) > c_i(x'_i, X_{-i}))$ **then**
6: Change strategy (go to RB j) with probability $1 - \frac{c_i(x'_i, X_{-i})}{c_i(x_i, X_{-i})}$
7: **end if**
8: **end for**

In each round in parallel, every eNodeB picks an available RB at random and decides probabilistically whether or not to migrate a UE to that RB. To compute the cost of the former strategy (x_i) and actual strategy (x'_i), any eNodeB i makes use of signaling information already present in the downlink of an LTE system. In fact, as already explained, a UE assigned to a specific RB l measures its channel quality based on pilots and sends a report in the form of CQI to its serving eNodeB. Hence, the eNodeB can easily infer the cost function based on the CQI sent every TTI by serviced UE to their eNodeBs.

4.4 Distributed learning of PNE

This section is devoted to prove the convergence to PNE of the proposed algorithm in a bounded time. Recall that n is the number of eNodeBs and m the number of RBs.

Theorem 4.1. *A Nash Equilibrium is reached in expected time $O(m\log(\bar{w}))$, with :* $\bar{w} = \frac{1}{m}\sum_{i\in N}\left(\sum_{k\in M} x_{i,k}\right)$.

We give in what follows a concise proof of the theorem. A detailed one can be found in the Appendix B.

Démonstration. Let $W(t) = (w_1, w_2, \ldots, w_m)$ be the vector containing the number of UEs on each resource RB at time t, with $w_k = \sum_{i\in N} x_{i,k}$ corresponding to the number of UEs on RB k. b is the number of active RB. Each UE to whom RB k is allocated will have a weight equal to 1.

Let $P_{k,\ell}$ be the probability that any UE migrate from RB k to RB ℓ :

$$P_{k,\ell} = \begin{cases} \frac{1}{b(m-(b-1))}\left(1 - \frac{w_\ell}{w_k}\right) & \text{if } \ell \neq k,\ w_k > w_\ell + 1 \\ 0 & \text{if } \ell \neq k,\ w_k \leq w_\ell + 1 \\ 1 - \sum_{j\in M, w_k > w_j} P_{k,j} & \text{if } \ell = k \end{cases} \tag{4.4.1}$$

We define our potential function $\Phi(W)$ as :

$$\begin{aligned} \Phi(W) &= \sum_{k\in M} (w_k - \bar{w})^2 \\ &= \frac{1}{m}\sum_{k=1}^{m}\sum_{\ell=k+1}^{m} (w_k - w_\ell)^2 \end{aligned}$$

with $\bar{w} = \frac{1}{m}\sum_{i\in N}\sum_{k\in M} x_{i,k}$ the average load.

This potential function is a standard one according to [BFHH12], [Gol04]. We adapt the analysis of convergence of such a potential function proposed by Berenbrink et al. for load balancing of unweighted tasks [BFHH12]. The objective is to prove that for any time t, $\mathbb{E}[\Phi(W(t+1))] < \mathbb{E}[\Phi(W(t))]$. Indeed, the potential function Φ is the sum of the difference between the load of each resource and the global mean $\bar{w}$, all squared. For a weight of $W = \{\bar{w}, \bar{w}, \ldots, \bar{w}\}$ where all resources have a load that equals the global mean $\bar{w}$, the potential function attains its lowest value $\Phi(W) = 0$. Thus, if we prove that $\mathbb{E}[\Phi(W(t+1))] < \mathbb{E}[\Phi(W(t))]$, it means that the potential function decreases on average at each time step and since it is lower bounded by 0, convergence time is finite.

In order to prove this theorem, we first prove that $\mathbb{E}[W_k(t+1)|W(t) = w_k] < \mathbb{E}[W(t)]$.

For that, we define the expected potential at time $t+1$:

$$\begin{aligned}
&\mathbb{E}[\Phi(W(t+1))|W(t)] \\
&= \mathbb{E}[\sum_{k=1}^{m}(W_k(t+1)-\bar{w})^2|W_k(t)=w_k] \\
&= \sum_{k=1}^{m}(\mathbb{E}[(W_k(t+1))|W_k(t)=w_k]-\bar{w})^2 \\
&\quad + \sum_{k=1}^{m} Var[(W_k(t+1))|W_k(t)=w_k]
\end{aligned} \tag{4.4.2}$$

According to this equation bounding the two sums on expectation and variance leads us to a bound on $\mathbb{E}[\Phi(W(t+1))|W(t)]$.

The proof of Lemmas 1 and 2 are built on the model of Berenbrink et al. for load balancing, details are displayed in the appendix. To overcome general understanding problems, we define $\mathbb{E}[W_{k,\ell}]$ to be the average total load of UEs which move from RB k to RB ℓ. Without loss of generality, we assume that $w_1 \geq w_2 \geq \cdots \geq w_m$. Further, $\forall k \in M$, let $S_k(t)$ be the set of UEs using RB k at time t and let u be the index of a given UE, we have what follows :

$$\begin{aligned}
\mathbb{E}[W_{k,\ell}] &= \sum_{u\in S_k} P^u_{k,\ell} = \frac{w_k - w_\ell}{b(m-b+1)} \\
&\leq \left(\frac{w_k - w_\ell}{m}\right)
\end{aligned}$$

Lemma 1.

$$\begin{aligned}
&\sum_{k=1}^{m}(\mathbb{E}[(W_k(t+1))|W_k(t)=w_k]-\bar{w})^2 < \\
&\Phi(W) - \sum_{k=1}^{m}\sum_{\ell=k+1}^{m} 2\mathbb{E}[W_{k,\ell}](w_k - w_\ell)
\end{aligned} \tag{4.4.3}$$

Lemma 2.

$$\begin{aligned}
&\sum_{k=1}^{m} Var[(W_k(t+1))|W_k(t)=w_k] \\
&\quad \leq 2\sum_{k=1}^{m}\sum_{\ell=k+1}^{m}\mathbb{E}[W_{k,\ell}]
\end{aligned} \tag{4.4.4}$$

Lemma 3.

$$\begin{aligned}\mathbb{E}[\Phi(W(t+1))|W(t)] &< \Phi(W(t)) \\ -\sum_{k=1}^{m}\sum_{\ell=k+1}^{m} 2\mathbb{E}[W_{k,\ell}](w_k - w_\ell)\end{aligned} \tag{4.4.5}$$

Recall that $w_k > w_\ell + 1$, otherwise $\mathbb{E}[W_{k,\ell}] = 0$. Hence, we get $w_k - w_\ell > 1$ and thus $w_k - w_\ell > (w_k - w_\ell - 1)$. From Equation (4.4.2) and both previous Lemmas, this lemma holds.

Lemma 4.

$$\mathbb{E}[\Phi(W(t+1))|W(t)] < \Phi(W(t))(1 - \frac{8}{(m+2)}) \tag{4.4.6}$$

By definition, $\mathbb{E}[W_{k,\ell}] = \frac{w_k - w_\ell}{b(m-b+1)}$. Since $\Phi(W) = \frac{1}{m}\sum_{k=1}^{m}\sum_{\ell=k+1}^{m}(w_k - w_\ell)^2$, we deduce that

$$\sum_{k=1}^{m}\sum_{\ell=k+1}^{m}\mathbb{E}[W_{k,\ell}]\,(w_k - w_\ell) = \frac{m\Phi(W)}{b(m-b+1)}$$

Furthermore, from Lemma 3, we have that $\mathbb{E}[\Phi(W(t+1))|W(t)] < \Phi(W(t)) - 2\frac{m\Phi(W(t))}{b(m-b+1)}$. Given that $m \geq b > 0$ for any b since $b \in M$ is the number of used RBs, by computation, we have that $\frac{m}{b(m-b+1)} \geq \frac{2}{(m+2)}$ and hence this lemma holds.

From Lemma 4, we have that $\mathbb{E}[\Phi(W(t+\tau))|W(t)] \leq \Phi(W(t))(1 - \frac{8}{(m+2)})^\tau$. From the definition of $\Phi(W)$, we have that $0 \leq \Phi(W) \leq \bar{w}^2$. Hence, after $\tau = m\log(\bar{w})$ steps, $\mathbb{E}[\Phi(W(t+\tau))|W(t)] \leq \bar{w}(1 - \frac{8}{(m+2)})^{m\log(\bar{w})} \leq 2$.

By Markov's inequality, the probability that $W(t+\tau)$ is a Nash equilibrium is greater than 1/2. Now for each new run of τ steps, the probability to reach a Nash Equilibrium is at least 1, hence the expected time to reach such a PNE is at most 2τ. Hence the theorem holds. □

4.5 Simulation results

We consider a system of 19 hexagonal eNodeBs, we only consider the performances in eNodeBs with 6 surrounding eNodeBs and suppose that further away eNodeBs do not interfere with them. UEs are uniformly disposed in every cell. eNodeBs have a frequency reuse of 1, with PRBs bandwidth of 180 KHz. Simulations were conducted for several LTE frequency bands : $\{1.4, 3, 5, 10, 15, 20\}$ MHz. The distance between two neighboring eNodeBs is 2 Km and transmission power is constant and set to 20 Watt (43 dBm). The propagation loss factor is set to 3.

4.5.1 Convergence

We assessed through extensive simulations the convergence of our proposed algorithm to PNE. We are interested in evaluating in what follows the speed of convergence of our Distributed Load Balancing scheme (denoted DLB). In Figure 4.1, the mean number of iterations to reach convergence is drawn as a function of the number of RBs for a constant load of 50%. 400 simulations were run for every scenario. The results show that convergence time increases linearly as a function of the number of RBs as proven in the previous section. Since the number of possible strategies depend on the number of RB, when the number of RBs becomes high, there are much more strategies for the algorithm to test, which leads to a longer convergence time. Further, we deduce that our algorithm is much more suited for relatively narrow band systems with a small amount of RBs.

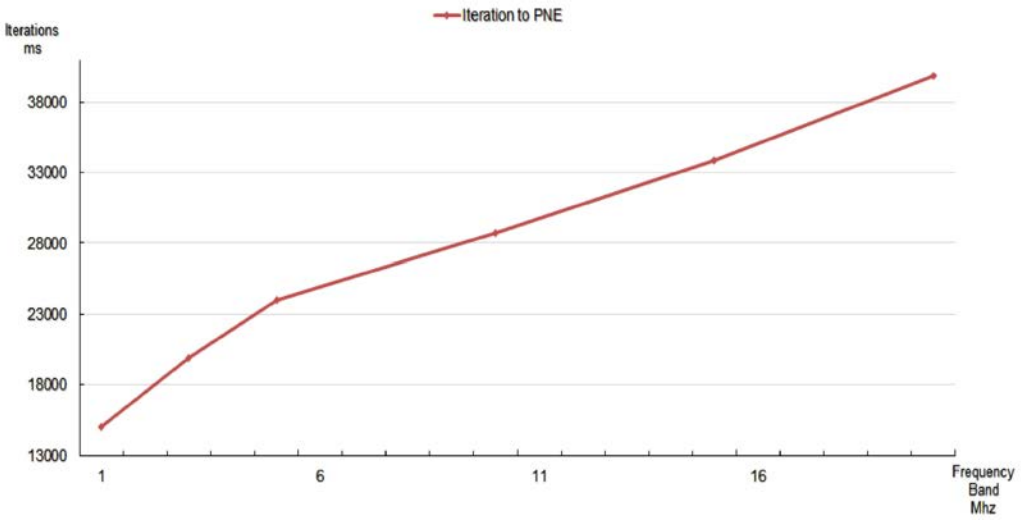

FIGURE 4.1: Convergence time as a function of frequency band

In Figure 4.2, we evaluate the impact of load on convergence time. Simulations were run with a frequency band of 5 MHz (25 RBs) and a load varying from 10% to 80%. The results show that convergence time increases linearly as a function of load which again verifies the proven bound on convergence time.

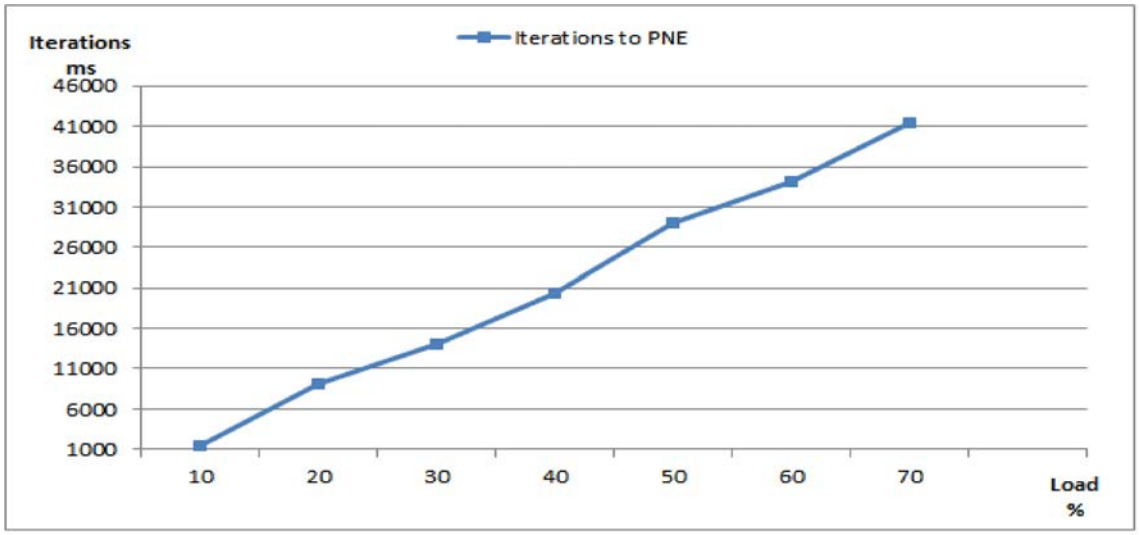

FIGURE 4.2: Convergence time as a function of load

4.5.2 Performances

To corroborate the good performances of the proposed scheme, we compared it against a trivial algorithm that selects randomly RBs in any cell once and for all. In Figure 4.3, the mean cost, which is an image of average interference, is depicted for a bandwidth of 5 MHz and a load spanning from 10% to 80%. For our distributed algorithm, we reported the mean cost after 100 iterations and after convergence is reached. We can clearly see that the major part of improvement is achieved during the first 100 iterations in comparison with the trivial algorithm. If we consider that an iteration is equivalent to a TTI (1ms), this result is quite attractive since we obtain good results for any eNodeB before its neighboring eNodeBs send new RNTP messages where certain RBs may be precluded due to the advertised high power on them.

In the lower sub-figure, the mean relative change of cost is displayed where the relative change in eNodeB i is given by $\frac{c_i^{DLB} - c_i^{Random}}{c_i^{Random}} * 100$ with c_i^{DLB} and c_i^{Random} are the cost function according to equation (4.3.1) for our distributed load balancing game and the random algorithm respectively. We capture results at three different instants : $\{100, 200, convergence\}$ iterations. In particular, we notice an improvement greater than 20% for a load smaller than 40% in a time coherent with the RNTP signaling time, the impact of load at high level is due to the fact that the majority of RBs are already selected, and there is fewer chance for the algorithm to improve the resource allocation.

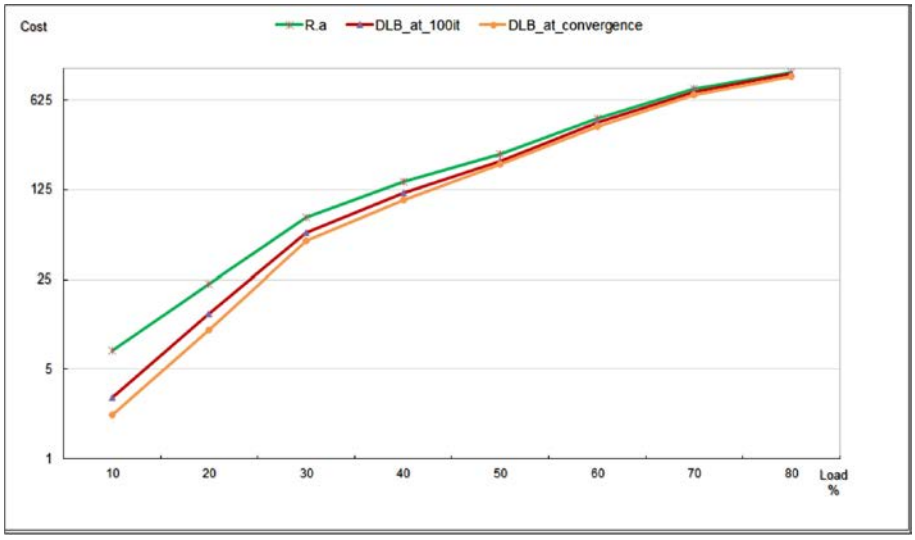

(a) Mean Cost

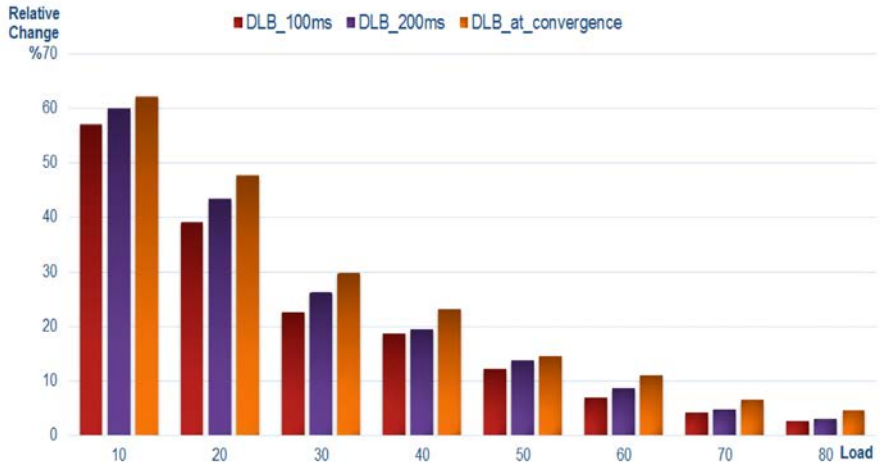

(b) Relative Change in Cost

FIGURE 4.3: Random algorithm vs. Distributed Load Balancing algorithm as a function of Load

Again, we conducted in Figure 4.4 further simulations to show the impact of the total available number of RBs at a moderate load (50%). We conclude from those results that the improvement achieved in comparison with the random approach decreases when the available bandwidth increases. In fact, when the number of UEs is relatively small in comparison with the available resources, there is limited latitude to achieve improvement.

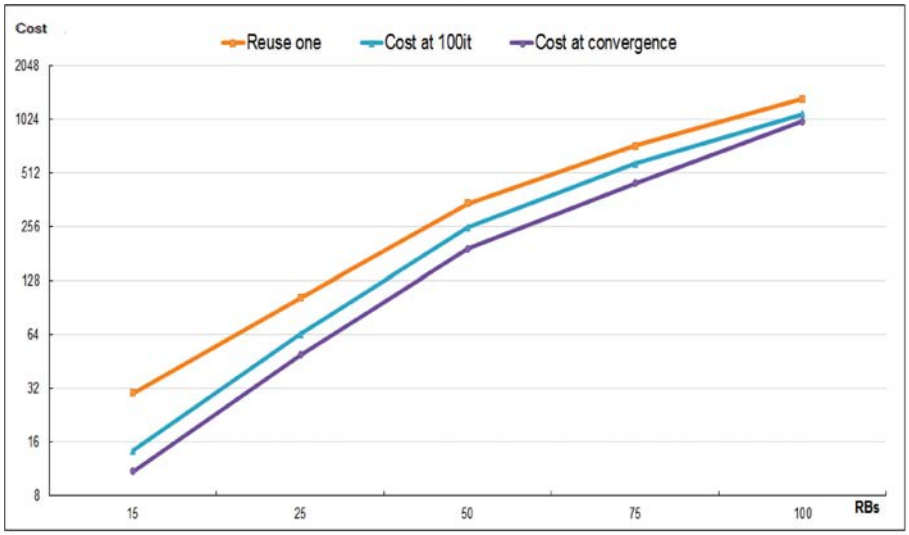

(a) Mean Cost

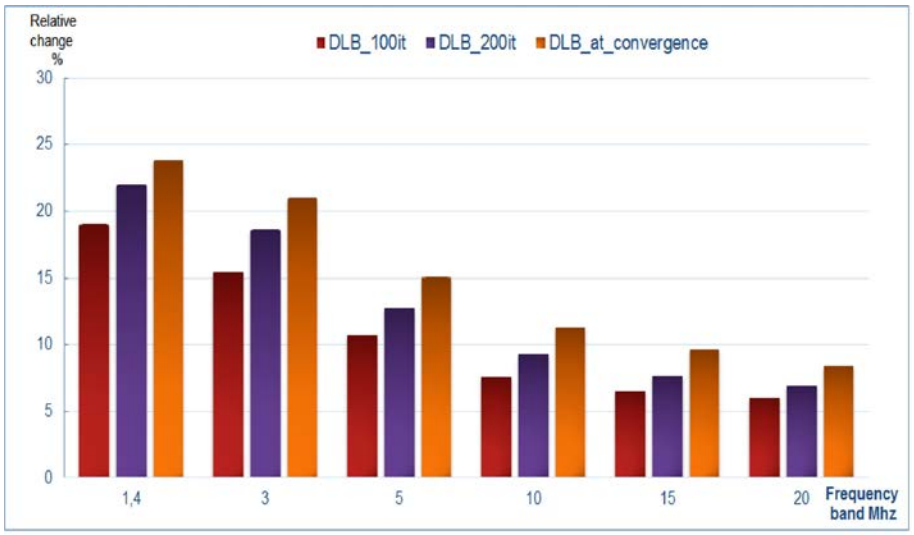

(b) Relative Change in Cost

FIGURE 4.4: Random algorithm vs. Distributed Load Balancing algorithm as a function of Frequency Band

4.6 Conclusion

In this chapter, RBs are judiciously assigned in LTE or OFDM based networks in the scope of Inter-Cell Interference coordination process. We proposed a fully distributed load balancing algorithm to reach the PNE of the portrayed game where eNodeBs only rely on local information. Proof of convergence in a finite time to PNE is provided and good performances of the proposed approach are assessed through extensive simulations.

Chapitre 5

A Greedy approach of Distributed Load Balancing Game for ICIC

This chapter reconsiders the problem tackled in Chapter 4 where the ICIC resource selection process is apprehended as a load balancing game in the downlink of a cellular OFDMA system. However, contrary to the work displayed in the previous chapter, we consider here the impact of UEs distance from their serving eNodeB. Unfortunately, the increased accuracy in the network model is obtained at the cost of increased complexity. Hence, we only provide proof of convergence of the proposed algorithm to PNE but without any guarantee of convergence in a bounded time. However, we propose here a greedy algorithm that gives interesting performance results, and reaches stability in a time coherent with RNTP signaling time[ARK+14b]

5.1 Introduction

In this chapter, the model at hand is an exact potential game that is known to have at least one PNE, since the potential function is strictly decreasing in any sequence of pure best responses [Ros73]. A stochastic version of the best-response dynamics, where agents only have a local view of the system, has been investigated by Berenbrink et al. [AB12, BFHH12]. We adapt the proposed approach where eNodeBs are able to simultaneously change their strategy in a distributed way with a local view of the system. The result of the devised coordination process in each cell will be a pool of RBs that is not too highly interfered and can then be used for fast intra-cell scheduling by the eNodeB. Extensive simulations were conducted to assess the convergence of the adapted distributed algorithm to PNEs. The rest of the chapter is organized as follows. The system model and cost characterization are given in Section 5.2. The RB selection scheme is presented as a non-cooperative congestion game in Section 5.3. The distributed learning algorithm is presented

in Section 5.4. Simulation results are portrayed in Section 5.5. Conclusion is given in Section 5.6.

5.2 The network model

We use the reference model of Section 2.1 presented in Chapter 2. However, to model the amount of interference endured by eNodeBs, we consider the SINR which is a much more exact performance indicator. In particular, we consider the bit transfer time defined in (2.1.4) where the position of UEs is accounted for.

5.3 Congestion game for RBs selection

Non-Cooperative game theory is a good fit to model the decentralized ICIC where selfish eNodeBs share common resource blocks in a way to enhance their own local performances. We adopt the multi-player game $\mathcal{G}$ between the n eNodeBs defined in Section 2.2 while using the same cost function of Chapter 3. Recall that the cost function of eNodeB i that selected strategy x_i is as follows :

$$\begin{aligned} c_i(x_i, X_{-i}) &= \sum_{k\in M}\sum_{u\in\mathcal{U}} x_{i,k}\cdot T_{i,k,u} \\ &= \sum_{k\in M}\sum_{u\in\mathcal{U}} x_{i,k}\frac{\sum_{\substack{j\in N,\\ j\neq i}} x_{j,k}\cdot H_{i,j}}{H_{i,u}} \end{aligned} \tag{5.3.1}$$

Any eNodeB will single out the strategy that minimizes the total bit transfer time in its cell.

The potential game at hand is a congestion game where players may differ from one another in their intrinsic preferences (the benefit they get from using a specific RB), their contribution to congestion, or both. In fact, the cost sustained by a given eNodeB on any selected RB depends indeed upon the congestion impact inflected by other BSs sharing the same RB. In other words, the cost of each player depends on the selected resources and the number of players choosing the same resources. In particular, $T_{i,k,u}$ is increasing in the number of UEs affected simultaneously to RB k.

5.4 Distributed learning of PNE

In [AB12, BFHH12], Berenbrinck et al. studied distributed load balancing in networks with selfish players. The proposed algorithm proceed in a round-based fashion. Players are initially assigned arbitrarily to the machines. In each round, every player picks a

neighboring machine at random and decides probabilistically whether or not to migrate to that machine. Rapid convergence to PNE of such protocols is proved.

In our case, every eNodeB (player) may choose concurrently many RBs (machines). Hence, we need to adapt our game so that we can implement one of the proposed protocols by Berenbrinck. Accordingly, we put forward an adapted algorithm in chapter 4 deemed algorithm 1 to reach the PNE : the system starts with an initial state where RBs are randomly alloted in any eNodeB such as all UEs are served ; then, in each round, every eNodeB migrates randomly and uniformly only one UE from an occupied RB to an available RB. In that case, our game boils down to a load balancing game according to algorithm 2 sketched hereafter.

Algorithm 2 Distributed Load Balancing Algorithm

1: At each iteration
2: **for** i = 1 to n **do**
3: eNodeB i selects a RB l uniformly at random among the b used RBs
4: eNodeB i selects a free RB j uniformly at random in $m - b$ (strategy x'_i)
5: **if** $(c_i(x_i, X_{-i}) > c_i(x'_i, X_{-i}))$ **then**
6: Change strategy (go to RB j) with probability $1 - \frac{c_i(x'_i, X_{-i})}{c_i(x_i, X_{-i})}$
7: **end if**
8: **end for**

To compute the cost of the former strategy (x_i) and actual strategy (x'_i), any eNodeB i makes use of signaling information already present in the downlink of an LTE system.

Although eNodeBs update their strategies in parallel, we noticed through extensive simulations portrayed in Section 5.5, that algorithm 2 is slow in convergence for systems with more than 25 RBs. Therefore, we propose another greedy version deemed algorithm 3 (Greedy algorithm) where,in parallel and for each iteration, every eNodeB re-affects randomly and uniformly all its UEs to the RBs according to the algorithm sketched below (we denote by n_i the number of UEs present in cell of eNodeB i).

Algorithm 3 Greedy algorithm

1: At each iteration
2: **for** i = 1 to n **do**
3: **for** l= 1 to n_i **do**
4: eNodeB i selects a RB uniformly at random among the $m - (l - 1)$ available RBs
5: **end for**
6: **if** $(c_i(x_i, X_{-i}) > c_i(x'_i, X_{-i}))$ **then**
7: Change strategy with probability $1 - \frac{c_i(x'_i, X_{-i})}{c_i(x_i, X_{-i})}$
8: **end if**
9: **end for**

Algorithm 3 is still a load balancing game if we consider that UEs in each cell are the

actual players. In that case, one RB is alloted to a UE (player) at a time. The eNodeB simply plays the role of a central entity that forbids the selection of the same RB by different UEs. Algorithm 2 is a regular load balancing game and is deemed to converge to PNE. However, for algorithm 3, we rely on extensive simulations to assess the convergence to PNEs.

5.5 Simulation results

We consider a system of 19 hexagonal eNodeBs, we only consider the performances in eNodeBs with 6 surrounding eNodeBs and suppose that further away eNodeBs do not interfere with them. Two zones are taken into account : zone 1 which stands for cell-center UEs located at a distance smaller than $R_0 = 0.5Km$ and zone 2 stands for cell-edge UEs located at a distance ranging between $R_0 = 0.5Km$ and $R_1 = R_{cell} = 1Km$. UEs are uniformly distributed in every cell. We assume that for cell-center UEs 64-QAM modulation is used while for cell-edge UEs 16-QAM modulation is used. The eNodeBs have a frequency reuse of 1, with PRBs bandwidth of 180 KHz. Simulations were conducted for several LTE frequency bands : $\{3, 5, 10, 15, 20\}$ MHz. The distance between two neighboring eNodeBs is 2 Km and transmission power is constant and set to 20 Watt (43 dBm). The propagation loss factor is set to 3.

5.5.1 Speed of convergence

We assessed through extensive simulations the convergence of algorithm 2 and algorithm 3 to PNE. We are interested in evaluating in what follows the speed of convergence of both algorithms. In Figure 5.1, the mean number of iterations to reach convergence is drawn as a function of the number of RBs for a constant load of 50%. 400 simulations were run for every scenario. We notice that although algorithm 2 converges faster for 15 RBs, the greedy algorithm largely outruns it for wider system bandwidths. Changing several RBs at the same time allows algorithm 3 to test relatively more strategies which leads to shorter convergence time.

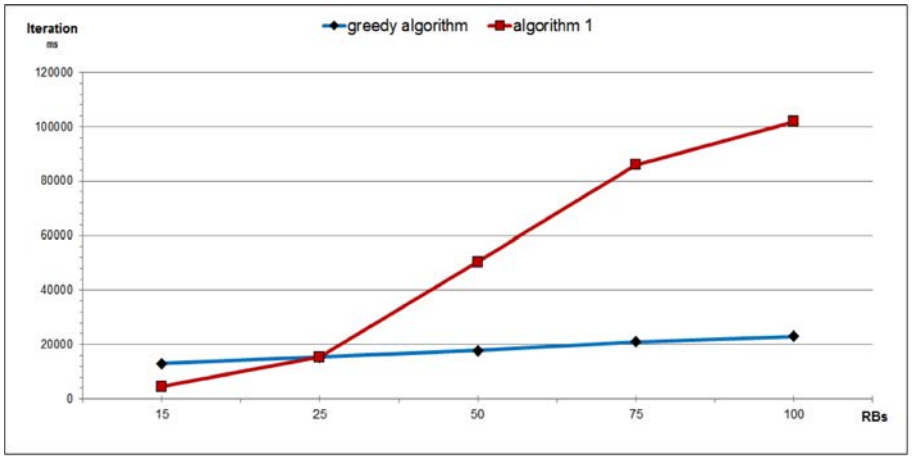

FIGURE 5.1: Speed of convergence as a function of frequency band

In Figure 5.2, we evaluate the impact of load on convergence time. Simulations were run with algorithm 3 with a frequency band of 20 MHz (100RB) and a load varying from 10% to 80%. The results show that convergence time increases linearly as a function of load which is a desired property.

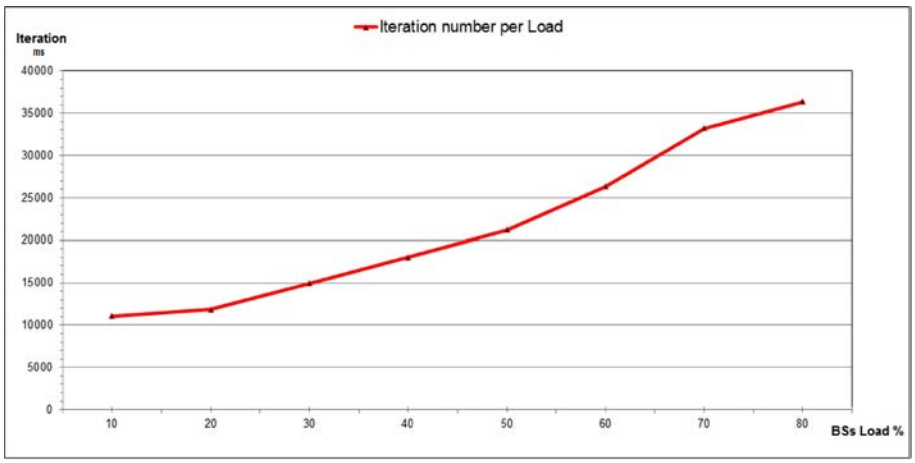

FIGURE 5.2: Speed of convergence as a function of load

5.5.2 Performances

To corroborate the good performances of algorithm 3, we compared it against a trivial approach (deemed trivial algorithm) that selects randomly RBs in any cell once and for all. In Figure 5.3, the mean cost (in ms) for algorithm 3 and trivial algorithm is depicted as a function of load for a frequency band of 20 MHz. For algorithm 3, we show results after 100 ms and after convergence is reached. In the lower subfigure, the mean relative change of cost

is displayed where the relative change in eNodeB i is given by $\frac{c_i^{Algo3}-c_i^{Triv}}{c_i^{Triv}} * 100$ with c_i^{Algo3} and c_i^{Triv} are the cost function according to equation (4.3.1) for algorithm 3 and trivial algorithm respectively. We captured results at three different instants : $\{100, 200, 1000\}$ iterations (ms).

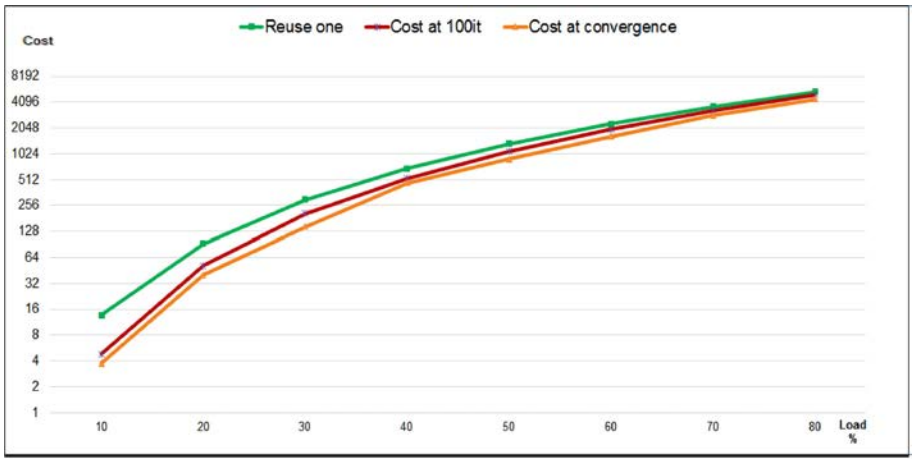

(a) Mean Cost

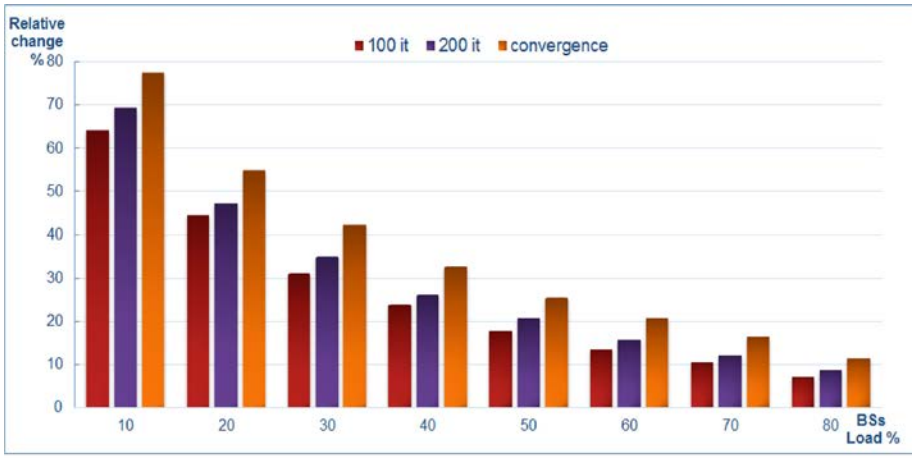

(b) Relative Change

FIGURE 5.3: Trivial algorithm vs. Greedy algorithm as a function of load

We can clearly see that the major part of improvement is achieved during the first 100 iterations in comparison with the trivial algorithm. If we consider that an iteration is equivalent to a TTI, this result is quite attractive since we obtain very good results before that neighboring eNodeBs exchange the RNTP (Relative Narrow-band Transmit Power) message where certain RBs may be precluded due advertised high interference on them. This behavior represent the strength of our algorithm. The relative change in the lower subfigure further highlights the good performances of our algorithm.

We conducted further simulations displayed in Figure 5.4 to show the impact of the total

available number of RBs at a load of 50%. We conclude from those results that the improvement achieved in comparison with the trivial approach decreases when the available bandwidth increases, in fact when the number of available RBs in the cell grows, the number of possibility become so high that finding a strategy that satisfies every one is difficult, hence, this leads to a lower improvement when the system bandwith grows.

(a) Mean Cost

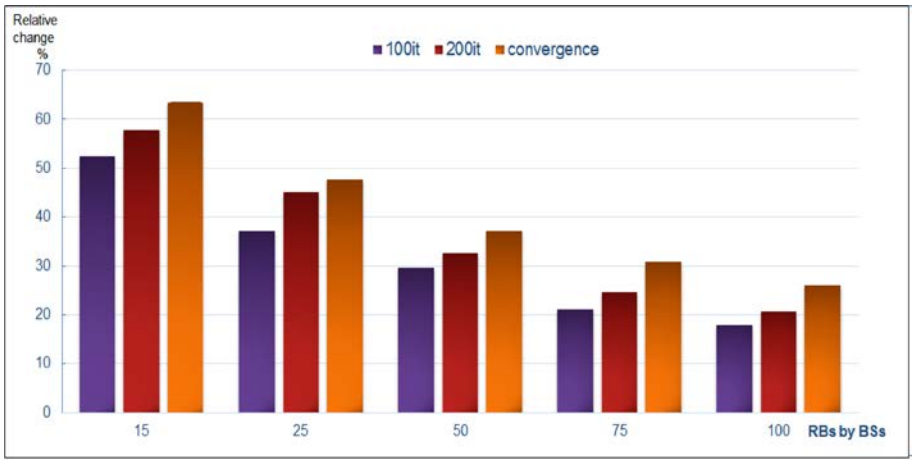

(b) Relative Change

FIGURE 5.4: Trivial algorithm vs. Greedy algorithm as a function of frequency band

5.5.3 Non homogeneous UEs distribution

We were interested in the behavior of the algorithm in a realistic non homogeneous UEs distribution in any cell. Two cases were handled :

– In the first scenario, the edge zone of the eNodeB is crowded (the majority of UEs are situated on the cell periphery),
– While in the second scenario, the center zone is crowded (the majority of UEs are close

to the eNodeB).

We show in this simulation the relative change between a random algorithm that selects randomly RBs in any cell once and for all, and our greedy algorithm.

Figure 5.5 shows the first scenario where 75% of the UE are situated in the cell-edge. In this case, the performance of the greedy algorithm decreased in comparison with the previous results (Chapter 5.5.2), this can be explained as most of the UEs are interfering with each other, which impacts negatively the channel quality of all the UEs. This case corresponds to a loaded scenario, except there are more free RBs, and hence, the algorithm manages to minimize the interference better than a fully loaded system.

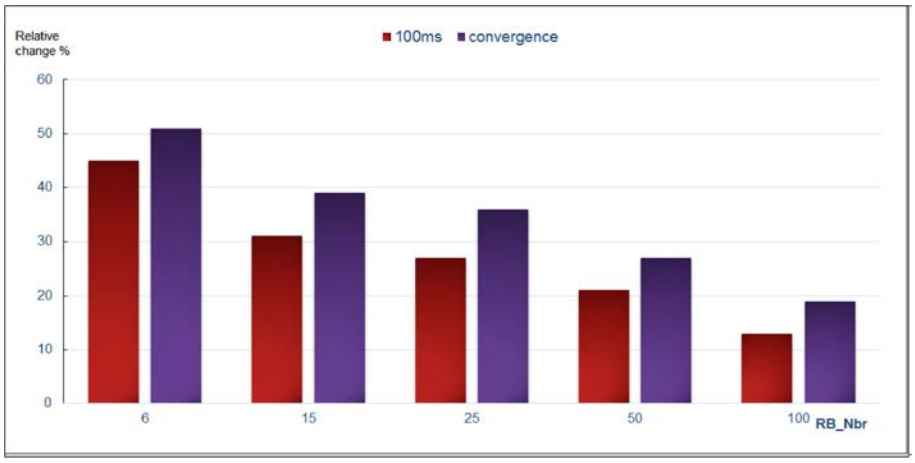

FIGURE 5.5: Greedy algorithm with crowded cell-edge

Figure 5.6 shows the case where 75% of the UEs are in the cell-center. Since UEs are far from neighboring cells, their channel quality is good, and hence, the greedy algorithm manages to allocate the RBs in a way that strongly boosts the performance of the system by decreasing the interference.

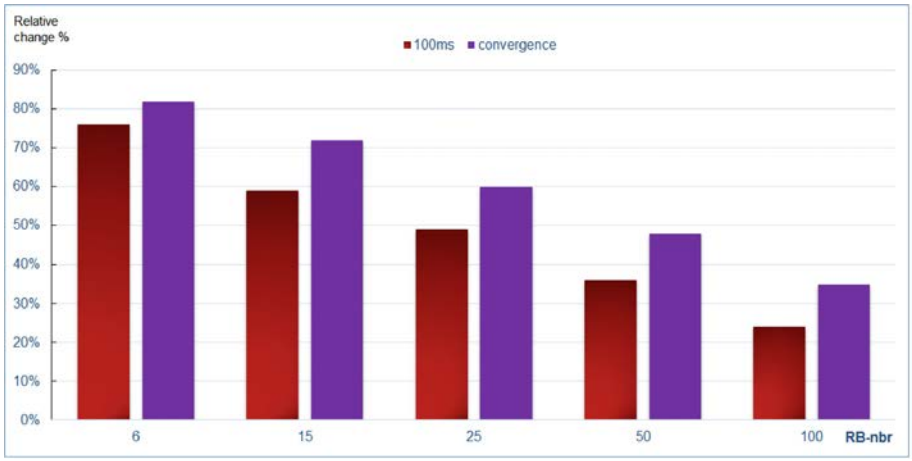

FIGURE 5.6: DLB algorithm with crowded cell-center

We can say that our algorithm is robust against any UE distribution with the advantage of using frequency reuse 1 contrary to the SFR scheme that is static and performs badly with non-uniform scenarios since there is no way to change the resource allocation along with the users distribution [YDH+10].

5.6 Conclusion

In this chapter, we smartly allocated the resources in the system to avoid the inter-cell interference. Using a load balancing game theoretic approach that is fully distributed shows good improvement over basic allocation. Hence, the enhanced greedy algorithm allows to obtain results in a time consistent with the signaling message latency, especially the RNTP message. This can be used to obtain better performance in a semi-distributed system that takes advantage from the RNTP message. Furthermore, using the RNTP message as an initial state will be addressed in future work.

Chapitre 6

Power Control for Distributed Inter-Cell Interference Coordination

This chapter addresses the problem of power control for ICIC in the downlink of cellular OFDMA systems. The power level selection process of resource blocks is apprehended as a sub-modular game. Here again, the existence of Nash equilibriums for that type of games shows that stable power allocations can be reached by selfish eNodeBs. We put forward a semi distributed algorithm based on best response dynamics to attain the NEs of the modeled game. Based on local knowledge conveyed by the X2 interface in LTE networks, each eNodeB will first select a pool of favorable RBs with low interference. Second, each eNodeB will strive to fix the power level adequately on those selected RBs realizing performances comparable with the Max Power policy that uses full power on selected RBs while achieving substantial power economy. Finally, we compare the obtained results to an optimal global solution, which is derived by solving an integer linear program. Hence, we are able to quantify the efficiency loss of the distributed game approach. It turns out that even though the distributed game results are sub-optimal, the low degree of system complexity and the inherent adaptability make the decentralized approach promising especially for dynamic scenarios[KAL+14].

6.1 Introduction

Contrary to previous chapters that stressed on RB selection for ICIC, we propose in this chapter to reduce ICI through efficient Power Control. Power control does not only reduce the impact of interfering signals by lowering their power level (signals usually belonging to cell-center UEs), but it can increase the power level on resource blocks that suffer of bad

radio conditions (usually RB allocated for cell-edge UEs). Therefore, it is considered as a method for ICIC. Here again, we have recourse to non-cooperative game theory to model the way selfish eNodeBs compete in a distributed manner for limited resources. Devising an optimal power level selection scheme depends on the existence of Nash equilibrium for the present game. In this chapter, we prove that the model at hand is a sub-modular game (see [Top79, Yao95]). Such games have always a Nash Equilibrium and it can be attained using a best response type algorithm (called algorithm I in both references). The result of the devised coordination process in each cell will be the power tuning on the least interfered RBs.

The rest of the chapter is organized as follows. The system model is given in Section 6.2. In Section 6.3, the framework of the RB selection and power control schemes is described. The power level selection scheme is presented as a non-cooperative sub-modular game in Section 6.4 where a semi distributed learning algorithm based on best response dynamics is presented in Subsection 6.4.2. Simulations results are portrayed in Section 6.5. The optimal centralized approach is given in Section 6.6 as a benchmark to evaluate the price of anarchy resulting from a decentralized approach. Conclusion is given in Section 6.7.

6.2 The system model

We consider the same system model described in Chapter 2, the UE distance is otherwise considered with a dynamic power control achieved with the proposed algorithm.

6.2.1 Data rate on the downlink

The SINR observed on RB k allotted to UE u in eNodeB i can be expressed as :

$$SINR_{i,k,u} = \frac{P_0 \cdot G_i \cdot p_{i,k} \cdot (\frac{1}{d^i_{u,i}})^\beta}{P_0 \cdot \sum_{\substack{j \in M, \\ j \neq i}} G_j \cdot p_{j,k} \cdot (\frac{1}{d^i_{u,j}})^\beta + P_N} \tag{6.2.1}$$

where P_0 represents the maximal transmitted power per RB, P_N represents the thermal noise power per RB, G_i the antenna gain of eNodeB i, $d^i_{u,j}$ is the distance between eNodeB j and UE u served by eNodeB i and β is the path-loss factor varying between 2 and 6. Finally, $p_{i,k}$ is the discrete variable that represents a fraction of the maximal transmitted power P_0. Hence, $p^l_{i,k} = P_0 \cdot p_{i,k}$ is one of the possible N_l power levels in eNodeB i on RB k allotted to UE u. It varies between $p^l_{i,k} = 0.0$ where RB k is not selected by eNodeB i and $p^l_{i,k} = P_0$ where full power is transmitted on that RB. However, our power control starts after the selection of a pool of RBs in any eNodeB i, denoted by N_i. Hence, $p^l_{i,k} \neq 0.0$.

We denote by $D_{i,k,u}$ the data rate achieved by UE u on RB k in eNodeB i given by what

follows :

$$D_{i,k,u} = \frac{W}{E_b/N_0} \cdot SINR_{i,k,u},$$

where W is the bandwidth per RB. Given a target error probability, it is necessary that $E_b/N_0 \geq \gamma$, for some threshold γ which is UE specific.

Each cell will be logically divided into N_Z concentric discs of radii R_z, $z = 1, ..., N_Z$, and the area between two adjacent circles of radii R_{z-1} and R_z is called zone z, $z = 1, ..., N_z$. UEs belonging to the same zone z have the same radio conditions leading to the same γ_z and the same mean rate per zone $D_{i,k,z}$ according to what follows :

$$\begin{aligned} D_{i,k,z} &= \frac{\frac{W}{\gamma_z} \int_{R_{z-1}}^{R_z} \rho_{zmobile} \frac{2\pi r dr}{r^\beta} \cdot G_i \cdot P_0 \cdot p_{i,k}}{P_0 \cdot \sum_{\substack{j \in M, \\ j \neq i}} G_j \cdot P_{j,k} \cdot \frac{1}{(d^i_{i,j})^\beta} + P_N} \\ &= \frac{\frac{W}{\gamma_z}(R_z^{2-\beta} - R_{z-1}^{2-\beta}) \cdot \rho_{zmobile} \cdot G_i \cdot P_0 \cdot P_{i,k}}{P_0 \cdot \sum_{\substack{j \in M, \\ j \neq i}} P_{j,k} \cdot \frac{G_j}{(\delta^z_{i,j} \cdot R_{cell})^\beta} + P_N} \end{aligned} \tag{6.2.2}$$

where R_{cell} is the cell radius. As for interference, we consider mainly for simplification the impact of eNodeB j on eNodeB i by replacing $d^i_{u,j}$ by $d^i_{z,j} = \delta^z_{i,j} \cdot R_{cell}$ the distance between eNodeB i and eNodeB j (the value of $\delta^z_{i,j}$ depends on how far is eNodeB j from zone z of eNodeB i).

6.2.2 Cost function

We denote by $T_{i,k,z}$ the amount of time necessary to send a data unit through RB k in eNodeB i for UEs in zone z. In fact, the delay needed to transmit a bit for a given UE is the inverse of the data rate perceived by this UE :

$$T_{i,k,z} = \frac{I_{i,k,z}}{x_{i,k}} \tag{6.2.3}$$

where $I_{i,k,z}$ is given by :

$$I_{i,k,z} = \frac{\sum_{\substack{j \in M, \\ j \neq i}} P_{j,k} \cdot H^z_{i,j} + P_N}{H_{i,z}} \tag{6.2.4}$$

where $H^z_{i,j} = \frac{P_0 G_j}{(\delta^z_{i,j} \cdot R_{cell})^\beta}$ captures distance-dependent attenuation of power between eNodeB j and eNodeB i and $H_{i,z} = \frac{W}{\gamma_z}(R_z^{2-\beta} - R_{z-1}^{2-\beta}) \cdot \rho_{zmobile} \cdot G_i$ captures distance-dependent attenuation of power inside zone z of eNodeB i.

We denote by N^i_z the pool of RBs used by UEs in zone z. eNodeB i will pay an amount α_z per power unit for the use of a given RB $k \in N^i_z$. This power unitary cost can decrease with the zone index to further protect UEs that are far away from the antenna ; or it can increase to favor cell-center UEs in order to enhance overall performances.

Accordingly, the goal of the power control scheme proposed in this chapter is to minimize the following cost function in eNodeB i for RB k allotted to a UE in zone z :

$$c_{i,k,z} = \begin{cases} \kappa \cdot T_{i,k,z} + \alpha_z \cdot P_0 \cdot y_{i,k}, & \text{if RB } k \text{ is used by eNodeB } j, \\ 0 & \text{If RB } k \text{ is not used in zone } z. \end{cases} \tag{6.2.5}$$

where κ is a normalization factor.

6.3 Proposed ICIC scheme

In this chapter, we propose that each eNodeB aggregates information about transmit power levels in adjacent cells and decides accordingly to choose the pool of RBs per zone. Recall that the RNTP indicator, received from neighboring eNodeBs every 200 TTI through the X2 interface, advertises on which RBs a neighboring eNodeB will use full power. In any eNodeB i, we associate with every RB k a variable $a_{i,k}$. This variable indicates the number of neighboring eNodeBs (thus $0 \leq a_{i,k} \leq 6$) that advertised the use of that same RB k with full power via the RNTP indicators. Thus, every eNodeB i updates its variables $a_{i,k}$ approximately every 200 TTI and makes use of those variables to update the pool of selected RBs per zone as described in algorithm 4 where n_z^i is the number of UEs in zone z of eNodeB i. Recall that N_z^i is the pool of RBs reserved to UEs in zone z.

Algorithm 4 Selecting the pool of RBs per zone

```
Every 200 TTI
for i=1 TO n do
    for k=0 TO m do
        eNodeB i updates the a_{i,k} variables according to the RNTP indicators.
        The updated a_{i,k} variables are sorted in ascending order list L_i.
        for z=0 TO N_Z − 1 do
            The n_z^i top values of L_i are a reserved pool RBs for UEs in zone N_Z − z
    (denoted by N_z^i) and removed from the sorted list.
        end for
    end for
end for
```

The idea behind the algorithm is to reserve the pool of least interfered RBs to UEs who are the furthest away from the eNodeB (the zones with the highest index). After selecting N_z^i, every eNodeB i proceeds to implementing the power control distributed algorithm described in the following section and which is the focal point of the chapter. We assume that the scheduler has already assigned UEs in a given zone z to RBs in N_z^i. Afterwards, our proposed power control scheme endeavors to find the optimal power levels on those allocated RBs. After convergence of the latter, each eNodeB i will obtain the optimal

power level $P^*_{i,k,z}$ to be assigned to RB k in zone z.

6.4 Non-cooperative game for power control

We define a multi-player game $\mathcal{G}$ between the m eNodeBs that make their decisions without knowing the decisions of each other.

The formulation of this non-cooperative game $G = \langle N, S, C \rangle$ can be described as follows :

- A finite set of players $M = (1, ..., m)$ and a finite set of RBs $N = (1, ..., n)$.
- For each eNodeB i, the space of strategies S_i is formed by the Cartesian product of each set of strategies $S_i = S_{i,1} \times ... \times S_{i,n}$, where n is the total number of RBs. An action of a eNodeB i is the amount of power $x_{i,k}$ sent on RB k. If RB $k \in N^i_z$ then $S_{i,k} = \{x^0_{i,k}, ..., x^{N_l-1}_{i,k}\}$ where $x^j_{i,k}$ is a fraction of P_0, else $S_{i,k} = \emptyset$. The strategy chosen by eNodeB i is then $X_i = (x_{i,1}, ..., x_{i,n})$. A *strategy profile* $X = (X_1, ..., X_m)$ specifies the strategies of all players and $S = S_1 \times ... \times S_m$ is the set of all strategies.
- A set of cost functions $C = (C_1(X), C_2(X), ..., C_m(X))$ that quantify players costs for a given strategy profile X where $C_i = (c_{i,1,z}, c_{i,2,z}, ..., c_{i,n,z})$ is the cost of eNodeB i where the cost $c_{i,k,z}$ of using RB k in zone z is given in Equation (6.2.5).
  As the frequencies allotted to different RBs are orthogonal, minimization of cost $c_{i,k,z}$ on RB k is done independently of other RBs. Hence, we denote by $x_{-i,k}$ the strategies played by all eNodeBs on the RB k except eNodeB i.

6.4.1 Sub-modular game

In this work, we turn to sub-modularity theory to show existence of Nash equilibriums. Sub-modularity was introduced into the game theory literature by Topkis [Top79] in 1979. Sub-modular games are of particular interest since they have Nash equilibriums, and there exists an upper and a lower bound on Nash strategies of each UE [OR94]. Furthermore, these equilibriums can be attained by using a best response type algorithm ([Top79, Yao95]).

Definition 6.1. Consider a game $G = \langle M, S, C \rangle$ with strategy spaces $S_i \subset \mathbb{R}^m$ for all $i \in M$ and for all $z \in N_Z, k \in N^i_z$. G is sub-modular if for each i and k, $S_{i,k}$ is a sublattice [1] of $\mathbb{R}^m$, and $c_{i,k,z}(x_{i,k}, x_{-i,k})$ is sub-modular in $x_{i,k}$.

Definition 6.2. The cost function $c_{i,k,z}$ is sub-modular iff for all $x, y \in S_{i,k}$,

$$c_{i,k,z}(min(x, y)) + c_{i,k,z}(max(x, y)) \leq c_{i,k,z}(x) + c_{i,k,z}(y) \tag{6.4.1}$$

1. A is a sublattice of $\mathbb{R}^m$ if $a \in A$ and $a' \in A$ imply $a \wedge a' \in A$ and $a \vee a' \in A$

Proposition 2. The cost function $c_{i,k,z}$ is sub-modular for every eNodeB i and every selected RB k.

Démonstration. We begin by defining the set A_1 such that $A_1 = \{x_{j,k}, y_{j,k} \in S_{j,k} | x_{j,k} < y_{j,k}, j \neq i\}$ and A_2 such that $A_2 = \{x_{j,k}, y_{j,k} \in S_{j,k} | x_{j,k} > y_{j,k}, j \neq i\}$. Accordingly, the inequality in (6.4.1) gives the following for $x = (x_{j,k}, j = 1, ..., m)$ and $y = (y_{j,k}, j = 1, ..., m)$ where $x_{j,k}, y_{j,k} \in S_{j,k}$:

$$\begin{aligned}
&\kappa \cdot \sum_{j \neq i} \frac{min(x_{j,k}, y_{j,k}) H^z_{i,j} + P_N}{H_{i,z} min(x_{i,k}, y_{i,k})} + \alpha_z P_0 min(x_{i,k}, y_{i,k}) \\
&+ \kappa \cdot \sum_{j \neq i} \frac{max(x_{j,k}, y_{j,k}) H^z_{i,j} + P_N}{H_{i,z} max(x_{i,k}, y_{i,k})} + \alpha_z P_0 max(x_{i,k}, y_{i,k}) \\
&\leq \kappa \cdot \sum_{j \neq i} \frac{x_{j,k} H^z_{i,j} + P_N}{H_{i,z} x_{i,k}} + \kappa \cdot \sum_{j \neq i} \frac{y_{j,k} H^z_{i,j} + P_N}{H_{i,z} y_{i,k}} \\
&+ P_0 \alpha_z (x_{i,k} + y_{i,k})
\end{aligned} \tag{6.4.2}$$

We notice in (6.4.2) that $P_0 \alpha_z (min(x_{i,k}, y_{i,k}) + max(x_{i,k}, y_{i,k})) = P_0 \alpha_z (x_{i,k} + y_{i,k})$ and $P_N \cdot (m-1)(\frac{1}{min(x_{i,k}, y_{i,k})} + \frac{1}{max(x_{i,k}, y_{i,k})}) = P_N \cdot (m-1)(\frac{1}{x_{i,k}} + \frac{1}{y_{i,k}})$ where m is the total number of eNodeBs. Thus, inequality (6.4.2) simplifies to :

$$\begin{aligned}
&\sum_{j \neq i} \frac{min(x_{j,k}, y_{j,k}) H^z_{i,j}}{min(x_{i,k}, y_{i,k})} + \sum_{j \neq i} \frac{max(x_{j,k}, y_{j,k}) H^z_{i,j}}{max(x_{i,k}, y_{i,k})} \\
&\leq \sum_{j \neq i} \frac{x_{j,k} H^z_{i,j}}{x_{i,k}} + \sum_{j \neq i} \frac{y_{j,k} H^z_{i,j}}{y_{i,k}}
\end{aligned} \tag{6.4.3}$$

Using the sets A_1 and A_2, inequality (6.4.3) is re-written as follows :

$$\begin{aligned}
&\sum_{j \in A_1} \frac{x_{j,k} H^z_{i,j}}{min(x_{i,k}, y_{i,k})} + \sum_{j \in A_2} \frac{y_{j,k} H^z_{i,j}}{min(x_{i,k}, y_{i,k})} \\
&\sum_{j \in A_1} \frac{y_{j,k} H^z_{i,j}}{max(x_{i,k}, y_{i,k})} + \sum_{j \in A_2} \frac{x_{j,k} H^z_{i,j}}{max(x_{i,k}, y_{i,k})} \\
&\leq \sum_{j \in A_1} \frac{x_{j,k} H^z_{i,j}}{x_{i,k}} + \sum_{j \in A_2} \frac{x_{j,k} H^z_{i,j}}{x_{i,k}} \\
&+ \sum_{j \in A_1} \frac{y_{j,k} H^z_{i,j}}{y_{i,k}} + \sum_{j \in A_2} \frac{y_{j,k} H^z_{i,j}}{y_{i,k}}
\end{aligned} \tag{6.4.4}$$

Here, before going further, we need to distinguish two cases :

– Case 1 : $x_{i,k} < y_{i,k}$. In this case, inequality (6.4.4) gives the following :

$$\begin{aligned}
&\sum_{j\in A_1} \frac{x_{j,k}H^z_{i,j}}{x_{i,k}} + \sum_{j\in A_2} \frac{y_{j,k}H^z_{i,j}}{x_{i,k}} \\
&\sum_{j\in A_1} \frac{y_{j,k}H^z_{i,j}}{y_{i,k}} + \sum_{j\in A_2} \frac{x_{j,k}H^z_{i,j}}{y_{i,k}} \\
&\leq \sum_{j\in A_1} \frac{x_{j,k}H^z_{i,j}}{x_{i,k}} + \sum_{j\in A_2} \frac{x_{j,k}H^z_{i,j}}{x_{i,k}} \\
&+ \sum_{j\in A_1} \frac{y_{j,k}H^z_{i,j}}{y_{i,k}} + \sum_{j\in A_2} \frac{y_{j,k}H^z_{i,j}}{y_{i,k}}
\end{aligned} \tag{6.4.5}$$

After some simplifications, inequality (6.4.5) gives what follows :

$$\sum_{j\in A_2} (x_{j,k} - y_{j,k}) H^z_{i,j} (\frac{1}{y_{i,k}} - \frac{1}{x_{i,k}}) < 0 \tag{6.4.6}$$

The latter inequality is obviously true as $x_{j,k} > y_{j,k}, \forall j \neq i$ and $x_{i,k} < y_{i,k}$.

– Case 2 : $x_{i,k} > y_{i,k}$. Similarly to case 1, inequality (6.4.4) simplifies to :

$$\sum_{j\in A_1} (y_{j,k} - x_{j,k}) H^z_{i,j} (\frac{1}{y_{i,k}} - \frac{1}{x_{i,k}}) > 0 \tag{6.4.7}$$

The latter inequality is obviously true as $y_{j,k} > x_{j,k}, \forall j \neq i$ and $x_{i,k} > y_{i,k}$.

□

Since $S_{i,k}$ is a single dimensional finite set, $S_{i,k}$ is a compact sublattice of $\mathbb{R}$. As we proved that the cost function $c_{i,k}$ is sub-modular for every eNodeB i on every selected RB k, our game is indeed sub-modular.

6.4.2 Attaining the Nash Equilibrium

6.4.2.1 The Best Response dynamics

The best response strategy of player i is the one that minimizes its cost given other players' strategies. A best response dynamics scheme consists of a sequence of rounds, each player i chooses the best response to the other players' strategies in the previous round. In the first round, the choice of each player is the best response based on its arbitrary belief about what the other players will choose. In some games, the sequence of strategies generated by best response dynamics converges to a NE, regardless of the players' initial strategies. S-modular games are part of those games.

To reach the NE, [AA03] proposes the following best response algorithm built on an

algorithm called algorithm I in [Top79, Yao95] : there are T infinite increasing sequences T_t^i for $t \in T$ and $i = 1, ..., m$. Player i uses at time T_k^i the best response policy (a feasible one) to the policies used by all other players just before T_k^i. This scheme includes in particular parallel updates (when T_t^i does not depend on t). Once this UE updates its strategy, the strategies of one or more other UEs need not be feasible anymore. In [AA03], proof is given for the following two results :

– If each player i either initially uses its lowest or largest policy in S_i, then the iterative algorithm converges monotonically to an equilibrium (that may depend on the initial state).
– If we start with a feasible policy, then the sequence of best responses monotonically converges to an equilibrium : it monotonically decreases in all components in the case of minimizing in a sub-modular game.

eNodeB i strives to find, for the pool of selected RBs in any zone z, the following optimal power level :

$$P_{i,k,z}^* = P_0 \cdot \arg \quad \min_{x_{i,k}} c_{i,k,z}(x_{i,k}, x_{-i,k}),$$

for $P_0 \cdot x_{i,k} \in \{x_{i,k}^0, ..., x_{i,k}^{N_l - 1}\}$.

By definition, $P_{i,k,z}^*$ is a best response of eNodeB i to the other eNodeBs strategies on RB k in zone z.

6.4.2.2 Distributed learning of NE

In a real environment, a best response type algorithm as the one proposed in [Top79, Yao95] cannot be practically applied as every eNodeB i needs to know the policy of all other eNodeBs $x_{-i,k}$ on every used RB k which necessitates expensive signaling and hinders the benefits of an efficient power control scheme. Fortunately, we can easily render our algorithm distributed by making use of signaling information already present in the downlink of an LTE system. In fact, $x_{-i,k}$ (or equivalently $x_{j,k} \, \forall j \neq i$) only intervene in the total interference $I_{i,k,z}$ endured on RB k in zone z of eNodeB i in equation (6.2.4). Interference can be easily inferred through the CQI sent every TTI by the UEs to which RB k is attributed. However, the eNodeBs should update their transmission powers on selected RBs sequentially in a predefined round robin fashion that need to be set once and for all.

We present in algorithm 5 the pseudo-code of best response algorithm , deemed DBR, which is a power control scheme under best response dynamics in distributed mode for our game.

Algorithm 5 DBR Power control algorithm

$t = 0, \quad conv = 0, stop = 0, NE = 0$
while $NE = 0$ **do**
  for $i = 1$ TO n **do**
    while $stop_i = 0$ **do**
      for $z = 0$ TO $N_Z - 1$ **do**
        while $conv_{i,k} = 0$ **do**
          for $l = 0$ TO $N_l - 1$ **do**
            eNodeB i allocates in parallel all selected RB $k \in N_z^i$ with power $x_{i,k}^l$ to a given UE,
            Serviced UEs send back CQI related to their assigned RB k,
            eNodeB i infers the corresponding value of $I_{i,k,z}(t)$ and then computes $c_{i,k,z}$ for $x_{i,k}^l$ at t,
            eNodeB i computes $P_{i,k,z}^*(t)$ and attributes it to RB k in zone z.
            if $|P_{i,k,z}^*(t+1) - P_{i,k,z}^*(t)| < \epsilon$ ▷ where ϵ is a very small positive quantity **then**
              $conv_{i,k} = 1$
            else
              $conv_{i,k} = 0$
            end if
          end for
        end while
        if $\sum_{k=1}^{m} conv_{i,k} = b$ ▷ where b is the number of active RB **then**
          $stop_i = 1$
        else
          $stop_i = 0$
        end if
      end for
    end while
    if $\sum_{i=1}^{n} stop_i = n$ **then**
      $NE = 1$
    else
      $NE = 0$
    end if
  end for
  $t = t + 1$
end while
Output : Each eNodeB i will obtain the optimal power level $P_{i,k,z}^*$ to be assigned to RB $k \in N_z^i$.

6.5 Simulation Results

We consider a bandwidth of 10 MHz with 50 RBs along with the following parameters listed in the 3GPP technical specifications TS 36.942 : the mean antenna gain in urban zones is 12 dBi (900 MHz). As for noise, we consider the following : UE noise figure 7.0

dB, thermal noise -104.5 dBm which gives a receiver noise floor of $P_N = -97.5$ dBm. We consider 10 hexagonal cells where each cell is surrounded with 6 other cells. The distance between two neighboring eNodeB is 2 Km. Transmission power is 43 dBm (according to TS 36.814) which corresponds to 20 Watts (On the downlink). We set $P_0 = 10$ Watts and $x_{i,k}$ for any eNodeB i on RB k belongs to $\{0.1, 0.2, 0.35, 0.5, 0.6, 0.7, 0.85, 1.0\}$. Various power unitary costs (α_1 ;α_2) were tested and for each scenario 400 simulations were run where in each cell a random number of UEs is chosen in every zone corresponding to a snapshot of the network state. Performances are compared against Max Power policy where full power P_0 is used on all RBs and against Trivial policy where power levels are set at random. For every simulation, 100 runs of Trivial policy were made. Further, for each simulation instance, the same pool of RBs per zone is given for the three policies : DBR, Max Power and Random policy. Hence, results only assess the impact of power control. We consider two zones : zone 1 which stands for cell-center UEs located at a distance smaller than $R_0 = 0.5Km$ and zone 2 stands for cell-edge UEs located at a distance ranging between $R_0 = 0.5Km$ and $R_1 = R_{cell} = 1Km$. We assume that for cell-center UEs we use 64-QAM modulation while for cell-edge UEs we use 16-QAM modulation.

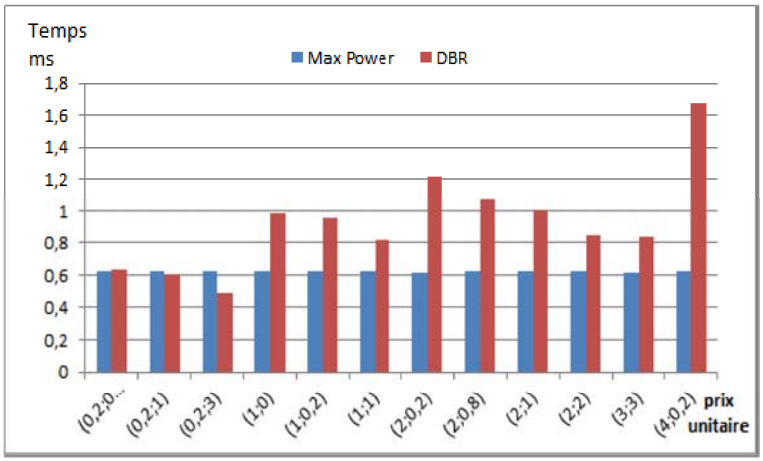

(a) Cell-center UEs

(b) Cell-edge UEs

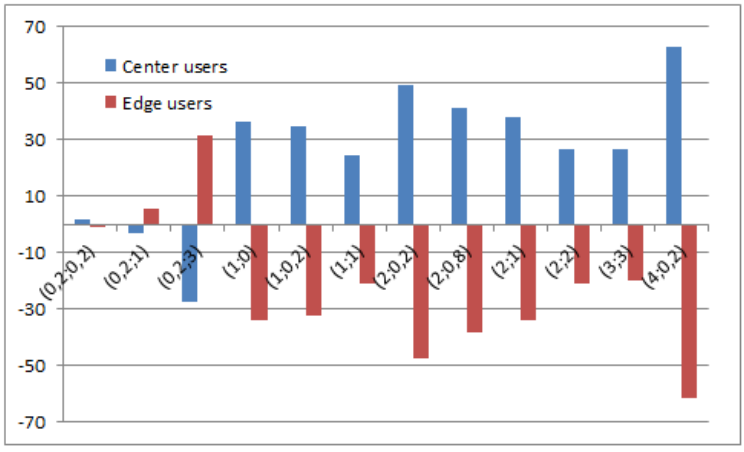

(c) Relative Deviation

FIGURE 6.1: Transfer time per zone as a function of power unitary cost for DBR vs. Max Power Policy

In Figure 6.1, we depict the total bit transfer time per zone $T_z = \sum_{i=1}^{m} \sum_{k=1}^{n} T_{i,k,z}$ for cell-center and cell-edge UEs as a function of various power unitary costs (α_1 ;α_2) for DBR and Max Power Policy. In most scenarios, we aimed at favoring cell-edge UEs by lowering the power unitary cost in comparison to that of cell-center UEs. We notice as expected that the improvement in one zone as compared to the Max Power policy is obtained at the expense of degradation of the other zone. This fact is highlighted in the lowest sub-figure where the relative deviation $\frac{T_z^{DBR} - T_z^{MaxPower}}{T_z^{DBR}} * 100$ is displayed. Further, we see that the improvement in one zone does not strictly depend on how low its power unitary cost is but how low it is relatively to the other zone : despite the fact that no power unitary cost is inflected on cell-edge UEs in scenario (1,0), the total transfer time is greater than that for scenarios (2 ;0.2) or (4 ;0.2).

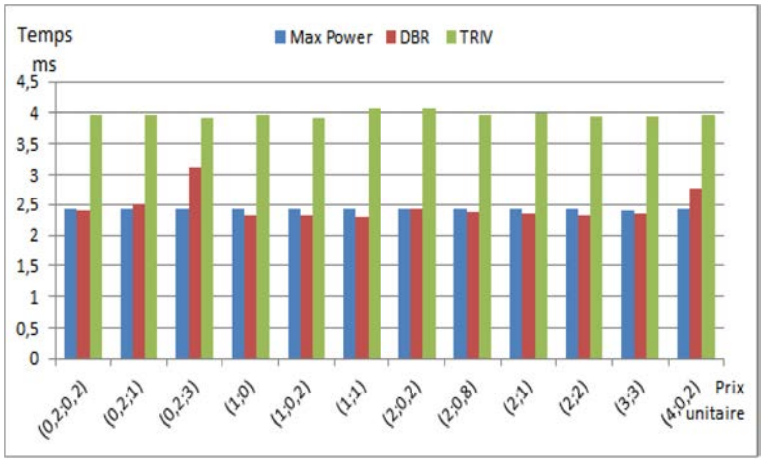

FIGURE 6.2: Total Transfer Time as a function of power unitary cost for DBR vs. Max Power Policy and Trivial Policy

In Figure 6.2, we depict the system bit transfer time $T = \sum_{z=1}^{2} \sum_{i=1}^{n} \sum_{k=1}^{m} T_{i,k,z}$ as a function of power unitary cost for DBR, Max Power policy and Trivial policy. Except for (0.2 ;3) and (4 ;0.2) where there is a large discrepancy between the power unitary cost of one zone in comparison with the other, for all other scenarios performances of DBR and Max Power policy are equivalent. However, DBR permits a considerable power economy in comparison with Max Power policy as we can see in figure 6.3 where the relative deviation between the total power in DBR and the Max Power policy is displayed as a function of power unitary cost. We can clearly see that the highest the power unitary cost in a zone, the highest the power economy and vice versa. The best performances are reached when the same (high) power unitary cost is assigned for both zones in scenarios (2 ;2) and (3 ;3) where power economy vary from 70% till 80% while the total transfer time is slightly lower than that in the Max Power policy. As the Trivial policy, we can see that performances are mediocre.

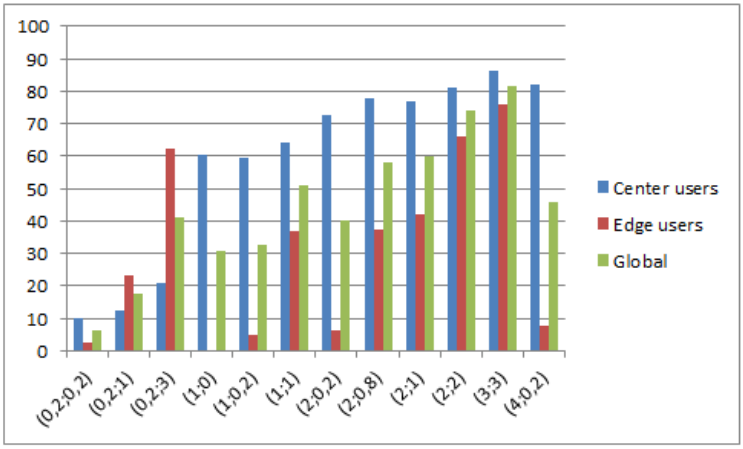

FIGURE 6.3: Power Economy

In figure 6.4, we report the mean convergence time as a function of power unitary cost. We note that DBR attains NE faster than 110 TTI and hence before the exchange of new RNTP messages (sent every 200 TTI).

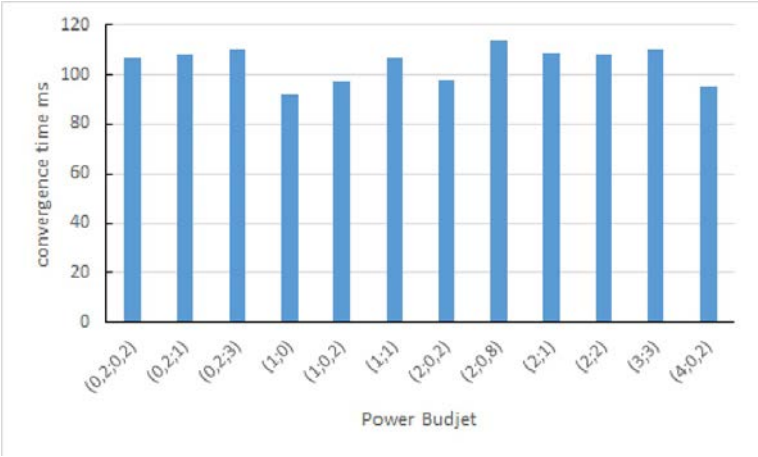

FIGURE 6.4: Convergence Time

6.6 The Price of Anarchy

In this section, we quantify the loss in efficiency suffered when a distributed scheme is adopted rather than a centralized optimization.

6.6.1 Optimal Centralized Approach

Unlike the distributed approach where precedence is given to the interests of each individual eNodeB, power control may be performed in a way that favors the overall system

performance. We do so by introducing a *centralized approach*, where a central controller assigns the power levels of each eNodeB in order to minimize the total network cost. To do that, we simply relax the integrality constraints on $x_{i,k}$, i.e., we assume that $0 < x_{i,k} \leq 1$ for all $i \in M$ and $k \in N$). After relaxing the integrality constraints, the obtained optimization problem is a non-linear convex problem :

$$\begin{aligned} &Minimize \sum_{i,z}(\frac{I_{i,k,z}}{x_{i,k}} + \alpha_z.P_0.x_{i,k}) \\ &Subject\ to : 0 \leq x_{i,k} \leq 1 \end{aligned} \tag{6.6.1}$$

6.6.2 Simulation Results

In Figure 6.5, we illustrate the mean time necessary to send a data unit for all UEs as a function of the system load for the optimal policy, our algorithm based on Best Response dynamics and the Max Power policy. We see that the performances of DBR and the Optimal policy are equivalent while we notice an expected improvement in comparison with the Max Power approach that systematically resorts to full power, especially for high load.

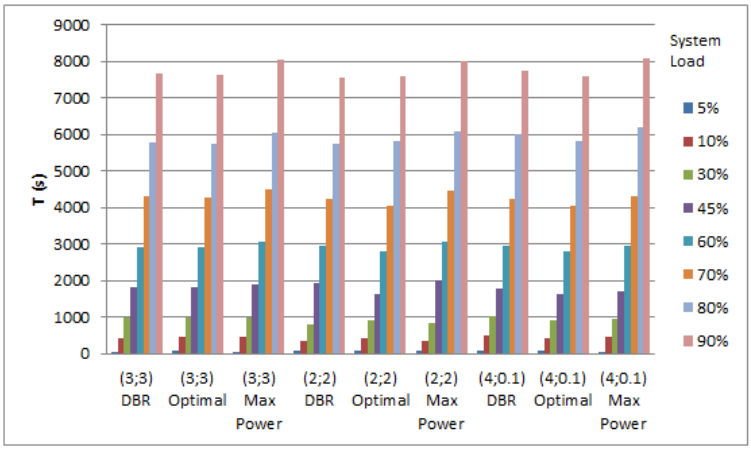

FIGURE 6.5: Global Transfer Time as a function of power unitary cost for DBR, Max Power and Optimal policies

However, the power economy made in the optimal approach as compared to DBR tempers its benefits as we can see from figure 6.6, where the relative deviation between the total power in DBR (respectively in the Optimal policy) and the Max Power policy is displayed as a function of power unitary cost. It is obvious that the optimal policy saves up much more power than the decentralized approach even in high load whereas the power economy in DBR withers slowly as load increases. Nevertheless, the slight discrepancy between the global transfer time in DBR and the Optimal policy which the primary goal sought for

and the low degree of system complexity of the decentralized approach makes it still an attractive solution.

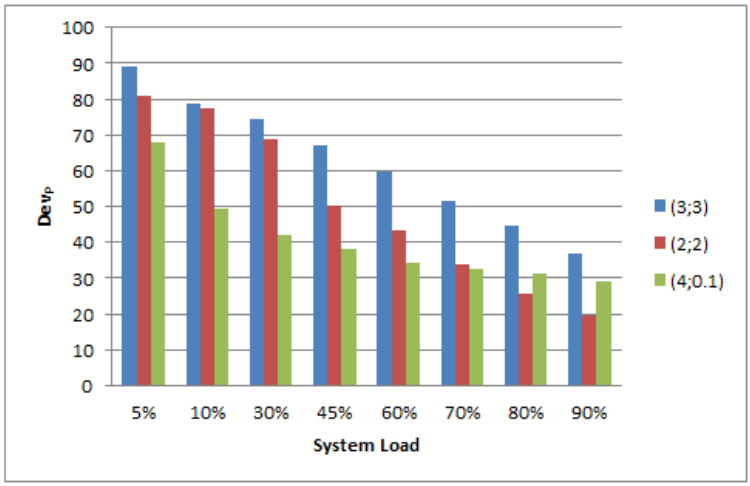

(a) DBR Policy

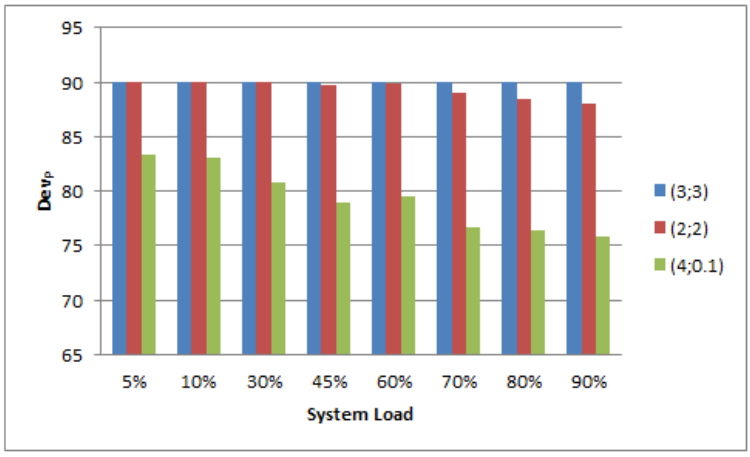

(b) Optimal Policy

FIGURE 6.6: Power Economy as a function of power unitary cost for DBR and Optimal policies

6.7 Conclusion

In this chapter, the power levels are astutely set as part of the LTE Inter Cell Interference coordination process. We proposed a game based semi distributed algorithm based on best response dynamics to reach NEs in a time coherent with the RNTP signaling time. Numerical simulations assessed the good performances of the proposed approach in comparison with a policy that services active UEs with full power. More importantly, considerable power economy can be realized.

Chapitre 7

General Conclusion

This chapter presents the general conclusion of the different studies described in this manuscript. We summarize the main contributions of our work and give the future research directions that stem from it.

7.1 Summary of Contribution

The exponential growth in the number of communications devices over the past decade has set out new ambitious targets to meet the ever-increasing demand for UE capacity in emerging wireless systems. However, the inherent impairments of communication channels in cellular systems pose constant challenges to meet the envisioned targets. In order to deal with the high cost and scarcity of suitable wireless spectrum, higher spectral reuse efficiency is required across the cells, inevitably leading to higher levels of interference. To combat interference, the ICIC concept is explored throughout this thesis in the downlink of cellular OFDMA systems. ICIC allows coordinated radio resources management between multiple cells. The eNodeBs can share resource usage information and interference levels over the X2 interface through LTE-normalized messages. Non-cooperative game theory is largely applied in this area were eNodeBs selfishly selects resource blocks (RBs) in order to minimize interference. Hence, we have recourse to this mathematical tool to model the interaction of eNodeBs over limited shared resources.

We focused our effort in this thesis on ICIC for the downlink of a cellular OFDMA system in the context of the SOAPS (Spectrum Opportunistic Access in Public Safety) project. This project introduces the LTE technologies for Broadband Services provision by PMR systems, it addresses low layers protocols issues with a particular focus on the improvement of frequency resource scheduling. Hence, our first work addresses the problem of downlink ICIC in the context of the SOAPS network, where the resource selection process is apprehended as a potential game for which we propose a fully decentralized algorithm

based on replicator dynamics to attain the pure Nash equilibriums of the game. Extensive simulations assessed the good performances of the algorithm for low to medium load, especially for systems with a limited number of RBs, where our algorithm produces efficient performances. These results comfort the adequacy of the proposed solution with the project needs and with the system latency constraints.

For the rest of our contributions, we were interested in a more general solution to overcome the ICIC problem for a full frequency band systems support (without a limited number of RBs). The downlink ICIC has been seen as a load balancing game, where an adaptation of a stochastic version of a best response dynamic algorithm is used to converge to the PNE of the game. Each eNodeB strives to select a pool of favorable resources with low interference based on local knowledge only. Proof of convergence is provided, and the efficiency of the tailored algorithm is proven through extensive simulations. However, in this first adaptation, the UE position in the cell is not taken into account for ease of computation. Simulation results show better performances than the replicator dynamics algorithm for systems using larger number of RBs.

The flaws of the previous proposed algorithm are treated in a second version using a more realistic scenario that taken into account the UEs positions, where a greedy algorithm is used to achieve faster convergence times. Simulation results of this new algorithm show a significant improvement for both time convergence and system performance even for larger system bandwidth.

As a final work, the ICIC issue was addressed through adequate power allocation on selected RBs. Finding a suitable power allocation allows to reduce both interference and power consumption. The power level selection process of RBs is apprehended as a sub-modular game and a semi distributed algorithm based on best response dynamics is proposed to attain the PNE of the modeled game. Using the RNTP message exchanged over the X2 link, each eNodeB will first select a pool of favorable RBs with low interference. Then, each eNodeB will strive to fix the power level adequately on those selected RBs realizing performances comparable with the Max Power policy that uses full power on selected RBs while achieving substantial power economy.

7.2 Future Directions

For our future work, we plan to enhance our RB selection algorithm by including position of the UE, in such a solution, each eNodeB will divide the cell in zones according to the adjacent cells, it will then compute the position of the UEs and locate them in one of the previously determined cells zone, then the RBs will be allotted to the UEs according to their positions. Each UE will get a RB in a way it minimizes the interference of that RB between the serving eNodeBs and the adjacent eNodeBs close to the UE. This po-

sition aware algorithm allows to use even highly interfered RB, this is done by finding the interferer eNodeB and avoiding using the RB in the shared region of both eNodeBs, while locating a non-interferer eNodeB to allocate that same RB to the UE located in the shared area. Another improvement of our game based algorithm is to determine an initial strategy for the considered ICIC game, based on the received RNTP message. It will build an initial strategy, taking into account the interference level of the adjacent eNodeB, this helps run the algorithm from a favourable state, and such an approach will induce better performances and quicker convergence time.

Another solution is to include a learning entity to our system, this algorithm will study the global behaviour of the chosen strategies after each convergence of our load balancing algorithm, it will then define some strategies as initial state or input for our algorithms in order to get faster convergence and better performances.

Some networks can propose priority between the UEs, the SOAPS project due to its critical aspect needs such prioritized UEs. hence, we are going to add this constraint to our algorithm. In this approach, each UE will get an ID in order to create UEs groups, and then the algorithm along with the position aware mechanism will take into account this priority in the RBs allocation, UEs with high priority will get best RBs according to their position to increase their throughput.

With the increasing demand of bandwidth, networks operator are using layered architecture with the macrocell being surrounded with many pico and femto cells. Managing the attribution of each UE to the cells become relevant, some macro cells could be loaded where there is some free of charge pico cells. This problem is a load balancing problem that we propose to tackle using a game theoretic approach. Using signaling between the cells to locate the loaded ones, the algorithm will perform the UEs reallocation in a semi distributed manner.

For the upcoming 5G networks, the main proposed solution is the heterogeneous wireless network, where each UE can access different RAN (Radio Access Network) technologies. To optimize network performance while enhancing user experience (by providing high rates with adequate QoS), efficient common radio resource management mechanisms need to be defined. Typically, when a new or a handover session arrives, a decision must be made as to what technology it should be associated with. This is known as the Radio Access Technology (RAT) selection. We propose a semi distributed approach where different networks exchange signaling information in order to find the suitable allocation (CoMP).

We plan to extend this type of methods to a SON environment, taking into account practical parameters expected for 5G and in a heterogeneous network with non-stationary situations due to channel variations and change in the traffic pattern. More importantly, resource allocation schemes with cooperation among eNodeBs will be investigated to avoid inefficient equilibrium.

Annexe A

Proof for Theorem of Chapter 3

The appendix is devoted to prove Theorem 3.1.

Démonstration. Let $Q = (q_1, q_2, \ldots, q_n)$ be a mixed profile of the game. $\mathbb{E}[\ c_i\ |Q\ ]$ denotes the expected cost of eNodeB i with respect to a mixed profile Q.

According to Sastry and al. [SPT94], the Linear Reward-Inaction algorithm converges weakly towards a replication dynamic :

$$\frac{dq_{i,x}}{dt}(Q) = q_{i,x}\left(\mathbb{E}[\ c_i\ |Q\ ] - \mathbb{E}[\ c_i\ |q_{i,x} = 1, Q_{-i}\ ]\right) \tag{A.0.1}$$

This equation, called the (multi-population) replicator dynamics, is well-known to have its limit points related to Nash equilibriums (through the so-called Folk's theorem of evolutionary game theory [HS03]). More precisely, we have the following theorem :

Theorem A.1. *The following are true for the solutions of Equation* (A.0.1) *: (i) All Nash equilibriums are stationary points. (ii) All strict Nash equilibriums are asymptotically stable. (iii) All stable stationary points are Nash equilibriums.*

From [BC13], the limit for $b \to 0$ of the dynamics of stochastic algorithms is some Ordinary Differential Equations (ODE) whose stable limit points, when $t \to \infty$ (if they exist), can only be Nash equilibriums. Hence, if there is convergence for the ordinary differential equation, then one expects the replicator dynamic algorithm to reach an equilibrium. Moreover, in [CTG09], Coucheney *et al.* proved that such Nash equilibriums are pure.

Let us see if the continuous dynamic converges with stability arguments. Given a pure profile $X = (x_1, x_2, \ldots, x_n)$, we denote by $\pi(X|Q)$ the probability that each eNodeB i chooses the pure strategy x_i according to the mixed profile Q :

$$\pi(X|Q) = \prod_{i=1}^{n} q_{i,x_i}. \tag{A.0.2}$$

To prove the convergence of the learning scheme Eq. (3.4.1), we define the following function $F : \mathbb{K} \to \mathbb{R}$:

$$F(Q) = \sum_{X \in \mathcal{S}} \pi(X|Q)\phi(X) \tag{A.0.3}$$

Let us study the evolution of function $F(Q)$ over time. We focus on $\frac{dF}{dt}(Q)$. By definition, we have

$$\frac{dF}{dt}(Q) = \sum_{i=1}^{n} \sum_{s \in S_i} \frac{\partial F}{\partial q_{i,s}} \frac{dq_{i,s}}{dt}(Q)$$

We will compute first $\frac{\partial \pi(X|Q)}{\partial q_{j,x'_j}}$ and then $\frac{\partial F}{\partial q_{j,x'_j}}(Q)$.

$$\frac{\partial \pi(X|Q)}{\partial q_{j,x'_j}} = \begin{cases} \prod_{i=1, i \neq j}^{n} q_{i,x_i} & \text{if} \quad x_j = x'_j, \\ 0 & \text{otherwise.} \end{cases} \tag{A.0.4}$$

This formula can be rewritten as

$$\frac{\partial \pi(X|Q)}{\partial q_{j,x'_j}} = \pi(X|q_{j,x'_j} = 1, Q_{-j}).$$

Hence, we get what follows :

$$\begin{aligned} \tfrac{\partial F}{\partial q_{j,x'_j}}(Q) &= \sum_{X \in \mathcal{S}} \frac{\partial \pi(X|Q)}{\partial q_{j,x'_j}} \phi(X) \\ &= \sum_{X \in \mathcal{S}} \pi(X|q_{j,x'_j} = 1, Q_{-j})\phi(X) \end{aligned}$$

From Equation (3.3.1), we can obtain :

$$\begin{aligned} &\tfrac{\partial F}{\partial q_{j,x'_j}} - \tfrac{\partial F}{\partial q_{j,x_j}} \\ &= \sum_{X \in \mathcal{S}} \pi(X|q_{j,x'_j} = 1, Q_{-j})(\phi(x'_j, X_{-j}) - \phi(x_j, X_{-j})) \\ &= \sum_{X \in \mathcal{S}} \pi(X|q_{j,x'_j} = 1, Q_{-j})(c_j(x'_j, X_{-j}) - c_j(x_j, X_{-j})) \\ &= \mathbb{E}[\ c_j\ |q_{j,x'_j} = 1, Q_{-j}\ ] - \mathbb{E}[\ c_j\ |q_{j,x_j} = 1, Q_{-j}\ ] \end{aligned}$$

So,

$$\frac{\partial F}{\partial q_{j,x'_j}} - \frac{\partial F}{\partial q_{j,x_j}} = \mathbb{E}[\ c_j\ |q_{j,x'_j} = 1, Q_{-j}\ ] - \mathbb{E}[\ c_j\ |q_{j,x_j} = 1, Q_{-j}\ ] \tag{A.0.5}$$

Hence, we have the following :

$$\frac{dF}{dt}(Q) = \sum_{i\in N}\sum_{x_i\in S_i}\frac{\partial F}{\partial q_{i,x_i}}\frac{dq_{i,x_i}}{dt}(Q)$$
$$= \sum_{i\in N}\sum_{x_i\in S_i} q_{i,x_i}\frac{\partial F}{\partial q_{i,x_i}}\left(\mathbb{E}[\ c_i\ |Q\ ] - \mathbb{E}[\ c_i\ |q_{i,x_i}=1, Q_{-i}\ ]\right)$$
$$= \sum_{i}\sum_{x_i\in S_i}\sum_{x'_i\in S_i} q_{i,x_i}q_{i,x'_i}\frac{\partial F}{\partial q_{i,x_i}}\cdot$$
$$\left(\mathbb{E}[\ c_i\ |q_{i,x'_i}=1, Q_{-i}\ ] - \mathbb{E}[\ c_i\ |q_{i,x_i}=1, Q_{-i}\ ]\right)$$
$$= \sum_{i}\sum_{x_i<x'_i} q_{i,x_i}q_{i,x'_i}\left(\frac{\partial F}{\partial q_{i,x_i}} - \frac{\partial F}{\partial q_{i,x'_i}}\right)\cdot$$
$$\left(\mathbb{E}[\ c_i\ |q_{i,x'_i}=1, Q_{-i}\ ] - \mathbb{E}[\ c_i\ |q_{i,x_i}=1, Q_{-i}\ ]\right)$$
$$= \textstyle\sum_i \sum_{x_i<x'_i} -q_{i,x_i}q_{i,x'_i}\cdot$$
$$\left(\mathbb{E}[\ c_i\ |q_{i,x'_i}=1, Q_{-i}\ ] - \mathbb{E}[\ c_i\ |q_{i,x_i}=1, Q_{-i}\ ]\right)^2$$

So, we can conclude that $\frac{dF}{dt}(Q) \leq 0$.

Thus F is non-decreasing along the trajectories of the replication dynamics. and, due to the nature of the learning algorithm, all solutions of the ODE (A.0.1) remain in the strategy space if initial conditions $\in [0,1]$. From the previous computations, we know that $\frac{dF(Q^*)}{dt} = 0$ implies that $\forall i \in N \forall x_i, x'_i \in S_i$:

$$q^*_{i,x_i} = 0, or\ (\mathbb{E}[\ c_i\ |q_{i,x_i}=1, Q_{-i}\ ] = \mathbb{E}[\ c_i\ |q_{i,x_i}=1, Q_{-i}\ ])$$

Such a Q^* is consequently a stationary point of the dynamics.

Since from Theorem A.1, all stationary points that are not Nash equilibriums are unstable, Theorem 3.1 holds. Thus all solutions have to converge to some stationary point corresponding to Nash Equilibrium. We can deduce that the learning algorithm, for any initial condition in $\mathbb{K} - \mathbb{K}^*$, always converges to a Nash Equilibrium of instance G. □

Annexe B

Proof for Theorem of Chapter 4

Let n be the total number of users and m the number of RBs, the resources and $M = \{1, 2, \ldots, m\}$. Let $W(t) = (w_1, w_2, \ldots, w_m)$ be the vector containing the weights of each resource RB at time t, with $w_k = \sum_{i \in N} x_{i,k}$ corresponding to the number of users on RB k. We defined our potential function as follows :

$$\Phi(W) = \frac{1}{2} \sum_{k \in M} (w_k - \bar{w})^2$$

, with $\bar{w} = \sum_{i \in N} \frac{x_{i,k}}{m}$ the average load.

This potential function is a standard one according to (ref Convergence Time to Nash Equilibria, Bounds for the Convergence Rate of Randomized Local Search in a Multiplayer Load-balancing Game, etc.). As stated in Chapter 4, the appendix is devoted to prove that a Nash Equilibrium is reached in expected time $O(m \log(\frac{n}{m}))$. We adapt the analysis proposed by Berenbrink et al.

Algorithm 6

for each BS **do**
  Select a RB i uniformly at random among the b used RBs
  Select a free RB j uniformly at random in $M - b$ (strategy x'_i)
  if $(c_i(x_i, X_{-i}) > c_i(x'_i, X_{-i})$) **then**
    Go to RB j with probability $1 - \frac{c_i(x_i, X_{-i})}{c_i(x'_i, X_{-i})}$
  end if
end for

Let $P_{i,j}$ be the random variable corresponding to the number of users moving from RB i to RB j

$$P_{i,j} = \begin{cases} \frac{1}{b} \times \frac{1}{m-(b-1)} \left(1 - \frac{w_j}{w_i}\right) \text{ if } j \neq i \text{ and } w_i \geq w_j + 1 \\ 0 \text{ if } j \neq i \text{ and } w_i \leq w_j + 1 \\ 1 - \sum_{k \in M, w_i > w_k} P_{i,k} \text{ if } j = i \end{cases}$$

The potential function is the following

$$\Phi(W) = \frac{1}{2} \sum_{k \in M} (w_k - \bar{w})^2 = \frac{1}{m} \sum_{i=1}^{m} \sum_{k=i+1}^{m} (w_i - w_k)^2$$

$$\begin{aligned} E[\Phi(W(t+1))|W(t)] &= \mathbb{E}[\sum_{i=1}^{m} (W_i(t+1) - \bar{w})^2 | W_i(t) = w_i] \\ &= \sum_{i=1}^{m} (\mathbb{E}[(W_i(t+1))|W_i(t) = w_i] - \bar{w})^2 + \sum_{i=1}^{m} Var[(W_i(t+1))|W_i(t) = w_i] \end{aligned} \tag{B.0.1}$$

Lemma 5.

$$\sum_{i=1}^{m} \left(\mathbb{E}[(W_i(t+1))|W_i(t) = w_i] - \bar{w}\right)^2 < \Phi(W) - \sum_{i=1}^{m} \sum_{k=i+1}^{m} 2\mathbb{E}[W_{i,k}] (w_i - w_k) \tag{B.0.2}$$

Démonstration. First, without loosing generality, we assume $w_1 \geq w_2 \geq \cdots \geq w_m$.

$$\mathbb{E}[W_i(t+1)|W(t) = w_i] = w_i + \sum_{j=1}^{i-1} \mathbb{E}[W_{j,i}] - \sum_{k=i+1}^{n} \mathbb{E}[W_{i,k}]$$

Let $S_i(t)$ be the set of BSs using resource i at time t. Let $\mathbb{E}[W_{i,j}]$ be the average total weight of players which move from resource i to j. Each player has a weight equals to 1.

$$\begin{aligned} \mathbb{E}[W_{i,j}] &= \sum_{\ell \in S_i} P_{i,j} \\ &= \frac{w_i}{b(m-b+1)} \left(1 - \frac{w_j}{w_i}\right) \leq \frac{w_i - w_j}{m} \end{aligned}$$

Let $d_{i,j} = \mathbb{E}[W_{i,j}]$ be the average weight transferred from i to j. We have $d_{i,j} \leq \frac{w_i - w_j}{m}$ if $i < j$, $d_{i,j} = 0$ otherwise.

These transitions can be represented by a complete graph with m vertices $S = \frac{m(m-1)}{2}$

edges. Each of these edges has a weight corresponding to the average transferred weight effected. Let e be an edge, $e = (i, j)$ has a weight $d_{i,j}$ for all $i \in M$, $j \in M$. Let $\mathbb{E} = \{e_1, e_2, \ldots, e_S\}$ with $e_1 \leq e_2 \leq \cdots \leq e_S$. The edges are activated sequentially from e_1 to e_S with e_1 the one of smaller weight.

Let $W^z = \{w_1^z, w_2^z, \ldots w_S^z\}$ be the weight vector of each resource after activating z edges. W^0 is the vector W without modification, $\forall i \in M,\ w_i^0 = w_i \Rightarrow \Phi(W^0) = \Phi(W)$. Similarly W^S is the vector W after activating S edges which correspond to all the possible weight transfers between the resources.

$$\begin{aligned} w_i^S &= w_i + \sum_{j=1}^{i-1} d_{j,i} - \sum_{k=i+1}^{n} d_{i,k} \\ &= \mathbb{E}[W_i(t+1) | W_i(t) = w_i] \end{aligned}$$

Let $\Delta_z(\Phi)$ be the potential difference associated with the activation of the edge $e_z = (i, k)$.

$$\forall z \in S,\ \Delta_z(\Phi) = \Phi(W^{z-1}) - \Phi(W^z)$$

The objective is to measure the potential difference between$\Phi(W^0)$ et $\Phi(W^S) = \sum_{z=1}^{S} \Phi(W^{z-1}) - \Phi(W^z) = \sum_{e_z \in \mathbb{E}} \Delta_z(\Phi)$

$$\begin{aligned} \Delta_z(\Phi) &= \Phi(W^{z-1}) - \Phi(W^z) \\ &= \sum_{j=1}^{m} (w_j^{z-1} - \bar{w})^2 - \sum_{j=1}^{m} (w_j^z - \bar{w})^2 \\ &= 2d_{i,k} \left(w_i^{z-1} - w_k^{z-1} - d_{i,k} \right) \end{aligned}$$

For all resources j activated before $e_z = (i, k)$ then $d_{i,j} \leq d_{i,k} \leq \frac{w_i - w_k}{m}$ because $j < k$. The resource i has $(m-2)$ resources different from k,so the average weight i could send to its neighbors before activating $e_z = (i, k)$ is at most $(m-2)d_{i,k} \leq m \left(\frac{w_i - w_k}{m} \right) - 2d_{i,k}$

$$w_i^{z-1} \geq w_i - (m-2)d_{i,k}$$

Similarly, the resource k has $(m-2)$ neighbors different from resource i. The average weight k may receive from them before the activation of $e_z = (i, k)$ is at most

$$w_k^{z-1} \leq w_k + (m-2)d_{i,k}$$

Using those two results

$$\Delta_z(\Phi) = 2d_{i,k}\left(w_i^{z-1} - w_k^{z-1} - d_{i,k}\right) \geq 2d_{i,k}\left(w_i - w_k\right)$$

This implies $\Phi(W^0) - \Phi(W^S) \geq \sum_{e_z \in E} 2d_{i,k}\left(w_i - w_k\right)$. Since $\Phi(W^S) \leq \Phi(W^0) - \sum_{e_z \in E} 2d_{i,k}\left(w_i - w_k\right)$ and $d_{i,k} = \mathbb{E}[W_{i,k}]$, the lemma holds. □

Lemma 6.

$$\sum_{i=1}^{m} Var[(W_i(t+1))|W_i(t) = w_i] \leq 2\sum_{i=1}^{m}\left(\sum_{k=i+1}^{m} \mathbb{E}[W_{i,k}]\right) \tag{B.0.3}$$

Démonstration. Recall that $S_i(t)$ is the set of players on resource i at time t. Let $Y^{\ell}_{(k,i)}$ be the unit vector indicating that player ℓ moves from resource k to i. Let ℓ et ℓ' be two different players, then $Y^{\ell}_{(k,i)}$ and $Y^{\ell'}_{(k,i)}$ are independents.

$$\begin{aligned}
Var[(W_i(t+1))|W_i(t) = w_i] &= Var[\sum_{\ell \in N} Y^{\ell}_{(k,i)}] \\
&= \sum_{\ell \in N} \sum_{\ell \in S_k(t)} Var[Y^{\ell}_{(k,i)}] \\
&= \sum_{\substack{k \in M \\ k \neq i}} \left(\sum_{\ell \in S_k(t)} P_{k,i}(1 - P_{k,i})\right) + \sum_{\ell \in S_i(t)} P_{i,i}(1 - P_{i,i}) \\
&< \sum_{\substack{k \in M \\ k \neq i}} \left(\sum_{\ell \in S_k(t)} P_{k,i}\right) + \sum_{\ell \in S_i(t)} (1 - P_{i,i}) \\
&< \sum_{\substack{k \in M \\ k \neq i}} (\mathbb{E}[W_{k,i}]) + \sum_{k \neq i} \mathbb{E}[W_{i,k}]
\end{aligned}$$

If $w_i > w_k$ then $\mathbb{E}[W_{k,i}] = 0$

$$\begin{aligned}
\sum_{i=1}^{m} Var[(W_i(t+1))|W_i(t) = w_i] &\leq \sum_{i=1}^{m}\left(\sum_{k \neq i} \mathbb{E}[W_{k,i}] + \sum_{k \neq i} \mathbb{E}[W_{i,k}]\right) \\
&\leq 2\sum_{i=1}^{m}\left(\sum_{k=i+1}^{m} \mathbb{E}[W_{i,k}]\right)
\end{aligned} \tag{B.0.4}$$

□

Lemma 7.

$$\mathbb{E}[\Phi(W(t+1))|W(t)] < \Phi(W(t)) - \sum_{i=1}^{m}\sum_{k=i+1}^{m} 4\mathbb{E}[W_{i,k}]\,(w_i - w_k) \tag{B.0.5}$$

Démonstration. Recall that $w_i > w_k$. So we get $w_i - w_k \geq 1$ and $2\,(w_i - w_k) \geq (w_i - w_k + 1)$. From Equation (B.0.1) and the both previous Lemmas, this lemma holds. □

Lemma 8.

$$\mathbb{E}[\Phi(W(t+1))|W(t)] < \Phi(W(t))(1 - \frac{16}{(m+2)}) \tag{B.0.6}$$

Démonstration. By definition, we have $\mathbb{E}[W_{i,k}] = \frac{w_i - w_k}{b(m-b+1)}$. Since $\Phi(W) = \frac{\sum_{i=1}^{m}\sum_{k=i+1}^{m}(w_i - w_k)^2}{m}$, we can deduce that

$$\sum_{i=1}^{m}\sum_{k=i+1}^{m}\mathbb{E}[W_{i,k}]\,(w_i - w_k) = \frac{m\Phi(W)}{b(m-b+1)}$$

So, from Lemma 7, we get $\mathbb{E}[\Phi(W(t+1))|W(t)] < \Phi(W(t)) - 4\frac{m\Phi(W(t))}{b(m-b+1)}$. By computation, we can obtain $\frac{m}{b(m-b+1)} \geq \frac{4}{(m+2)}$ for any b and m such that $m \geq b > 0$. So we can deduce $\mathbb{E}[\Phi(W(t+1))|W(t)] < \Phi(W(t))(1 - \frac{16}{(m+2)})$. □

From Lemma 8, we deduce that $\mathbb{E}[\Phi(W(t+\tau))|W(t)] \leq \Phi(W(t))(1 - \frac{16}{(m+2)})^{\tau}$. Recall that $\Phi(W) = \frac{1}{2}\sum_{k\in M}(w_k - \frac{n}{m})^2$, thus $0 \leq \Phi(W) \leq \frac{n^2}{2m}$. So, after $\tau = m\log(\frac{n^2}{m})$ steps, $\mathbb{E}[\Phi(W(t+\tau))|W(t)] \leq \frac{n^2}{2m}(1 - \frac{16}{(m+2)})^{m\log(\frac{n^2}{m})} \leq 2$ By Markov's inequality, the probability $W(t+\tau)$ is a Nash equilibrium given $W(t) = W$ is greater than $1/2$. Now for each new run of τ steps, the probability to reach a Nash Equilibrium is at least 1, hence the expected time to reach such a equilibrium is at most 2τ.

Bibliographie

[3GP08] 3GPP, *Requirements for further advancements for e-utra (lte-advanced) (release 8)*.

[3gp11a] *3gpp, evolved universal terrestrial radio access network (e-utran) x2 application protocol (x2ap)*.

[3GP11b] 3GPP, *Technical report : Coordinated multi-point operation for lte physical layer aspects*.

[3gp12] *3gpp, evolved universal terrestrial radio access (e-utra) ; physical layer procedures*, 2012.

[AA03] Eitan Altman and Zwi Altman, *S-modular games and power control in wireless networks*, Automatic Control, IEEE Transactions on **48** (2003), no. 5, 839–842.

[AADM07] Andrea Abrardo, Alessandro Alessio, Paolo Detti, and Marco Moretti, *Centralized radio resource allocation for ofdma cellular systems*, 5738–5743.

[AB12] Clemens PJ Adolphs and Petra Berenbrink, *Distributed selfish load balancing with weights and speeds*, Proceedings of the 2012 ACM symposium on Principles of distributed computing, ACM, 2012, pp. 135–144.

[AKC+14] Amine Adouane, Kinda Khawam, Johanne Cohen, Dana Marinca, and Samir Tohme, *Replicator dynamics for distributed inter-cell interference coordination*, Computers and Communication (ISCC), 2014 IEEE Symposium on, IEEE, 2014, pp. 1–7.

[AKG11] Alireza Attar, Vikram Krishnamurthy, and Omid Namvar Gharehshiran, *Interference management using cognitive base-stations for umts lte*, Communications Magazine, IEEE **49** (2011), no. 8, 152–159.

[AkI08] Ibrahim Ismail Mohammed Al-kebsi and Mahamod Ismail, *The impact of modulation adaptation and power control on papr clipping technique in ofdm of 4g systems*, Telecommunication Technologies 2008 and 2008 2nd Malaysia Conference on Photonics. NCTT-MCP 2008. 6th National Conference on, IEEE, 2008, pp. 295–299.

[AR11] Schwarz Andreas Roessler, Rohde, *Understanding downlink power allocation in lte*, http ://www.wirelessdesignmag.com/blogs/2011/02/understanding-downlink-power-allocation-lte, 02 may 2011.

[ARK+14a] Amine Adouane, Lise Rodier, Kinda Khawam, Johanne Cohen, and Samir Tohme, *Distributed load balancing game for inter-cell interference coordination*, European Wireless 2014 ; 20th European Wireless Conference ; Proceedings of, VDE, 2014, pp. 1–6.

[ARK+14b] ———, *Game theoretic framework for inter-cell interference coordination*, Wireless Communications and Networking Conference (WCNC), 2014 IEEE, IEEE, 2014, pp. 57–62.

[Ass08] Mohamad Assaad, *Optimal fractional frequency reuse (ffr) in multicellular ofdma system*, Vehicular Technology Conference, 2008. VTC 2008-Fall. IEEE 68th, IEEE, 2008, pp. 1–5.

[BC13] Olivier Bournez and Johanne Cohen, *Learning equilibria in games by stochastic distributed algorithms*, Computer and Information Sciences III, Springer, 2013, pp. 31–38.

[BCRG14] Erez Biton, Asaf Cohen, Guy Reina, and Omer Gurewitz, *Distributed inter-cell interference mitigation via joint scheduling and power control under noise rise constraints*, Wireless Communications, IEEE Transactions on **13** (2014), no. 6, 3464–3477.

[BFHH12] Petra Berenbrink, Tom Friedetzky, Iman Hajirasouliha, and Zengjian Hu, *Convergence to equilibria in distributed, selfish reallocation processes with weighted tasks*, Algorithmica **62** (2012), no. 3-4, 767–786.

[BPVG06] Paola Bisaglia, Silvano Pupolin, Daniele Veronesi, and Michele Gobbi, *Resource allocation and power control in a tdd ofdm-based system for 4g cellular networks*, Vehicular Technology Conference, 2006. VTC 2006-Spring. IEEE 63rd, vol. 4, IEEE, 2006, pp. 1595–1599.

[BZGA10] Stefan Brueck, Lu Zhao, Jochen Giese, and M Awais Amin, *Centralized scheduling for joint transmission coordinated multi-point in lte-advanced*, 177–184.

[CAM+09] Vikram Chandrasekhar, Jeffrey G Andrews, Tarik Muharemovict, Zukang Shen, and Alan Gatherer, *Power control in two-tier femtocell networks*, Wireless Communications, IEEE Transactions on **8** (2009), no. 8, 4316–4328.

[Cha13] Himanshu Chauhan, *Lte network topology and architecture*, http ://worldtechie.blogspot.fr/2013/04/lte-network-topology-and-architecture.html, 25 April 2013.

[CKKL04] Jung Min Choi, Jin Sam Kwak, Ho Seok Kim, and Jae Hong Lee, *Adaptive subcarrier, bit, and power allocation algorithm for mimo-ofdma system*,

Vehicular Technology Conference, 2004. VTC 2004-Spring. 2004 IEEE 59th, vol. 3, IEEE, 2004, pp. 1801–1805.

[CLL13] Bumkwi Choi, Seyoun Lim, and Tae-Jin Lee, *Sequential frequency reuse with power control for ofdma systems*, Wireless Communications and Mobile Computing **13** (2013), no. 1, 37–46.

[Com09] Anritsu Company, *Lte resource guide*, 2009.

[CTG09] Pierre Coucheney, Corinne Touati, and Bruno Gaujal, *Fair and efficient user-network association algorithm for multi-technology wireless networks*, INFOCOM 2009, IEEE, IEEE, 2009, pp. 2811–2815.

[DMMS14] Supratim Deb, Pantelis Monogioudis, Jerzy Miernik, and James P Seymour, *Algorithms for enhanced inter-cell interference coordination (eicic) in lte hetnets*, IEEE/ACM Transactions on Networking (TON) **22** (2014), no. 1, 137–150.

[DSZ12] A Daeinabi, K Sandrasegaran, and X Zhu, *Survey of intercell interference mitigation techniques in lte downlink networks*, Telecommunication Networks and Applications Conference (ATNAC), 2012 Australasian, IEEE, 2012, pp. 1–6.

[EASH09] Jan Ellenbeck, Hussein Al-Shatri, and Christian Hartmann, *Performance of decentralized interference coordination in the lte uplink*, Vehicular Technology Conference Fall (VTC 2009-Fall), 2009 IEEE 70th, IEEE, 2009, pp. 1–5.

[EE13] Mohammed S ElBamby and Khaled MF Elsayed, *Performance analysis of soft frequency reuse schemes for a multi-cell lte-advanced system with carrier aggregation*, Personal Indoor and Mobile Radio Communications (PIMRC), 2013 IEEE 24th International Symposium on, IEEE, 2013, pp. 1528–1532.

[EHB08] Jan Ellenbeck, Christian Hartmann, and Lars Berlemann, *Decentralized inter-cell interference coordination by autonomous spectral reuse decisions*, Wireless Conference, 2008. EW 2008. 14th European, IEEE, 2008, pp. 1–7.

[ENJA08] Jad El-Najjar, Brigitte Jaumard, and Chadi Assi, *Minimizing interference in wimax/802.16 based mesh networks with centralized scheduling*, 1–6.

[Gol04] Paul W Goldberg, *Bounds for the convergence rate of randomized local search in a multiplayer load-balancing game*, Proceedings of the twenty-third annual ACM symposium on Principles of distributed computing, ACM, 2004, pp. 131–140.

[HDDM13] Mesud Hadzialic, Branko Dosenovic, Merim Dzaferagic, and Jasmin Musovic, *Cloud-ran : Innovative radio access network architecture*, ELMAR, 2013 55th International Symposium, IEEE, 2013, pp. 115–120.

[HMLN13] Amir Helmy, Leila Musavian, and Tho Le-Ngoc, *Energy-efficient power adaptation over a frequency-selective fading channel with delay and power constraints.*

[HS03] Josef Hofbauer and Karl Sigmund, *Evolutionary game dynamics*, Bulletin of the American Mathematical Society **40** (2003), no. 4, 479–519.

[JL03] Jiho Jang and Kwang Bok Lee, *Transmit power adaptation for multiuser ofdm systems*, Selected Areas in Communications, IEEE Journal on **21** (2003), no. 2, 171–178.

[KAL+14] Kinda Khawam, Amine Adouane, Samer Lahoud, Johanne Cohen, and Samir Tohme, *Game theoretic framework for power control in intercell interference coordination*, Networking Conference, 2014 IFIP, IEEE, 2014, pp. 1–8.

[KLL03] Didem Kivanc, Guoqing Li, and Hui Liu, *Computationally efficient bandwidth allocation and power control for ofdma*, Wireless Communications, IEEE Transactions on **2** (2003), no. 6, 1150–1158.

[KM11] Bujar Krasniqi and Christoph F Mecklenbrauker, *Efficiency of partial frequency reuse in power used depending on user's selection for cellular networks*, Personal Indoor and Mobile Radio Communications (PIMRC), 2011 IEEE 22nd International Symposium on, IEEE, 2011, pp. 268–272.

[KW11] Martin Kasparick and Gerhard Wunder, *Autonomous distributed power control algorithms for interference mitigation in multi-antenna cellular networks*, Wireless Conference 2011-Sustainable Wireless Technologies (European Wireless), 11th European, VDE, 2011, pp. 1–8.

[KZM12] Xin Kang, Rui Zhang, and Mehul Motani, *Price-based resource allocation for spectrum-sharing femtocell networks : A stackelberg game approach*, Selected Areas in Communications, IEEE Journal on **30** (2012), no. 3, 538–549.

[LAV14] Sandra Lagen, Adrian Agustin, and Josep Vidal, *Decentralized beamforming with coordinated sounding for inter-cell interference management.*

[LCK08] Zhenyu Liang, Yong Huat Chew, and Chi Chung Ko, *A linear programming solution to subcarrier, bit and power allocation for multicell ofdma systems*, Wireless Communications and Networking Conference, 2008. WCNC 2008. IEEE, IEEE, 2008, pp. 1273–1278.

[LLK+11] Lars Lindbom, Robert Love, Sandeep Krishnamurthy, Chunhai Yao, Nobuhiko Miki, and Vikram Chandrasekhar, *Enhanced inter-cell interference coordination for heterogeneous networks in lte-advanced : A survey*, arXiv preprint arXiv :1112.1344 (2011).

[LPJZ09] David López-Pérez, A Juttner, and Jie Zhang, *Dynamic frequency planning versus frequency reuse schemes in ofdma networks*, Vehicular Technology Conference, 2009. VTC Spring 2009. IEEE 69th, IEEE, 2009, pp. 1–5.

[LYW+11] Zhaoming Lu, Yan Yang, Xiangming Wen, Ying Ju, and Wei Zheng, *A cross-layer resource allocation scheme for icic in lte-advanced*, Journal of Network and Computer Applications **34** (2011), no. 6, 1861–1868.

[MDV13] Marco Maso, Merouane Debbah, and Lorenzo Vangelista, *A distributed approach to interference alignment in ofdm-based two-tiered networks*, Vehicular Technology, IEEE Transactions on **62** (2013), no. 5, 1935–1949.

[MMT08] Xuehong Mao, Amine Maaref, and Koon Hoo Teo, *Adaptive soft frequency reuse for inter-cell interference coordination in sc-fdma based 3gpp lte uplinks*, Global Telecommunications Conference, 2008. IEEE GLOBECOM 2008. IEEE, IEEE, 2008, pp. 1–6.

[MPS07] Farhad Meshkati, H Vincent Poor, and Stuart C Schwartz, *Energy-efficient resource allocation in wireless networks*, Signal Processing Magazine, IEEE **24** (2007), no. 3, 58–68.

[NSV+14] Giovanni Nardini, Giovanni Stea, Antonio Virdis, Marco Caretti, and Dario Sabella, *Improving network performance via optimization-based centralized coordination of lte-a cells*, 18–22.

[OR94] Martin J Osborne and Ariel Rubinstein, *A course in game theory*, MIT press, 1994.

[Pro06] Third Generation Partnership Project, *Physical layer aspects for evolved universal terrestrial radio access (utra) (release 7)*, 2006.

[PTLa14] Harri Pennanen, Antti Tolli, and Matti Latva-aho, *Robust beamforming with decentralized interference coordination in cognitive radio networks*, Acoustics, Speech and Signal Processing (ICASSP), 2014 IEEE International Conference on, IEEE, 2014, pp. 7308–7312.

[PWSF13] Klaus I Pedersen, Yuanye Wang, Stanislaw Strzyz, and Frank Frederiksen, *Enhanced inter-cell interference coordination in co-channel multi-layer lte-advanced networks*, Wireless Communications, IEEE **20** (2013), no. 3.

[RLLS98] Ragunathan Rajkumar, Chen Lee, John P Lehoczky, and Daniel P Siewiorek, *Practical solutions for qos-based resource allocation problems*, Real-Time Systems Symposium, 1998. Proceedings., The 19th IEEE, IEEE, 1998, pp. 296–306.

[Ros73] Robert W Rosenthal, *A class of games possessing pure-strategy nash equilibria*, International Journal of Game Theory **2** (1973), no. 1, 65–67.

[RY07] Mahmudur Rahman and Halim Yanikomeroglu, *Multicell downlink ofdm subchannel allocations using dynamic intercell coordination*, Global Telecommunications Conference, 2007. GLOBECOM'07. IEEE, IEEE, 2007, pp. 5220–5225.

[SAR09] Sanam Sadr, Alagan Anpalagan, and Kaamran Raahemifar, *Radio resource allocation algorithms for the downlink of multiuser ofdm communication systems*, Communications Surveys & Tutorials, IEEE **11** (2009), no. 3, 92–106.

[SEH14] Ahmed Hamdi Sakr, Hesham ElSawy, and Ekram Hossain, *Location-aware coordinated multipoint transmission in ofdma networks*, Proc. of IEEE International Conference on Communications, ICC, 2014.

[SMB+14] Vincenzo Sciancalepore, Vincenzo Mancuso, Albert Banchs, Shmuel Zaks, and Antonio Capone, *Interference coordination strategies for content update dissemination in lte-a.*

[SPT94] PS Sastry, VV Phansalkar, and M Thathachar, *Decentralized learning of nash equilibria in multi-person stochastic games with incomplete information*, Systems, Man and Cybernetics, IEEE Transactions on **24** (1994), no. 5, 769–777.

[SQ09] Rainer Schoenen and Fei Qin, *Adaptive power control for 4g ofdma systems on frequency selective fading channels*, Wireless Communications, Networking and Mobile Computing, 2009. WiCom'09. 5th International Conference on, IEEE, 2009, pp. 1–6.

[SSC11] Akram Bin Sediq, Rainer Schoenen, and Zhijun Chao, *A novel distributed inter-cell interference coordination scheme based on projected subgradient and network flow optimization*, Personal Indoor and Mobile Radio Communications (PIMRC), 2011 IEEE 22nd International Symposium on, IEEE, 2011, pp. 1595–1600.

[SV09] Alexander L Stolyar and Harish Viswanathan, *Self-organizing dynamic fractional frequency reuse for best-effort traffic through distributed inter-cell coordination*, INFOCOM 2009, IEEE, IEEE, 2009, pp. 1287–1295.

[Top79] Donald M Topkis, *Equilibrium points in nonzero-sum n-person submodular games*, SIAM Journal on Control and Optimization **17** (1979), no. 6, 773–787.

[WCLM99] Cheong Yui Wong, Roger S Cheng, K Ben Lataief, and Ross D Murch, *Multiuser ofdm with adaptive subcarrier, bit, and power allocation*, vol. 17, IEEE, 1999, pp. 1747–1758.

[WKSV10] Gerhard Wunder, Martin Kasparick, Alexander Stolyar, and Harish Viswanathan, *Self-organizing distributed inter-cell beam coordination in cellular networks with best effort traffic*, Modeling and Optimization in Mobile, Ad Hoc and Wireless Networks (WiOpt), 2010 Proceedings of the 8th International Symposium on, IEEE, 2010, pp. 295–302.

[WWS+] Jiao Wang, Jay Weitzen, Volkan Sevindik, Oguz Bayat, and Mingzhe Li, *Dynamic centralized interference coordination in femto cell network with qos provision.*

[Yao95] David D Yao, *S-modular games, with queueing applications*, Queueing Systems **21** (1995), no. 3-4, 449–475.

[YDH+10] Yiwei Yu, Eryk Dutkiewicz, Xiaojing Huang, Markus Mueck, and Gengfa Fang, *Performance analysis of soft frequency reuse for inter-cell interference coordination in lte networks*, Communications and Information Technologies (ISCIT), 2010 International Symposium on, IEEE, 2010, pp. 504–509.

[YKS13] Wei Yu, Taesoo Kwon, and Changyong Shin, *Multicell coordination via joint scheduling, beamforming, and power spectrum adaptation*, Wireless Communications, IEEE Transactions on **12** (2013), no. 7, 1–14.

[ZCM+12] Haijun Zhang, Xiaoli Chu, Wenmin Ma, Wei Zheng, and Xiangming Wen, *Resource allocation with interference mitigation in ofdma femtocells for co-channel deployment*, EURASIP Journal on Wireless Communications and Networking **2012** (2012), no. 1, 1–9.